

Electronic Thesis and Dissertation Repository

6-24-2011 12:00 AM

Development of a Novel TiO₂-polymeric Photocatalyst for Water Purification both under UV and Solar illuminations

Debjani Mukherjee, *The University of Western Ontario*

Supervisor: Dr. Ajay K. Ray, *The University of Western Ontario*

Joint Supervisor: Dr. S. Barghi, *The University of Western Ontario*

A thesis submitted in partial fulfillment of the requirements for the Doctor of Philosophy degree in Chemical and Biochemical Engineering

© Debjani Mukherjee 2011

Follow this and additional works at: <https://ir.lib.uwo.ca/etd>

 Part of the [Other Chemical Engineering Commons](#)

Recommended Citation

Mukherjee, Debjani, "Development of a Novel TiO₂-polymeric Photocatalyst for Water Purification both under UV and Solar illuminations" (2011). *Electronic Thesis and Dissertation Repository*. 187.
<https://ir.lib.uwo.ca/etd/187>

This Dissertation/Thesis is brought to you for free and open access by Scholarship@Western. It has been accepted for inclusion in Electronic Thesis and Dissertation Repository by an authorized administrator of Scholarship@Western. For more information, please contact wlsadmin@uwo.ca.

Development of a Novel TiO₂-polymeric Film Photocatalyst for Water Purification both under UV and Solar Illuminations

(Spine Title: Water Purification by Photocatalysis)

(Thesis format: Integrated-article)

by

Debjani Mukherjee

Graduate Program in Chemical and Biochemical Engineering
Department of Chemical and Biochemical Engineering

Submitted in partial fulfillment
of the requirements for the degree of
Doctor of Philosophy

The School of Graduate and Postdoctoral Studies
The University of Western Ontario
London, Ontario, Canada
July 2011

CERTIFICATE OF EXAMINATION

Supervisors

Dr. Ajay Ray

Dr. Shahzad Barghi

Supervisory Committee

Dr. Hassan Goma

Dr. Amarjeet Bassi

Examiners

Dr. Anand Prakash (Program Examiner)

Dr. Hassan Goma (Program Examiner)

Dr. Clare Robinson (University Examiner)

Dr. Xianshe Feng (External Examiner)

The thesis by

Debjani Mukherjee

entitled:

**Development of novel TiO₂-polymeric film photocatalyst for
water purification both under UV and solar illuminations**

is accepted in partial fulfillment of the
requirements for the degree of
Doctor of Philosophy

Date

Chair of the Thesis Examination Board

Abstract

Comprising about 70% of the Earth's surface, water is undoubtedly the most precious natural resource. According to the W.H.O, around 3.5 million people are dying every year from different water related diseases. Different kinds of dyes and pharmaceutical products have been detected in drinking water, all over the world. These organic compounds being non removable by traditional water purification processes, made advanced oxidation processes come into existence. Among all kind of advanced oxidation processes, photocatalytic oxidation is the most promising one. The photocatalytic process is based on aqueous phase hydroxyl radical chemistry and couples low energy UV light with semiconductors acting as photocatalyst. The slurry form of TiO_2 though being efficient has several disadvantages (particularly, post treatment expensive separation steps) which brings the immobilization of the catalysts on surfaces into existence. In this study, a TiO_2 -polymeric film photocatalyst was synthesized by reaction of gelatin, polyvinyl alcohol and polyvinyl pyrrolidone. TiO_2 Degussa P25 powder was embedded into the polymeric matrix. The characterization of the film by OM, SEM, FTIR, revealed the topography of the catalyst films. Optimization of photocatalysts functionality was carried out by varying the cross linking methods and conducting several photodegradation reactions both under UV and solar light. Aspirin and methyl orange were chosen as model compounds, as traces of these compounds were detected in the drinking water of South-Western Ontario. The freeze-dried film photocatalyst was observed to degrade organic compounds efficiently, under both UV and solar illuminations. Degradation of high concentrated organic pollutant, was observed to follow Langmuir-Hinshelwood kinetics while at low concentration, first-order kinetics was observed. The effects of initial concentration, flow rate, pH, light intensity, photocatalyst loading, and thickness of the film on the degradation rates were studied. Mechanism of degradation of aspirin was studied from LC/MS analysis. The TOC analysis was carried out to analyse the organic carbon content of the intermediates formed during the course of degradation. Finally, photocatalytic degradation reaction was carried out in a continuous flow reactor under LED lights. In brief this TiO_2 -polymeric

film photocatalyst holds the potential of being an efficient and economical form of future photocatalyst for water purification.

Keywords

Water purification, Photocatalysis, Titanium dioxide Degussa P25, Gelatin, Polyvinyl alcohol, Polyvinyl pyrrolidone, TiO₂-polymeric film photocatalyst, Methyl orange, Acetyl salicylic acid, UV lamps, Solar simulator, Total organic carbon content, Langmuir-Hinshelwood kinetics.

Acknowledgement

I would like to extend my deepest appreciation and gratitude to my supervisors, Dr. Ajay K. Ray and Dr. Shahzad Barghi, for their continuous encouragement, constructive criticism, enthusiastic guidance, support and understanding throughout my doctoral program. Besides, I have been extremely fortunate to work with them during this important period of my life and have them as one of the best examples for my future research and career.

My gratitude is also extended to the University of Western Ontario for the financial support of the research program. I gratefully acknowledge the faculty of Engineering Science in the University of Western, Ontario for the WGRS.

My sincere thanks to my advisory committee members, Dr. Gomaa and Dr. Bassi for being there to support and constructively criticise my work, which lead me to this final stage.

I am also thankfully acknowledging University Machine Services, Information Technology Service and Engineering Financial store. Moreover, the anytime advice and support from Mr. Pastor, Mr. Souheil Afara, Mr. Brian Dennis and Mr. Joel Eckert are greatly appreciated. I have been fortunate to have friendly colleagues, who made these four years of research quite enjoyable and memorable. I greatly appreciate their friendships.

Last but not the least, I would like to thank my parents for all their guidance and support, which made me achieve all my goals, till now. All my honours are dedicated to my parents. Without, their encouragement, moral support, love, trust and guidance any accomplishment would not have been possible. I owe everything that I am and would be in the future to my friends, philosophers and guides of my life, my parents.

Contents

CERTIFICATE OF EXAMINATION	ii
Abstract.....	iii
Acknowledgments.....	v
Table of Contents.....	vi
List of Tables.....	xiv
List of Figures.....	xv
List of Appendices.....	xix
Chapter 1.....	1
1 « Introduction ».....	1
1.1 « Scopes and Objectives ».....	3
Chapter 2.....	6
2 « Literature review ».....	6
2.1 « Photocatalyst and its functions ».....	7
2.2 « TiO ₂ as photocatalyst ».....	8
2.3 « Modes of TiO ₂ addition ».....	10
2.4 « Factors influencing photocatalytic degradation ».....	11
2.4.1 « Effect of pollutant concentration ».....	11
2.4.2 « Effect of TiO ₂ loading ».....	12
2.4.3 « Effect of different type of catalysts ».....	13
2.4.4 « Effect of pH ».....	13

2.4.5 « Light sources ».....	15
2.4.5.1 « Solar vs UV ».....	16
2.4.6 « Effect of light intensity and radiation time ».....	16
2.4.7 « Substrate catalyst / liquid catalyst illumination ».....	17
2.4.8 « Effect of naturally occurring ions and solvents ».....	18
2.5 « Methods of increasing TiO ₂ efficiency ».....	18
2.5.1 « Polymer/TiO ₂ complex ».....	18
2.5.2 « Doping of TiO ₂ ».....	19
2.6 « Immobilization of catalyst ».....	20
2.7 «Physical and chemical properties of polymers».....	21
2.7.1 « Polyvinyl alcohol ».....	21
2.7.2 « Gelatin ».....	22
2.7.3 « Polyvinylpyrrolidone ».....	22
2.8 « Types of water pollutants and their effects ».....	22
2.8.1 « Organic water pollutants ».....	23
2.9 « Photodegradation of methyloange and aspirin ».....	27
2.10 « Mineralization of pollutants and analysis of end product ».....	27
2.11 « References ».....	30
Chapter 3.....	35
3 « Experimental summary ».....	35
3.1 « Materials and Methods ».....	35
3.1.1 « Materials ».....	35
3.1.1.1 « Polyvinyl alcohol».....	35
3.1.1.2 « Gelatin ».....	36
3.1.1.3 « Polyvinyl pyrrolidone ».....	37

3.1.2 « Methods ».....	38
3.1.2.1 « Preparation of TiO ₂ -polymeric photocatalyst ».....	38
3.1.2.2 « Photodegradation of Methyl orange ».....	39
3.1.2.3 « Photodegradation of aspirin ».....	40
3.1.2.4 « Photodegradation of methyl orange in large scale reactor ».....	41
3.1.2.5 « Reactor setup ».....	42
3.1.2.6 « Advantages and Disadvantages of reactor ».....	43
3.1.2.7 « Instrumental analysis ».....	43
3.2 « Nomenclature ».....	44
3.3 « References ».....	44
Chapter 4.....	45
4 « Preparation and characterization of TiO ₂ -polymeric film photocatalysts ».....	45
4.1 « Introduction ».....	45
4.2 « Materials and Methods ».....	47
4.2.1 « Materials ».....	47
4.2.2 « Methods ».....	47
4.2.2.1 « Preparation of TiO ₂ -PVP composite ».....	47
4.2.2.2 « Preparation of coating ».....	48
4.2.2.3 « Immobilization ».....	48
4.2.2.4 « Preparation of polymeric-TiO ₂ film ».....	48
4.2.2.5 « C-L methods ».....	49
4.2.2.5.1 « Freeze-dried ».....	49
4.2.2.5.2 « Heat treated ».....	50
4.2.2.5.3 « Aldehyde treated ».....	51
4.2.2.5.4 « UV treated ».....	52

4.2.2.5.5« Freedried/UV treated».....	52
4.2.2.5.6 «Characterization of film catalyst ».....	53
4.2.2.5.7 « Photocatalytic efficiency».....	53
4.3 « Results and Discussions ».....	54
4.3.1 « Analysis of optical microscopy ».....	54
4.3.2 «Analysis of SEM images ».....	55
4.3.3 « Degradation of acetylsalicylic acid ».....	58
4.4 « Conclusions ».....	61
4.6 « References ».....	63
Chapter 5.....	64
5 « Photodegradation of MeO under UV light ».....	64
5.1« Introduction ».....	64
5.2« Experimental ».....	67
5.2.1« Materials».....	67
5.2.2 « Preparation of TiO ₂ -polymeric film ».....	67
5.2.3 « Immobilization ».....	68
5.2.4 « Activity test ».....	68
5.2.5 « Photocatalytic efficiency ».....	68
5.3 « Results and discussions ».....	69
5.3.1 « SEM analysis ».....	69
5.3.2 « Blank experiment ».....	70
5.3.3 « Effect of flow rate».....	71
5.3.4 « Photodegradation of MeO ».....	72
5.3.5 « Effect of initial concentration ».....	74
5.3.6 « Kinetic study ».....	76

5.3.7 « TOC ».....	78
5.3.8 « Effect of pH ».....	78
5.3.9 « Effect of light intensity ».....	82
5.4 « Conclusions ».....	85
5.5 « Nomenclature ».....	86
5.6 « References ».....	87
Chapter 6.....	89
6 « Photodegradation of aspirin under solar and UV light by slurry TiO ₂ ».....	89
6.1« Introduction ».....	89
6.2 « Materials and Methods ».....	91
6.2.1 « Materials ».....	91
6.2.2 « Methods ».....	91
6.2.2.1 « Blank reaction ».....	91
6.2.2.2 « Photodegradation of aspirin under UV lamp ».....	91
6.2.2.3 « Photodegradation under solar stimulator ».....	92
6.3« Results and Discussions ».....	92
6.3.1« Photodegradation under UV light ».....	92
6.3.1.1« Rate constant ».....	92
6.3.1.2 « Effect of initial concentration ».....	93
6.3.1.3 « Effect of catalyst loading ».....	94
6.3.2 « Photodegradation under solar lights ».....	95
6.3.2.1 « Calculation of rate constant ».....	95
6.3.2.2 « Effect of initial concentration ».....	96
6.3.2.3 « Kinetic study ».....	97
6.3.2.4 « Effect of catalyst loading ».....	98

6.4 « Conclusions ».....	99
6.5 « Nomenclature ».....	99
6.6 « References ».....	100
Chapter 7.....	101
7 « Degradation of aspirin under solar and UV lights in presence of TiO ₂ -polymeric ».....	101
7.1 « Introduction ».....	101
7.2 « Materials and Methods ».....	102
7.2.1 « Materials ».....	102
7.2.2 « Methods ».....	102
7.2.2.1 « Preparation of photocatalyst ».....	102
7.2.2.2 « Experimentation under UV lamp ».....	102
7.2.2.3 « Experiment under solar lamp ».....	103
7.3 «Results and Discussions ».....	103
7.3.1 « Photodegradation under UV lamp ».....	103
7.3.1.1 « Effect of initial concentration ».....	103
7.3.1.2 « Kinetic study ».....	104
7.3.1.3 « Effect of Light intensities ».....	106
7.3.1.4 « Effect of catalyst loading ».....	107
7.3.1.5 « Effect of film thickness ».....	108
7.3.2 « Photodegradation under solar lights ».....	109
7.3.2.1 « Effect of initial concentration ».....	109
7.3.2.2 « Kinetic study».....	111
7.3.2.3 « Effect of catalyst loading ».....	112
7.3.2.4 « Effect of film thickness ».....	113

7.3.2.5 « Effect of pH ».....	114
7.3.2.6 « Effect of light intensities ».....	117
7.4 « Conclusions ».....	118
7.5 « Nomenclature ».....	119
7.6 « References ».....	120
Chapter 8.....	121
8 « Mechanism of aspirin degradation under solar light in presence of TiO ₂ /polymeric ».....	121
8.1 « Introduction ».....	121
8.2 « Materials and Methods ».....	123
8.2.1 « Materials ».....	123
8.2.2 « Methods ».....	123
8.2.2.1 « Photocatalyst preparation ».....	123
8.2.2.2 « Photodegradation and analysis ».....	123
8.2.2.3 « Fourier transform infra-red ».....	124
8.2.2.4 « High performance liquid chromatography ».....	124
8.3 « Results and Discussions ».....	125
8.3.1 « Assumption of reaction mechanism ».....	126
8.3.2 « Pathways of aspirin degradation ».....	129
8.4 « Conclusions ».....	131
8.5 « Nomenclature ».....	132
8.6 « References ».....	133
Chapter 9.....	134
9 « Photodegradation of MeO in large scale continuous reactor under LED lights in presence of TiO ₂ /polymeric film ».....	134
9.1 « Introduction ».....	134

9.2 « Materials and Methods ».....	136
9.2.1 « Materials ».....	136
9.2.2 « Methods ».....	136
9.2.2.1 « Photodegradation of MeO under LED lights ».....	136
9.2.2.2 « Preparation of photocatalyst ».....	137
9.2.2.3 « Blank reaction ».....	138
9.3 « Results and Discussions ».....	138
9.3.1 « Photocatalytic oxidation ».....	138
9.3.2 « Effect of flow rates ».....	138
9.3.3 « Photodegradation of MeO under LED lights ».....	139
9.3.4 « Effect of initial concentration ».....	140
9.3.5 « Kinetic study ».....	142
9.3.6 « TOC ».....	143
9.4 « Conclusions ».....	144
9.5 « Recommendations ».....	145
9.6 « Nomenclature ».....	145
9.6 « References ».....	146
Chapter 10.....	147
10 « Final Conclusions ».....	147
Appendices.....	149
Curricular Vitae.....	159

List of Tables

Table 5.1.....	78
Table 8.1.....	126
Table 8.2.....	131
Table 9.1.....	144

List of Figures

Figure 1.1: Photocatalysis by TiO ₂	3
Figure 2.1: Mechanism of TiO ₂ as photocatalyst.....	9
Figure 2.2: Structure of methyl orange in alkaline pH.....	24
Figure 2.3: Structure of methyl orange in acidic pH.....	24
Figure 2.4: Structure of aspirin.....	25
Figure 2.5: Thesis outline.....	29
Figure 3.1: Structure of Polyvinyl alcohol.....	36
Figure 3.2: Structure of Gelatin.....	37
Figure 3.3: Structure of Polyvinyl pyrrolidone.....	38
Figure 3.4: Photodegradation of MeO under UV lights.....	39
Figure 3.5: Aspirin photodegradation.....	40
Figure 3.6: MeO photodegradation under LED lights.....	41
Figure 3.7: Reactor setup.....	42
Figure 4.1: Structure of aspirin.....	45
Figure 4.2: TiO ₂ /PVP photocatalyst.....	48
Figure 4.3: Freeze-drying photocatalyst.....	50
Figure 4.4: Heat treated photocatalyst.....	51
Figure 4.5: Aldehyde treated photocatalyst.....	51
Figure 4.6: UV treated photocatalyst.....	52
Figure 4.7 Freeze-dried/UV treated photocatalyst.....	53
Figure 4.8: Optical microscopy of photocatalysts.....	54

Figure 4.9: SEM images of Freeze-dried photocatalyst.....	56
Figure 4.10: SEM of heat treated photocatalyst.....	56
Figure 4.11: SEM of UV treated photocatalyst.....	57
Figure 4.12: SEM of UV treated/freeze dried.....	57
Figure 4.13: SEM of aldehyde treated.....	58
Figure 4.14:Effect of C-L on the aspirin degradation under UV.....	59
Figure 4.15: Effect of C-L on aspirin degradation under solar light.....	60
Figure 5.1: Structure of MeO.....	64
Figure 5.2: SEM of TiO ₂ /polymeric photocatalyst.....	70
Figure 5.3: Dark reaction of MeO.....	71
Figure 5.4: Effects of flow rates	72
Figure 5.5: Photodegradation of MeO under UV lamp.....	73
Figure 5.6: Effect of initial concentration.....	75
Figure 5.7: Plot of r_0^{-1} Vs C_0^{-1}	77
Figure 5.8:Effect of pH.....	80
Figure 5.9: Effect of pH.....	80
Figure 5.10: Effect of pH.....	81
Figure 5.11: Effect of pH.....	81
Figure 5.12: Effect of pH.....	82
Figure 5.13:Effect of light intensity.....	83
Figure 5.14: Effect of light intensity.....	83
Figure 5.15: Effect of light intensity.....	84
Figure 5.16: Effect of light intensity.....	84
Figure 6.1: Photodegradation of aspirin with slurry.....	92
Figure 6.2: Effect of initial concentration.....	93

Figure 6.3: Plot of $1/r_0$ Vs $1/C_0$	94
Figure 6.4: Effect of catalyst loading.....	95
Figure 6.5: Photodegradation of aspirin under solar light.....	96
Figure 6.6: Effect of initial concentration.....	97
Figure 6.7: Plot of $1/r_0$ Vs $1/C_0$	97
Figure 6.8: Effect of catalyst loading.....	98
Figure 7.1: Effect of initial concentration.....	104
Figure 7.2: Degradation of aspirin under UV.....	105
Figure 7.3: Plot of $1/r_0$ Vs $1/C_0$	105
Figure 7.4: Effect of light intensity.....	106
Figure 7.5: Effect of light intensity.....	107
Figure 7.6: Effect of catalyst loading.....	108
Figure 7.7: Effect of film thickness.....	109
Figure 7.8: Effect of initial concentration.....	110
Figure 7.9: Aspirin degradation under solar light.....	111
Figure 7.10: Plot of $1/r_0$ Vs $1/C_0$	112
Figure 7.11: Effect of catalyst loading.....	113
Figure 7.12: Effect of film thickness.....	114
Figure 7.13: Effect of pH.....	115
Figure 7.14: Effect of light intensity.....	117
Figure 7.15: Effect of light intensity.....	118
Figure 8.1: FTIR spectrum.....	128
Figure 9.1: Structure of MeO.....	134
Figure 9.2: Photodegradation of MeO.....	137
Figure 9.3: Effect of flow rates.....	139

Figure 9.4: Photodegradation of MeO.....	140
Figure 9.5: Effect of initial concentration.....	141
Figure 9.6: Photodegradation by LED lights.....	142
Figure 9.7: Plot of $1/r_0$ Vs $1/C_0$	143

List of appendices

Appendix I: Photodegradation of methyl orange under UV light in presence of TiO ₂ /polymeric film.....	149
I.1 « Calculation of residence time ».....	149
I.2 « Calculation of total organic carbon content ».....	149
Appendix II: Photodegradation of aspirin with slurry TiO ₂ under both solar and UV lights.....	150
II.1 « Dark reactions ».....	151
Appendix III: Photodegradation of aspirin under solar and UV light in presence of TiO ₂ /polymeric film.....	152
III.1 « Dark reactions ».....	153
Appendix IV: Mechanism of aspirin degradation under solar light.....	154
IV.1 « LC/MS Analysis ».....	154
IV.2 « Total organic carbon content ».....	157
Appendix V : Photodegradation of MeO in large scale continuous flow reactor under LED lights.....	158
V.1 Calculation of residence time.....	158
V.2 Total organic carbon content.....	159

Chapter 1

Introduction

Environmental contamination, which is growing around the world, is a serious problem not to be neglected. Among all contaminations, water pollution is a major problem. One of the most pressing environmental issues of the present and most probably the future is the effective protection and utilization of the precious fresh water resources of the world. 88% of the 4 billion annual cases of diarrheal disease are attributed to unsafe water and inadequate sanitation and hygiene, and 1.8 million people die from diarrheal diseases each year, all over the world [1]. The WHO estimates that 94% of these diarrheal cases are preventable through modifications to the environment, including access to safe water. As a consequence of human activities, organic compounds are often present as pollutants in waste water. Water pollution occurs when a body of water is adversely affected due to the addition of large amounts of materials to the water. When it is unfit for its intended use, water is considered polluted. Two types of water pollutants exist; point source and nonpoint source. Point sources of pollution occur when harmful substances are emitted directly into a body of water. A nonpoint source delivers pollutants indirectly through environmental changes. The technology exists for point sources of pollution to be monitored and regulated. Nonpoint sources are much more difficult to control. The pollution which is arising from the non-point sources accounts for a majority of the contaminants in streams and lakes [2]. It is necessary to remove these contaminants to protect our water resources to produce water of desired quality. Many treatment technologies have been developed over the years and are currently being employed to remove these contaminants (dyes, pesticides, drugs) or degrade them into non-toxic ones. Azo dyes are one of the largest groups of pollutants found in the drinking water, coming from, and the food and textile industries. Many studies indicate that these dyes are toxic or carcinogenic [3]. If these dyes come in contact with certain drugs in the human body they can induce allergic and asthmatic reactions. Physical, chemical and biological treatment technologies are currently applied to degrade these pollutants. Unfortunately, many types of organic pollutants in water are not removable by those

conventional technologies. Advanced oxidation processes (AOPs) show the potential to become a preferred future treatment technology, attributed to their capability of completely degrading almost all organic pollutants into the ultimate products (carbon-dioxide and water). Currently the main disadvantage of AOPs is their high cost. Among all the AOPs, photo catalytic oxidation (PCO) is the most promising one [4]. Photo catalytic oxidation is a process where degradation of organic compounds occur by the illumination of photo catalyst without introducing any other chemicals. Under such circumstances, it can be concluded that a new material is needed to degrade the contaminants into non-toxic products by using UV lamps and solar light. A novel Polymeric-TiO₂ film was synthesized, which not only immobilizes the TiO₂ in the cross-linked polymer fibres but also efficient enough to degrade organic pollutants (e.g. Methyl orange and Aspirin), both under solar and UV lights. Both batch and continuous flow reactors have been tested in these studies. Rates of photodegradation of Methyl orange and Aspirin under the solar light were observed to be higher than under UV lights, which can be explained due to the photocatalysts unique nature. The exposure of the photocatalyst film to the UV light cures the polymeric substrate, which in turn makes the interstitial TiO₂ particles unavailable for the reaction. The methyl orange decolourization was about 100% and the decrease in carbon content was measured by TOC. Though other researchers reported decolourisation of the dye by different sources of light, they have not studied the carbon content of the degraded samples [5]. The photocatalytic efficiency was 85%. The aspirin photodegradation has also been observed to have higher rates under solar light than the UV. The effects of initial concentration, flow rates, pH, catalyst loading, thickness of film photocatalyst and light intensities have been studied. Increase of initial concentration increased the rate initially which decreased on further increase of concentration. Increase of flow rates showed diminishing effects of mass transfer limitations, on the degradation rates. Acidic and alkaline pH changed the surface charges on both TiO₂ particles and the organic pollutant, which in turn varied the degradation rates. It was observed that increase of the TiO₂ amount also affected the degradation rates. It was also observed that the increased photocatalyst film thickness decreased the degradation rate. The instrumental analysis (HPLC, LC/MS, TOC, and FTIR) of the photo degraded samples of aspirin and methyl orange showed the mechanism of the

degradation reactions. These principles were applied in a large-scale reactor, where methyl orange was degraded in presence of visible LED lights and the effects of flow rates and initial concentrations were studied.

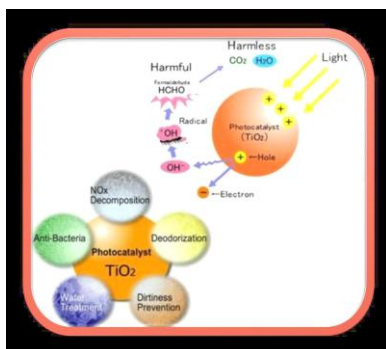


Figure 1.1: Photocatalysis by TiO₂ [6]

1.1 Scopes and Objectives

In our study, a two-phase swirl-flow monolithic-type photocatalytic reactor and a batch reactor were used to investigate the kinetics of heterogeneous photocatalytic degradation of Methyl orange and Aspirin respectively in presence of polymeric-TiO₂ film photocatalyst under ultraviolet as well as visible light illumination.

This thesis has nine chapters. Following the introduction in this chapter, detailed literature review about photocatalysis is provided by chapter 2. In chapter 3, experiment details are illustrated, including experimental set-up, photocatalytic reactor structure and methodology of experiments. Chapter 4 presents the preparation and characterization of TiO₂/polymeric film photocatalysts. Chapter 5 presents results and discussion of the photocatalytic degradation of methyl orange under UV light. Detailed experiments were conducted to study the effects of various operating parameters on the photocatalytic degradation performance. Photocatalytic kinetic models are developed and the kinetic parameters are obtained. Chapter 6 deals with the photocatalytic degradation of Aspirin

under visible and UV illumination with suspended catalysts. While, chapter 7 presents results in presence of TiO₂/polymeric film. Chapter 8 describes mechanism of aspirin degradation under solar light. Chapter 9 presents some results for photo-degradation of Methyl orange in a large-scale continuous reactor under LED lights in presence of TiO₂/polymeric film. Finally, chapter 10 summarizes conclusions reached as a result of this study and some recommendations for further studies.

1.2 References

1. Terry, LA Water Pollution, Environ. Law practice, 4, (1996), 19-29.
2. Poppe, Wayne, Hurst, Renee, Water qual. Int., (1997), 37-39.
3. Richman, M Ind. Wastewater, 5, (1997), 24-29.
4. Tibbetts, J Anon. Water Environ. Solns. 9, (1996), 5-7.
5. M. N. Rashed, A. A. El-Amin, Int. J. of Phys. Sc.,2, (2007), 073-081.
6. Tomorrow Nano Science and Technology Ltd,
<http://0769mt.en.alibaba.com/product/286574840-> Retrieved Dec. 2009.

Chapter 2

Literature Review

Approximately, 14,000 people die because of the water pollution, everyday all over the world. According to official classification, 41.3% of the United States' water is polluted [1]. China is the latest victim of impure water tragedies. The environment is extremely fragile. Recent pollution offenses include mountaintop mining in the Appalachians, oil drilling at both the Arctic and Antarctic poles which results in massive wildlife death, and oil spills that sicken people, as was recently the case in United States [2]. Canada flushes some 200 billion liters of raw sewage directly into natural waterways every year, from the St. Lawrence River to the Strait of Juan de Fuca and the Pacific Ocean [3]. Scientists detected the traces of prescription drugs in the water that comes from many people's faucets. "Everything from antidepressants to heart medication to birth control pills to caffeine" has been found in the drinking water all over the world [4]. A vast array of pharmaceutical products, including antibiotics, anti-convulsants, mood stabilizers and sex hormones — have been found in drinking water supplies of at least 41 million Americans, as shown in Associated Press investigation. To be sure, the concentrations of these pharmaceuticals are tiny, measured in quantities of parts per billion or trillion, far below the levels of a medical dose. It has been proved by scientists that the traces of these drugs can cause several health problems to both human and wild life [5]. These, organic pollutants are not completely removable by traditional water treatment technologies like Distillation, reverse osmosis, ion-exchange, carbon adsorption, micro porous membrane filtration. Distillation and reverse osmosis remove a wide range of water supply contaminants. However, one of their major disadvantages is that they also remove the good stuff - that is, the trace mineral elements (heavy metals e.g. copper, zinc, iron) that are also present in water and vital to human health [6]. The premier activated carbon water filter on the market would not strip away these organic pollutants completely, either. Therefore, advanced oxidation processes have been introduced, to degrade these pollutants in water. Advanced Oxidation Processes (abbreviation: AOPs), refers to a set of chemical treatment procedures designed to remove organic and inorganic materials in

waste water by oxidation. In AOPs, the OH radicals are produced in the solution which helps in degradation of the organic pollutant. In recent years, different oxidation processes, which produce OH radicals, e.g. O₃/UV, O₃/H₂O₂ and UV/H₂O₂, photocatalytic oxidation etc., have been applied in wastewater treatment [7]. Among all kind of advanced oxidation processes, photocatalytic oxidation is the most promising one. In recent years, photocatalytic degradation mediated by illuminated TiO₂ has received considerable attention as an alternative for treating polluted water. The semiconductor photocatalytic process is based on aqueous phase hydroxyl radical chemistry and couples low energy UV–A Light with semiconductors acting as photocatalyst. It has been proved that this process can degrade many toxic compounds in waste water into carbon dioxide and water. The most suitable semiconductor for the photocatalytic reaction is TiO₂ [8].

2.1. Photo-catalyst and its functions

Photo-catalyst activated by UV lights can oxidize organic pollutants into non-toxic materials, such as carbon dioxide, water and also disinfect certain bacteria. Photo-Catalysis is defined as "acceleration of photoreaction in presence of a catalyst". A catalyst does not change in itself or being consumed in the chemical reaction. In catalyzed photolysis, light is absorbed by an adsorbed substrate. In photo generated catalysis the photo catalytic activity (PCA) depends on the ability of the catalyst to create electron–hole pairs, which generate free radicals (hydroxyl radicals: OH) able to undergo secondary reactions. Its comprehension has been made possible ever since the discovery of water electrolysis by means of the titanium dioxide [9]. In photo catalytic oxidation (PCO) process, it is generally conceded that the semiconductor photo-catalysts can act as sensitizers for light-induced redox processes, due to the electronic structures of these photo-catalysts that are characterized by a filled valence band and an empty conduction band [2, 7, 9]. Adsorption of a photon of energy greater than the band gap energy leads to the formation of an electron/photo hole pair. In the absence of suitable scavengers, the stored energy is dissipated within few nanoseconds by recombination. If a suitable scavenger or surface defect state is available to trap the electron or the photo-hole, the recombination is prevented and subsequent redox reaction may occur. The valence band holes are powerful oxidants (+1.0 to +3.5V), while the conduction band electrons are

good reductant (+0.5 to -1.5V). Most organic photo degradation reactions utilize the oxidizing power of the holes either directly or indirectly. The interaction of the positive holes or the negative electrons with the absorbed organic pollutants can give rise to unstable intermediates which are further attacked by hydroxyl or proxy species occasioning a carbon-carbon bond rupture (or aromatic ring opening) with concomitant release of low molecular weight products which may in turn be further oxidized to CO₂. The attacking hydroxyl radical presumably comes from the photo splitting of water by photo generated hole. Alternatively, the peroxy radical may come from the protonation of a superoxide anion, O₂⁻ produced from electron uptake of dissolved O₂. Among all semiconductors photo-catalysts studied including TiO₂, ZNO, Fe₂O₃, CdS and ZNS most researchers focused on TiO₂ because of its low cost and relatively high photo-catalytic activity, as well as its chemical stability in aqueous systems [8, 9]. As the band gap energy of TiO₂ is about 3.0-3.2 eV, only the light that have short wavelength within the UV range (< 380nm) are powerful enough to activate the photo catalytic reaction. As a result, the high cost associated with the generation and supply of UV light from electricity has constituted one of the major drawbacks hindering the commercial application of the current photo catalytic oxidation technology in actual water and wastewater treatment. A solution to this problem may resort to the utilization of the solar energy that is naturally available [8-10]. However, the UV light only accounts for about 3-4% of the sunlight. It is therefore of great use to develop photo-catalysts that can work under sunlight.

2.2 TiO₂ as photo catalyst

Titanium Dioxide has proved itself to be the most efficient semi-conductor available for photocatalysis. Indeed there are already a large number of commercial photocatalytic TiO₂ products available [4, 5]. TiO₂ is available in 3 forms-anatase, rutile and brookite. Degussa is a mixture of anatase and rutile form with higher efficiency. The high activity is due to the more positive conduction band of anatase and the light promoted e⁻ may pass from rutile to anatase phase enhancing the separation of h⁺ and e⁻. There is a great deal of research currently trying to improve the photocatalytic potential of titanium dioxide, both in effectiveness and in trying to expand the light spectrum with which it reacts into the

visible range. The most common technique currently tried is to dope titanium dioxide with another element and more recently two elements, co-doping has been tried. However, many factors, within the preparation process of photocatalyst affect the degradation reactions. The basic process of photo catalysis consists of ejecting an electron from the VB (Valence band) to conduction band of the TiO₂ semi-conductor creating an “h_{vb}⁺” hole in the valence band. This is due to UV irradiation of TiO₂ with an energy equal/superior to the band gap (> 3.2 eV)

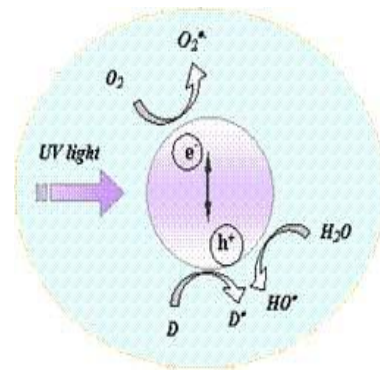
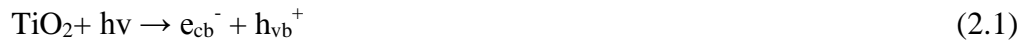
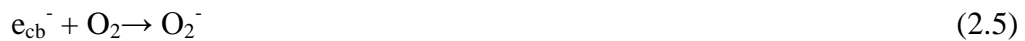


Figure 2.1: TiO₂ as photocatalyst [10]

This is followed by the formation of extremely reactive radicals (like OH[•]) at the semi-conductor surface and a direct oxidation of the polluting species.



The ejected electron reacts with the electron acceptors such as O₂ absorbed or dissolved in H₂O



Also the electron and holes may recombine together without electron donor or acceptors



In general, the goal of the application of photocatalysis in water treatment is the transformation, deactivation and finally mineralization of environmentally persistent compounds [11, 12].

2.3 Modes of TiO₂ addition

In photocatalytic degradation using TiO₂, two modes of TiO₂ application are adopted: (1) TiO₂ immobilized on rigid inert support materials, e.g., quartz sand, glass, glass wool matrix, ceramic membrane, noble metal, carbon fibres etc., and (2) TiO₂ suspended in aqueous medium [13,14]. In terms of technical application, immobilized TiO₂ is preferable [15] compared to dispersed TiO₂ because it does not need additional post-treatment for the recovery of catalyst particles after oxidation.

In large-scale applications, however, the catalyst particles must be filtered prior to the discharge of the treated water, even though TiO₂ is harmless to the environment. Hence, a liquid-solid separator must follow the slurry reactor. The installation and operation of such a separator will raise the cost of the overall process because the separation of the ultrafine catalyst particles is a slow and expensive process. Besides, the penetration depth of the UV light is limited because of the strong absorption by TiO₂ and dissolved organic species, particularly for dyes. All of these disadvantages render the scale-up of a slurry reactor very difficult. The preceding problem can be eliminated by immobilizing the TiO₂ catalyst over suitable supports [16]. The immobilization has a few advantages over slurry system. First, they eliminate the need for the ultra fine expensive filtration system for separation of the catalyst particles from the treated liquid and enable the contaminated water to be treated continuously. However, immobilization of TiO₂ on supports also creates its own problems [17]. At least two obvious problems have been reported to arise from this arrangement: the accessibility of the catalytic surface to the photons and the reactants and a significant influence of the external mass transfer particularly at low fluid flow rate, because of the increasing diffusional length of the reactant from bulk solution to the catalyst surface [17]. On the other hand, with an increase of the catalyst film thickness, it has been reported that the internal mass transfer might play a dominant role

by limiting the utilization of the catalyst near the support surface. All of these usually led to a lower overall degradation rate when the catalyst is immobilized compared with the suspended system [16, 17].

2.4 Factors influencing the photocatalytic degradation

2.4.1 Effects of pollutant concentration

It is important both from a mechanistic and from an application point of view to study the dependence of the photocatalytic reaction rate on the substrate concentration. It is generally noted that the degradation rate increases with the increase of dye concentration to a certain level and a further increase in dye concentration leads to decrease the degradation rate of the dye [18, 19]. The rate of degradation relates to the probability of $\bullet\text{OH}$ radicals formation on the catalyst surface and to the probability of $\bullet\text{OH}$ radicals reacting with dye molecules. With the increase in initial concentrations of the dye, the increase in the probability of reaction between dye molecules and oxidizing species also increases, which leads to an enhancement in the decolourization rate. On the contrary, the degradation efficiency of the dye decreases as the dye concentration increases further. The presumed reason is that at high dye concentrations the generation of $\bullet\text{OH}$ radicals on the surface of catalyst are reduced since the active sites are covered by dye ions [19]. Another possible cause for such results is the UV-screening effect of the dye itself. At a high dye concentration, a significant amount of UV may be absorbed by the dye molecules rather than the TiO_2 particles and that reduces the efficiency of the catalytic reaction because the concentrations of $\bullet\text{OH}$ and $\text{O}_2\bullet^-$ decrease [20 - 25]. The major portion of degradation was reported to occur in the region near to the irradiated side (termed as reaction zone) where the irradiation intensity was much higher than in the other side [26]. Thus at higher dye concentration, degradation decreased at sufficiently long distances from the light source or the reaction zone due to the retardation in the penetration of light. Hence, it was concluded by researchers that as initial concentration of the dye increased, the requirement of catalyst surface needed for the degradation also increased [27]. In case of other organic compounds, the photonic efficiency increased as

the initial concentration of organic pollutant concentration was raised up. As reported in several publications [4, 28, 29] the rate, and therefore the photonic efficiency (maximum numbers of photons adsorbed, which increased the e^- and h^+ formation, increasing the degradation in turn.), of the degradation process is a function of the initial pollutant concentration, at least in a certain concentration range, when other parameters, such as the concentration of molecular oxygen, the ionic strength, and the light intensity, were kept constant. The effect of the initial concentration of organic dyes on its initial degradation rate during UV-A illumination was investigated [4, 5, 6, 10, 28, and 29].

2.4.2 Effect of TiO_2 loading

Whether in static, slurry or dynamic flow reactors the initial reaction rates were reported to be directly proportional to catalyst concentration indicating the heterogeneous regime [30-33]. However, it was observed by researchers that above a certain level of concentration the reaction rate even decreased and became independent of the catalyst concentration [34]. Most of studies reported enhanced degradation rates for catalyst loading up to 400–500 mg/l [30-34]. Only a slight enhancement or decrease was observed when TiO_2 concentration further increased up to 2000 mg/l [35]. This can be rationalized in terms of availability of active sites on TiO_2 surface and the light penetration of photo activating light into the suspension. The availability of active sites increased with the increase of catalyst loading, but the light penetration, and hence, the photo activated volume of the slurry form of photocatalyst decreased, due to catalyst agglomeration. Agglomeration and sedimentation of the TiO_2 particles were observed elsewhere when 2000 mg/l of TiO_2 was added to the dye solution [35, 36]. In such a condition, part of the catalyst surface probably became unavailable for photon absorption and dye adsorption, thus bringing little stimulation to the catalytic reaction. On the contrary, continuous increase of the photocatalytic degradation rate of pollutant was found up to 3500 mg/l TiO_2 [37]. The crucial concentration of TiO_2 depends on the geometry, the working conditions of the photo reactor and the type of UV-lamp (power, wavelength). The optimum amount of TiO_2 has to be added in order to avoid unnecessary excess catalyst

and also to ensure better absorption of light photons for efficient photo mineralization. This optimum loading of photo catalyst was found to be dependent on the initial solute concentration [38].

2.4.3 Effect of different kinds of catalysts

Several researches have been carried out all around the world by applying different kind of doped, polymer complexed TiO₂ and also different forms of TiO₂. The photocatalytic degradation of methyl orange in aqueous solutions was examined by treating with slurry TiO₂, Hombikat UV 100, TiO₂ nano composites, TiO₂-FeZSM5 composite and also TiO₂ immobilized on carbon fibres, by several researchers. It has been reported by many researchers that Degussa is the most efficient form of TiO₂ [37-41].

2.4.4 Effect of pH

Although the pH can be one of the most important parameters for the photocatalytic process, its influence on the photocatalytic degradation has been investigated in detail only by a few research groups. The interpretation of pH effects on the efficiency of dye photodegradation process is a very difficult task because of its multiple roles. Firstly, it is related to the ionization state of the surface according to the following reactions. Also, related to that of reactant dyes and products such as acids and amines.



pH changes can thus influence the adsorption of dye molecules onto the TiO₂ surfaces, an important step reported by scientists [39-41] have already reviewed that acid-base properties of the metal oxide surfaces can have considerable implications upon their photocatalytic activity. The point of zero charge (pzc) of the TiO₂ (Degussa P25) is at pH 6.2 [42]. Thus, the TiO₂ surface is positively charged in acidic media (pH < 6.2), whereas

it is negatively charged under alkaline conditions ($\text{pH} > 6.2$). Second, hydroxyl radicals can be formed by the reaction between hydroxide ions and positive holes. The positive holes were considered as the major oxidation species at low pH whereas hydroxyl radicals were considered as the predominant species at neutral or higher pH levels [43, 44]. It was stated that in alkaline solution $\bullet\text{OH}$ radicals were easier to be generated by oxidizing more hydroxide ions available on TiO_2 surface, thus the efficiency of the process was logically enhanced [45-49]. Similar results were reported in the photocatalysed degradation of acidic azo dyes and triazine containing azo dyes [50, 51], although it should be noted that in alkaline solution there is a Coulombic repulsion between the negative charged surface of photocatalyst and the OH^- ion. Formation of more $\bullet\text{OH}$ and thus decreased the photooxidation. Very high pH has been found favourable even when anionic azo dyes should hamper adsorption on the negatively charged surface [56]. At low pH, reduction by electrons in conduction band may play a very important role in the degradation of dyes due to the reductive cleavage of azo bonds. Third, the TiO_2 particles tend to agglomerate under acidic condition and the surface area available for dye adsorption and photon absorption would be reduced [57]. Hence, pH played an important role both in the characteristics of textile waters and in the reaction mechanisms that can contribute to dye degradation, namely, hydroxyl radical attack, direct oxidation by the positive hole and direct reduction by the electron in the conducting band. The degradation rate of some azo dyes increased with decrease in pH as reported elsewhere [58]. At $\text{pH} < 6$, a strong adsorption of the dye on the TiO_2 particles was observed as a result of the electrostatic attraction of the positively charged TiO_2 with the dye. At $\text{pH} > 6.2$ as dye molecules were negatively charged in alkaline media, their adsorption is also expected to be affected by an increase in the density of TiO_2 . Thus, due to Coulombic repulsion the dyes were scarcely adsorbed [59]. For the above reasons the photocatalytic activity of anionic dyes (mainly sulphonated dyes) reached a maximum in acidic conditions followed by a decrease in the pH range 7–11 [55-60]. Moreover, the higher degradation rate at acid pH was seen also for Vis/ TiO_2 experiments due to the efficient electron-transfer process due to strong surface complex bond formation. This effect was less marked in neutral/basic pH solutions [61]. On the contrary, different optimal pHs [6, 7] have been observed for the photocatalytic degradation of other azo dyes, and a

decrease of degradation in both acidic and alkaline pH was reported [62 - 64]. The inhibitory effect seems to be more pronounced in the alkaline range (pH = 11–13). At high pH values the hydroxyl radicals were rapidly scavenged and they do not have the opportunity to react with dyes.

An additional explanation for the pH effects can be related with changes in the specification of the dye. That was, protonation or deprotonation of the dye can change its adsorption characteristics and redox activity [65]. Since the influence of the pH is dependent on dye type and on properties of TiO₂ surface therefore the effect on the photocatalytic efficiency must be accurately checked before any application.

2.4.5 Light sources

TiO₂ absorbs radiation below the visible range of light spectrum. Hence, photo activation of TiO₂ requires radiation with light of wavelength less than or equal to 384 nm, with an absorbance maximum at approximately 340 nm. The vast majority of studies quoted in the literature have been carried out between the wavelengths 320- 380 nm [10, 12, 15, 25, and 28]. The light that gives rise to the required radiation field can be produced by artificial lamps or by solar irradiation. In a photocatalytic reactor, UV-A (320-380 nm) radiation was provided by fluorescent low-pressure mercury lamps emitting low-intensity UV-A radiation. Medium pressure mercury lamps have also been used, which emit high intensity UV light in the short, medium and long UV spectrums. However, short (UV-C; 200-280 nm) and medium (UV-B; 280-320 nm) UV radiation emitted by the mercury were usually cut off by the transparent photo reactor material, unless it is made of quartz. Some studies had also reported increased efficiency with UV-C radiation than UV-A for the degradation of certain organic materials [77, 78]. Direct photolysis and the higher probability of trapping of electron-hole pairs with shorter wavelength excitation were thought to be the possible reasons for such an effect. It has been estimated that only 5% of the incident solar irradiation is of use for the TiO₂ band gap photocatalytic reaction. This significantly limits its practical application.

2.4.5.1 Solar Vs UV lamps

More significantly, the current photo catalytic oxidation processes generally applies the photo catalyst within the water medium, either in the suspended slurry or immobilized form. This has resulted in a major problem of low light utilization efficiency because UV light, attenuate very fast in water [79]. As a result, the prospect of direct use of natural sunlight as the sole energy source for photo catalytic reaction in water is greatly limited with the current status of photo catalytic technology. The preference to use solar or UV lamps as the irradiation source depends largely on light intensity and the cost of the light-producing or light collecting equipment. UV lamps are conventionally used for photocatalysis, but more efficient, longer life and safe UV light-emitting diodes (LEDs) are prospective replacements. The costs still remain a challenge, however, and much focus has been given to sunlight as the initiator of the photochemical reaction. Solar photochemical systems are based on the collection of only high-energy short-wavelength UV or near-UV sunlight (300–400 nm) to promote photochemical reactions especially with TiO_2 as the catalyst. A useful overview of solar photocatalysis was provided by a group of researchers [40-45]. Solar photocatalytic treatment with TiO_2 as a catalyst, however, poses some challenges. Solar photocatalysis uses only the UV portion of sunlight and as much as 50% or more of this may be present in diffused form. As would be expected, local variability in cloud cover and other factors may change actual levels. Even under the limitations of solar applications, by far the greatest advantages are the cleanness, cheapness, and abundance of the energy source.

2.4.6 Effect of light intensity and irradiation time

Ollis et al. [68] reviewed the studies reported for the effect of light intensity on the kinetics of the photocatalysis process and stated that (i) at low light intensities (0–7 mW/cm^2), the rate would increase linearly with increasing light intensity (first order), (ii) at intermediate light intensities beyond a certain value (approximately 17 mW/cm^2), the rate would depend on the square root of the light intensity (half order), and (iii) at high light intensities the rate is independent of light intensity. This might be likely because at

low light intensity reactions involving electron–hole formation are predominant and electron–hole recombination would be negligible. However, at increased light intensity electron–hole pair separation competes with recombination, thereby causing lower effect on the reaction rate. The enhancement of the rate of decolourization as the light intensity increased was also observed [67-69]. It was evident that the percentage of decolourization and photodegradation increased with increase in irradiation time. The reaction rate decreased with irradiation time since it followed apparent first-order kinetics and additionally a competition for degradation might occur between the reactant and the intermediate products [69]. The slow kinetics of dyes degradation after certain time limit was due to: (a) the difficulty in converting the N-atoms of dye into oxidized nitrogen compounds (b) the slow reaction of short chain aliphatic with •OH radicals, and (c) the short life-time of photocatalyst because of active sites deactivation by strong by-products deposition [100].

2.4.7 Substrate catalyst/ Liquid catalyst illumination

Experiments were performed to study the photocatalytic degradation rate when catalyst was immobilized either on the bottom plate or on the top plate [70, 71]. In the latter case, light intensity falling on the catalyst surface would be considerably reduced, as it would have to travel through the absorbing liquid medium. The two circumstances can be depicted as substrate-catalyst SC and liquid-catalyst LC illumination, depending on whether the catalyst is activated from the substrate side or from the liquid side.

SC Illumination:- In this case, light passes from the side of substrate to the catalyst film.

LC illumination:- In this case, the light passes through the liquid to the catalyst film. The light source can be positioned either on the top - LC illumination or at the bottom - SC illumination. Sequences of events have been postulated for photocatalytic degradation of benzoic acid under both SC and LC illumination [70]. It has been observed by researchers that SC illumination was more efficient as in LC illumination light gets absorbed by the liquid. It has been reported by a researcher [71], that an optimum catalyst layer thickness

existed for SC illumination, while the rate reached a saturation value for LC illumination, and increasing the catalyst layer thickness had no effect on the rate thereafter.

2.4.8 Effect of natural occurring ions and solvents

The occurrence of dissolved inorganic ions is rather common in dye-containing industrial wastewater. Often, wastewater contains a mixture of pollutants, organic solvents as well as dissolved organic matter and humic substances, if mixed with other waste streams. These substances may compete for the active sites on the TiO₂ surface or deactivate the photocatalyst and, subsequently, decrease the degradation rate of the target dyes. Alternatively, they may act as light screens, thus reducing the photon receiving efficiency. The photocatalytic degradation of different classes of dyes in presence of TiO₂ is reported to get slowed down by many commonly used industrial solvents and acids, as well as by many naturally abundant mineral species and dissolved organic matter. The retardation by humic substances might be by the combined effects of light attenuation, competition for active sites and surface deactivation. Finally, various solvents such as acetonitrile and ethanol were found to have a significant retardation effect on the photo bleaching of dyes even at low concentrations as it is also stated for phenols and aromatic products [72].

2.5 Methods of increasing TiO₂ efficiency

2.5.1 Polymer/TiO₂ complex

A polymer–metal complex is composed of synthetic polymer and metal ions bound to the polymer ligand by a coordinate bond. A polymer ligand contains anchoring sites like nitrogen, oxygen or sulphur obtained either by the polymerization of monomer possessing the coordinating site or by a chemical reaction between a polymer and a low molecular weight compound having the coordinating ability. The polymer–metal complexes may be classified into different groups according to the position occupied by the metal, which was decided by the method of preparation [72]. Various works on the

co-ordination complexes have revealed that the heterogeneous systems possess more economical potentials and advantages over homogeneous systems. In addition these TiO₂-polymer complexes were reported to help in ion selectivity in waste water treatment, recovery of trace metal ions, and hydrometallurgy are enlightened in the final part [72, 73]. Researchers showed how PVP affects the structure of TiO₂ - PVP composite which in turn affects the gelation time [73].

2.5.2 Doping of TiO₂ for better efficiency (Metal oxides)

Metal oxides of low band gap energy have been considered as the candidate photo catalyst for visible light activity, but many of these photo catalysts lose their photo catalytic activity fast and therefore are rarely used [9]. Recently attempts have been made to modify those metal oxides, particularly TiO₂, that are photo catalytically stable even though have large band gap energies. The modification has been done though doping TiO₂ with small amount of noble metals, other metal compounds or non-metals. When a small amount of a noble metal was doped into the TiO₂, the electrons and photo hole produced by the light irradiation were retained respectively on the noble metal and TiO₂ semiconductor because the noble metal trapped the electrons, which limited the recombination of the electrons and photo holes and thus improved the reactivity of the photo catalyst [65, 67]. However, through this approach, the large band gap of TiO₂ was not significantly reduced. Doping of TiO₂ with precious metal (Pt), metal oxides such as ZnO, Fe₂O₃ and inorganic components such as N for extended visible light activities has been successfully conducted [65-70]. A recent preliminary investigation by a team of researchers revealed a significant enhancement of visible light activity (up to 60-70% absorbance) by doping a combination of N and C or silver into TiO₂ in a nano sol-gel system. Many researchers had already reported that photo catalysts with visible light activity have only achieved light absorbance at < 30%. It has also been revealed that in surface modification and grafting technology through chemical oxidation or plasma treatment would serve as the basis for solving the challenge of immobilizing inorganic photo catalysts on inert substrates [74 - 77].

2.6 Immobilization of catalyst on organic or inorganic substrates

These micro or nano-sized catalysts are usually applied to water treatment directly in a form of suspension slurry. Although, researches showed that the reaction rates were high, in the slurry systems but it required the separation of these small catalysts particles from the treated slurry, which has been found to be difficult to accomplish and hence reduce the economical viability [23]. The immobilization of nano catalyst particles on macro supports is a process to solve the separation problem encountered in the slurry systems. To avoid the separation problem, photocatalyst particles have been immobilized onto macro supports. So far, the immobilization has been more successfully done on inorganic substrates such as metal tubes or glass plates [24-25], because the crystallization and immobilization reaction of TiO₂-based photocatalysts usually has to be conducted at a high temperature (300-400° C or higher). However, the use of an inorganic substrate has limited the possibility to make buoyant or floating photocatalysts, and the required high temperature reactions to be carried out. Studies have been carried out to immobilize the catalyst on a buoyant support that can float on the surface of water to effectively absorb the sunlight energy for the photo catalytic degradation of organic pollutants [73]. Immobilizations were carried out through sol-gel method at low temperature and also at elevated temperature. More preferably, the support materials should be selected from organic materials that can concentrate through sorption, the organic contaminants from water or waste water and thus enhance the photo catalytic degradation rate by providing sufficient organic compounds in contact with the catalyst particles. Organic support materials are readily available and cheap or can be easily recovered from plastic wastes. In another method of catalyst immobilization, inorganic substrate has been used and treated at elevated temperature as inorganic substrates can endure (300°- 400 °C) [74]. A new method for immobilization has been reported by researchers [75]. Several unique reaction processes has been developed to immobilize nano catalyst particles on polymeric substrates directly through the in-situ production of the nano catalyst particles at a moderately low temperature (150° C) [75].

2.7 Physical and chemical properties of polymers employed for photocatalyst preparation

2.7.1 Polyvinyl alcohol

Polyvinyl alcohol (synonyms, vinyl alcohol polymer, PVA) is a water-soluble synthetic resin, prepared by the polymerization of vinyl acetate, followed by partial or complete catalyzed hydrolysis. PVA is fully degradable and is a quick dissolver. PVA has a melting point of 230°C and 180° – 190°C for the fully hydrolysed and partially hydrolysed grades, respectively. It decomposes rapidly above 200°C as it can undergo pyrolysis at high temperatures. PVA is an atactic material but exhibits crystallinity as the hydroxyl groups are small enough to fit into the lattice without disrupting it. FDA has approved this polymer as additives in food and drugs [76].

2.7.2 Gelatin

Gelatin is a protein produced by partial hydrolysis of collagen extracted from the boiled bones, connective tissues, organs and some intestines of animals such as domesticated cattle, pigs, and horses. The natural molecular bonds between individual collagen strands are broken down into a form that rearranges more easily. Gelatin melts to a liquid when heated and solidifies when cooled again [77]. Together with water, it forms a semi-solid colloid gel. Gelatin forms a solution of high viscosity in water, which sets to a gel on cooling, and its chemical composition is, in many respects, closely similar to that of its parent collagen. Gelatin solutions show viscoelastic flow and streaming birefringence. Gelatin gels exist over only a small temperature range, the upper limit being the melting point of the gel, which depends on gelatin grade and concentration and the lower limit, the freezing point at which ice crystallizes.

2.7.3 Polyvinyl pyrrolidone

Polyvinylpyrrolidone (PVP), also called Polyvidone, is a water-soluble polymer made from the monomer N-vinylpyrrolidone [78]. PVP is soluble in water and other polar solvents. When dry it is a light flaky powder, which readily absorbs up to 40% of its weight in atmospheric water. In solution, it has excellent wetting properties and readily forms films. This makes it good as a coating or an additive to coatings [79].

2.8 Types of water pollutants and their effects

Water pollution is caused by different sources. Water bodies are getting polluted by microbes, chemicals, radioactive contaminants and metals [80].

Microbiological organisms in drinking water: Can cause gastrointestinal illnesses, legionnaire's disease and nausea. Examples of such organisms are cryptosporidium and giardia lamblia.

Inorganic chemicals: Potential health effects include learning disorders, kidney and liver damage. Examples of inorganic compounds are copper, lead and fluoride.

Inorganic chemicals in water : Potential health effects include learning disorders, kidney and liver damage. Examples of inorganic compounds are copper, lead and fluoride.

Organic chemicals in drinking water: Potential health effects include, Eye, kidney and liver damage as well as increased risk of cancer. Organic compounds include benzene, carbofuran and lindane.

Radioactive contaminants or radio nuclides: Most water supplies have very low levels of these contaminants. The ones that are present in your water are usually naturally occurring, but man-made radioactive contamination can occur. Increased risks of cancer and kidney toxicity are potential health hazards of these contaminants

2.8.1 Organic water pollutants

Textile dyes and other industrial dyestuffs constitute one of the largest groups of organic compounds that represent an increasing environmental danger. About 2–20% of the total world production of dyes are lost during the dyeing process and are released in the textile effluents [81]. The release of those coloured waste waters in the environment is a considerable source of nonaesthetic pollution and eutrophication and can originate dangerous by-products through oxidation, hydrolysis, or other chemical reactions taking place in the waste water treatment. Decolourization of dye effluents has therefore received increasing attention. For the removal of dye pollutants, traditional physical techniques (adsorption on activated carbon, ultra filtration, reverse osmosis, coagulation by chemical agents, ion exchange on synthetic adsorbent resins, etc.) can generally be used efficiently. Nevertheless, they are non-destructive, since they just transfer organic compounds from water to another phase, thus causing secondary pollution. Consequently, regeneration of the adsorbent materials and post-treatment of solid-wastes, which are expensive operations, are needed. Due to the large degree of aromatics present in dye molecules and the stability of modern dyes, conventional biological treatment methods are ineffective for decolourization and degradation [82]. Furthermore, the majority of dyes is only adsorbed on the sludge and is not degraded. Therefore several researches are ongoing by applying photo catalysis oxidation process to degrade these organic dyes in water.

Methyl orange is an organic dye used as pH indicator in titration. Many studies revealed the toxicity and carcinogenic nature of this dye. If this colorant comes in contact with certain drugs in the human body it can induce allergic and asthmatic reactions in sensitive people. An additional difficulty is that, when present, this dye is not removed normally by conventional waste water treatment systems. Therefore, the effluents must be treated before being released into water. In this research methyl orange has been used as a model compound. TiO_2 degrades organic pollutants in water. Methyl orange is an indicator in strong acid-weak base titrations. It changes from red (at pH 3.1) to orange-yellow (at pH 4.4). The colour of methyl orange changes because it absorbs light in the visible part of the electromagnetic spectrum. Its molecule contains an extended system of

delocalised electrons called chromophores. The differences in energy between the quantised electronic energy levels correspond to the energies of photons of visible light. Electrons are promoted when these photons are absorbed, removing their frequencies from those that enter the eye. In methyl orange, when the molecule becomes protonated in acidic solution, the differences in energy between the electron energy levels change slightly from the unprotonated form. This results in the absorption of different frequencies of visible light and so a change in colour of the indicator. Methyl orange in acidic solution absorbs blue-green light, which makes its solution appear red. In alkaline solution it absorbs blue-green and red light making it appears yellow [79]. Methyl orange is one of the indicators commonly used in titrations. In an alkaline solution, methyl orange is yellow and the structure is:

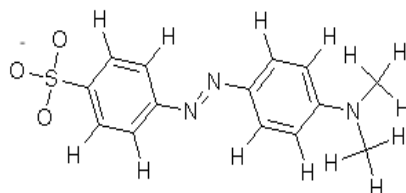


Figure 2.2: Structure of methyl orange in alkaline pH [81]

In fact, the hydrogen ion attaches to one of the nitrogen in the nitrogen-nitrogen double bond to give a structure which might be drawn like this:

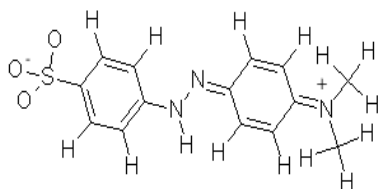


Figure 2.3: Structure of methyl orange in acidic pH [81]

Since, TiO_2 is known to possess positive surface charges at specific pH range (3 - 6.2). Also, TiO_2 shows zero charge at pH 6.3 and beyond this it possesses negative charges up to pH 14 [83]. The change in reactivity occurs due to the surface charge change with pH and methyl orange charge (acidic/alkaline). At low pH methyl orange has positive

charges and TiO₂ also possessing positive surface charges showed very less attraction or repulsion, while at pH 4.4-6.2 methyl orange having negative charges and TiO₂ surface carrying positive charges showed strong attraction beyond this point again weak attraction to repulsion occurs with the rise in pH [84].

NSAIDs are non steroidal anti-inflammatory drugs, used as pain killer, antipyretics and anti-inflammatory medicine. Aspirin, known as acetylsalicylic acid (ASA), is a commonly used Non-steroidal anti-inflammatory drug (NSAIDs) to relieve minor aches and pains. Aspirin was the first discovered member of the class of drugs known as non steroidal anti-inflammatory drugs (NSAIDs), not all of which are salicylates. Although they all have similar effects and most have inhibition of the enzyme cyclooxygenase as their mechanism of action. They are widely used for the treatment of inflammatory disorders and painful conditions such as rheumatoid arthritis, gout, bursitis, painful menstruation, and headache. They are effective in the relief of pain. It is also used as an antipyretic to reduce fever and as an anti-inflammatory medication. ASA can also be used during a heart attack to reduce the death risk.

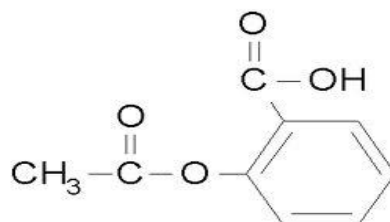


Figure 2.4: Structure of Aspirin [85]

The main undesirable side effects of aspirin are gastrointestinal ulcers, stomach bleeding, and tinnitus, especially in higher doses. Today, aspirin is one of the most widely used medications in the world, with an estimated 40,000 tonnes of it being consumed each year. Aspirin degrades in aqueous medium into several toxic intermediates causing environmental pollution and affect human health in several ways. Aspirin is a transparent, colourless, odourless crystals having solubility of 1g per 100ml of water at 37° Centigrade. Specific gravity of 1.40. Its boiling point is 130° Centigrade. Stable in dry air (hydrolyzes in moist air, decomposes in hot water) and have acidic pH [85].

NSAIDs inhibit the cyclooxygenase (COX) activity resulting in decreased synthesis of prostaglandin, leukotriene and thromboxane precursors such as the ubiquitous enzyme which catalyzes the initial step in the synthesis of prostanoids. Prostanoid is any of a group of C-20 fatty acids complex with an internal five or six carbon rings such as prostaglandins, prostanic acid, prostacyclins, and thromboxane; derived from arachidonic acid (C-20 polyunsaturated fatty acid with four cis double bonds). The action or the synthesis of prostanoids are involved in the modulation of a variety of patho-physiologic processes which include inflammation, hemostasis, thrombosis, cytoprotection, ulceration, hemodynamic and other the progression of kidney diseases. Thus, NSAIDs as non-selective inhibitors of the cyclooxygenases (both the cyclooxygenase-1 and cyclooxygenase-2 isoenzymes) may have beneficial as well as untoward effects on a variety of human diseases. Low stomach prostanoid levels caused by COX-1 inhibitors can result in ulceration and internal bleeding and perforation. The selective COX-2 inhibitors such as oxicam, meloxicam, and coxibs (celecoxib, rofecoxib, valdecoxib, parecoxib and etoricoxib) do not interfere with COX-1. The most prominent NSAID is aspirin [85]. Removal of these organic compounds by traditional techniques (charcoal adsorption, ozonization) is challenging and costly. These methods usually generate concentrated effluent streams, which are harmful to environment. Recent advanced technologies in photocatalytic oxidation of organic materials can be safely employed in treatment of organic wastes as the final products are mostly carbon dioxide and water.

2.9 Photo degradation of methyl orange and aspirin

Several researches have been conducted on degradation of organic compounds with TiO_2 powder or doped form under solar rays and UV/Hg lamps. Researchers have shown photo degradation of methyl orange under solar rays is faster than that with UV lamp [86]. Doped forms of TiO_2 and TiO_2 films have been studied by many researchers to demonstrate the degradation kinetics of methyl orange under solar ray and UV lamp [18-20].

2.10 Photocatalytic mineralization of pollutants and Analysis of the end products

In order to assess the degree of mineralization reached during the photocatalytic treatment the formation of CO₂ and inorganic ions were generally determined. However, in the presence of real wastewaters the monitoring of inorganic ions and CO₂ gives only a global estimation on the well functioning of the treatment, but does not provide information on the real decay of the contaminant. In such cases the determination of total organic carbon (TOC) and/or the measurement of the chemical oxygen demand (COD) or the biological oxygen demand (BOD) of the irradiated solution were generally used for monitoring the mineralization of the dye [85-87]. In general, it has been reported that at low reactant levels or for compounds which do not form important intermediates, complete mineralization and reactant disappearance proceed with similar half lives, but at higher reactant levels where important intermediates occur, mineralization were reported to be slower than the degradation of the parent compound [86, 87]. Until now, total mineralization has been observed for the photocatalytic degradation of most of the azo dyes even at longer irradiation periods. Usually, it was observed by researchers that the COD or TOC values decrease with increase in irradiation time whereas the amount of NH₄⁺ and NO₃⁻ ions increase with increase in irradiation time [87]. Titanium dioxide (TiO₂) has been employed in photocatalytic oxidation processes due to its capability of producing hydroxyl radical ([•]OH) when exposed to ultraviolet/solar light. Contradictory results have been reported for the contribution of TiO₂ in degradation of organic materials. It was shown that at low pH the positive holes were considered as the major oxidizing species, whereas hydroxyl radicals were considered as the predominant species at neutral or high pH levels [83]. Interestingly it was claimed in another report that holes are the major oxidizing species at pH = 3, while below and above this pH the hydroxyl radicals were the major degrading agents [84]. Such a discrepancy is most probably due to the nature of the organic compounds and operating conditions. Therefore it can be concluded that aspirin undergoes the following reactions when exposed to the catalyst illuminated by solar light:



Several mechanisms have been proposed to account for the initial steps of semiconductor-mediated photo degradation of aliphatic and aromatic organics. The heterogeneous reaction mechanisms proposed were similar to their homogeneous counterparts [96]. These mechanisms can be summarized as;

(i) Direct charge transfer from the semiconductor to the dissolved molecule.

(ii) Generation of radicals from water decomposition, which then attack the aromatic ring. Most of the studies on photocatalytic degradation of several drugs include a detailed examination of the so-called primary processes under different working conditions, while little information is available on the reaction mechanisms involved in the degradation process.

In this research the applications of the polymeric-TiO₂ film photocatalysts were examined. TiO₂ got immobilized in the polymeric networks, which prevented the TiO₂ particles to agglomerate during the reaction process and in turn prevented ultrafiltration process. This photocatalyst being buoyant can utilize the light more effectively. In one study, the developed photo catalyst was immobilized on inorganic substrates. Photo degradations of organic pollutants were carried out both under solar and UV light, in presence of both film catalyst and immobilized film on glass plates. The degradation kinetics of methyl orange and aspirin were studied in details. The effects of initial concentration, flow rates, catalyst loading, film thickness and light intensity were studied. Also, in this study, mechanism of degradation of aspirin in the presence under solar light was investigated. The most probable reactions and the mechanisms were suggested based on the qualitative and quantitative analysis. My investigations have enabled natural sunlight to be used as the light source and also eradicated the ultra filtration method, thereby reducing the cost of the treatment. Besides, a new type of film photo catalyst has been introduced which holds the potential of oil/chemical spill recovery.

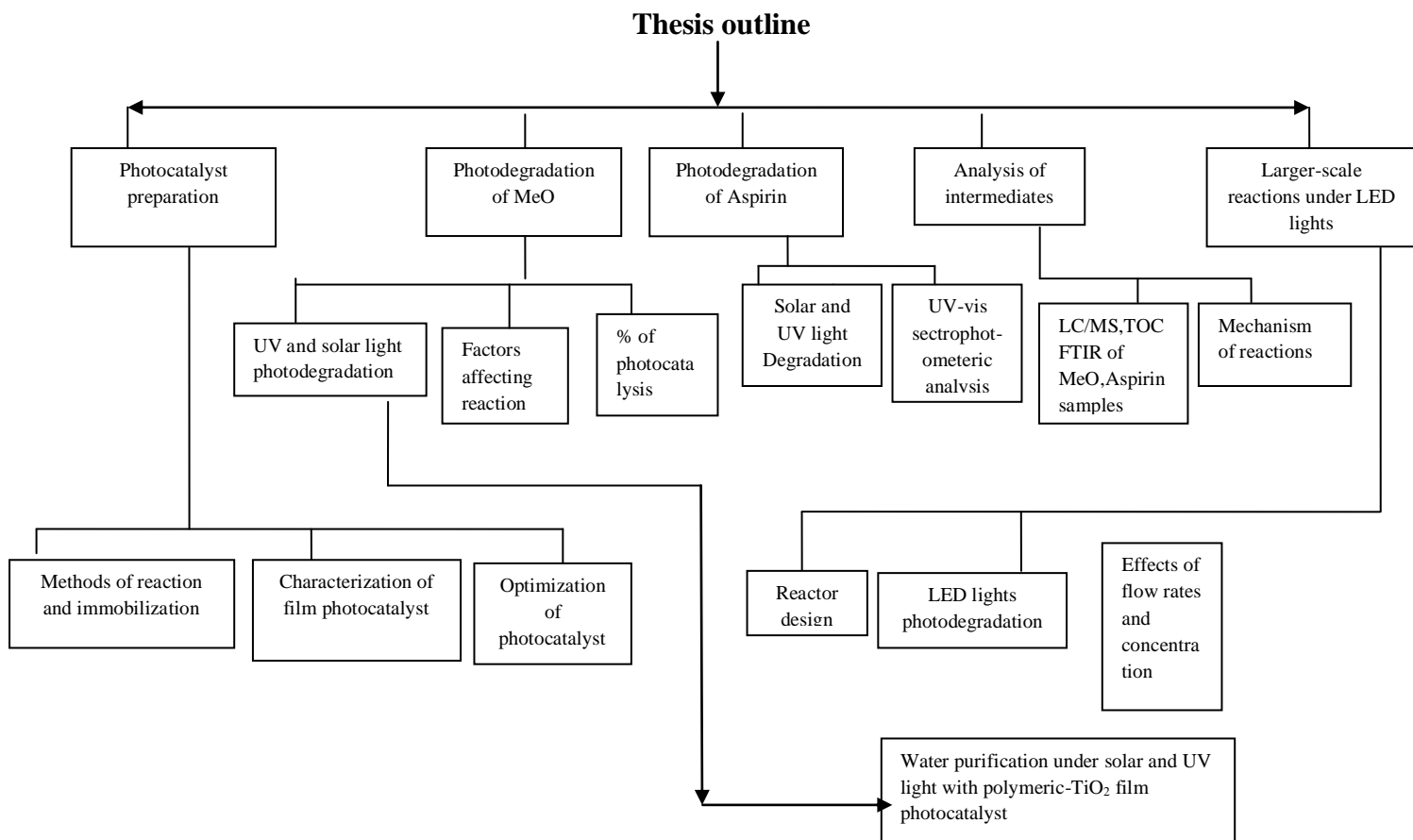


Figure 2.5: Thesis Outline

2.11 Reference

1. http://en.wikipedia.org/wiki/Water_crisis, Retrieved April 2009.
2. Richman, M IND. Wastewater, 5, (1997), 24-29.
3. Tibbetts, J Anon. Water Environ. Soln., 9, (1996),5-7.
4. http://www.NaturalNews.com/001891_prescription_drugs_pharma_industry.html
Retrieved May 2009.
5. Paul E. Stackelberg, Jacob Gibs, Edward T. Furlong, Michael T. Meyer, Steven D. Zaugg , R. Lee, Lippincott, Science of the Total Environment , 377, (2007), 255–272.
6. <http://www.lenntech.com/processes/heavy/heavy-metals.com>. Retrieved April 2009.
7. Alexander A. Mofidi, Joon H. Min, Leslie S. Palencia, Bradley M. Coffey, Sun Liang, James F. Green, California Energy Commission Sacramento, California, (2002).
8. A. Fujishima, K. Honda, and S. Kikuchi, Kogyo, Kagaku Zasshi, 72, (1969), 108 .
9. A. Fujishima, K. Honda, Nature, 238, (1972), 37-38.
10. Electron lifestyle product, http://www.electronline.com.au/about_us.htm. Retrieved April 2009.
11. Allen, J., Allen, S., Baertischi, S., J. Pharm. Biomed. Anal. 24, (2000), 167–178.
12. Bauer, R., Waldner, G., Fallmann, H., Hager, S., Klare, M., Krutzler, T., Malato, S., Maletzky, P., Catal. Today 53, (1999), 131–141.
13. Blanco, J., Malato, S. Renewable Energy Series. France, UNESCO Publishing, (2003).
14. Boyd, G., Reemtsma, H., Grimm, A., Mitra, S., USA and Ontario, Canada. Sci. Total Environ., 311, (2003), 135–149.
15. L. Andronic , S. Manolache , and A. Duta, J. of nanosci. and nanotech, 8, (2008), 2.
16. P.S. Mukherjee, A.K. Ray, Chem. Eng. Technol. 22, (1999), 253–260.
17. I. Arslan and I. Akmehmet Balcioglu, *Dyes and Pigments*, (1993), 43.
18. T. Ohsaka, Y. Ohnuki, N. Oyama, K. Katagiri, K. Kamisako, J. Electroanal. Chem., 161, (1984), 399.
19. S.K. Kansal, M. Singh, and D. Sud, J. Hazardous Mat. 12, (2007), 141.

20. A. A. Karyakin, A. K. Strakhova, A. K. Yatsimirsky, *J. Electroanal. Chem.*, 371, (1994), 259.
21. C. Hatchard, C. Parker, *Proceedings of R. Soc. A*, 235, (1956), 518–536.
22. J. De Laat, G.T. Le, B. Legube, *Chemosphere* ,55, (2004), 715–723.
23. X. Liu, N. Deng, *Environ. Sci. Technol.*, 38, (2004), 296–299.
24. H. Krysova, J. Jirkovsky, G. Mailhot, M. Bolte, *Appl. Catal. B: Environ.*, 40, (2003), 1–12.
25. H. Mestankova, G. Mailhot, J. Jirkovsky, J. Krysa, M. Bolte, *Catal. B: Environ.* 57, (2005), 257–265.
26. Y. Sun, J. Pignatello, *J. Environ. Sci. Technol.* 27, (1993), 304–310.
27. G. Mailhot, M. Sarakha, B. Lavedrine, J. Caceres, S. Malato, *Chemosphere*, 49, (2002), 525–532.
28. Gerd Sagawe, Mara L. Satuf, Rodolfo J. Brandi, Jan P. Muschner, Christian Federer, Orlando , 35, (2001), 230-237.
29. A.L. Boreen, W.A. Arnold, K. Mc Neill, *Environ. Sci. Technol.* 38, (2004), 3933–3940.
30. J. Pawlaczyk, W. Turowska, B. Rozniak, *Acta Pol. Pharm.* 33, (1976), 87–91.
31. T. Ahmad, I. Ahmad, *Pharmazie* 36, (1981), 619–621.
32. W. Baran, E. Adamek, A. Makowski, *Chem. Eng. J.*, 145, (2008), 242–248.
33. P. Sukul, M. Spiteller, *Environ. Contam. Toxicol.*, 187, (2006), 67–101.
34. K. Berger, B. Peterson, H. Buening-Pfaune, *Arch. Lebensmittelsh.*, 37, (1986), 99–102.
35. Y. Kim, K. Choi, J. Jung, S. Park, P.-G. Kim, J. Park, *Environ. Int.* 33, (2007), 370–375.
36. T.A. Ternes, M. Bonerz, N. Herrmann, B. Teiser, H.R. Andersen, *Chemosphere* 66 (2007), 894–904.
37. P. Kay, P.A. Blackwell, A.B.A. Boxall, *Environ. Pollut.* 134, (2005), 333–341.
38. B. Halling-Sørensen, S. Nors Nielsen, P.F. Lanzky, F. Ingerslev, H.C. Holten Lützholt, S.E. Jørgensen, *Chemosphere*, 36, (1998), 357–393.
39. K. Kummerer, *Chemosphere* 45, (2001), 957–969.

40. K. Ku`mmerer (Ed.), *Risks*, Springer-Verlag, Heidelberg, (2001).
41. T. Heberer, *Toxicol. Lett.*, 131, (2002), 5–17.
42. M. Carballa, F. Omil, J.M. Lema, M. Llompert, C. Garcia-Jares, I. Rodriguez, M. Gomez, T. Ternes, *Water Res.* 38, (2004), 2918–2926.
43. C.C. Liu, Y.H. Hsieh, P.F. Lai, C.H. Li , and C.L. Kao, *Dyes and Pigments*,68, (2006), 2-3.
44. C.F. Daughton, T.A. Ternes, *Environ. Health Persp.*, 107, (1999), 907–938.
45. European conference on pharmaceuticals in the environment: *Envirpharma*: 14–16 Lyon, France, (2003).
46. E.R. Campagnoloa, K.R. Johnsonb, A. Karpatia, C.S. Rubinb, *Sci. Total Environ.* 299 , (2002), 89–95.
47. A.C. Capleton, C. Courage, P. Rumsbya, P. Holmesa, E. Stutt, A.B.A. Boxall, L.S. Levy,*Toxicol. Lett.* 163, (2006), 213–223.
48. M. Clara, B. Strenn, O. Gans, E. Martinez, N. Kreuzinger, H. Kroiss, *Water Res.* 39 (2005), 4797–4807.
49. W. Baran, J. Sochacka, W. Wardas, *Chemosphere*, 65, (2006), 1295–1299.
50. M.N. Abellan, B. Bayarri, J. Gimenez, J. Costa, *Appl. Catal. B: Environ.* ,74 , (2007), 233–241.
51. S. Gartiser, E. Urich, R. Alexy, K. Ku`mmerer, *Chemosphere*, 66, (2007), 1839–1848.
52. Eliassaf, J., *Polym.Lett.*, 16, (1972), 225-235.
53. G. El-Kodsi, & Schurz J. Papier (Darmstadt), 27, (1973), 253-255.
54. V.I. Maslov & F.M. Kolerko, *Lab. Delo*, 5,(1972), 295-297
55. H.A. Al-Ekabi, and D.Ollis, Elsevier, Amsterdam, (1993).
56. Y.M.Slokar, and A.M Le Marechal, *Dyes and Pigments*, (1998), 37.
57. S.B. Sakthivela, M.V. Neppolianb, B. Shankarb , M. Arabindoob, V.Palanichamyb, and V. Murugesanb, *Sol. Energy Mater. Sol. Cells*,77, (2003), 65-82.
58. F. Debeaufort, J.A. Quezada-Gallo, Voilley, A. *Crit. Rev. Food Sci.* (1998), 38, 298-331.
59. R.N. Tharanathan *Trends Food Sci. Tech.* (2003), 14, 71-78.

60. D.S. Cha, M.S. Chinnan, *Crit. Rev. Food Sci.* (2004), 44, 223–237.
61. V. Siracusa, P. Rocculi, S. Romani, M. Dalla Rosa, *Trends Food Sci. Tech.* 19, (2008), 634-643.
62. N. Daneshvar, D. Salari, A.R. Khataee, *J. of Photochemistry and Photobiology A: Chemistry*, 12, (2003), 157-165.
63. D. Lin, Zhao, Y. *Comp. Rev. Food Sci. Food Saf.* 6, (2007), 60-75.
64. M.Varga, C. Pastor, A. Chiralt, D.J. McClements, C. González-Martínez, *Rev. Food Sci.* (2008), 48, 496-511.
65. E.A. Baldwin, M.O. Nisperos-Carriedo, Ed., Lancaster Technomic Publishing, (1994), 1-24.
66. P.A. Williams, G.O. Phillips, In *Handbook of hydrocolloids*, CRC Press, Cambridge, England, (2000), 1-19.
67. J.J. Kester, O.R. Fennema, *Food Technol.* 40, (1986), 47-59.
68. Y.L. Tu, *J. Mater. Res.* 11, (1996), 2566- 2574.
69. K. Maki, *J. Am. Ceram. Soc.* 83, (2000), 1914-1920.
70. D. Chen, A.K. Ray, *Applied Catalysis B: Environmental*, 23, (1999), 143-147.
71. Dingwang Chen, Fengmei Li, and Ajay K. Ray, *J. of AIChE*, 46, (2000), 846-1100.
72. T. Araki, I. Hirabayashi, *Supercond. Sci. Technol.* 16, (2003), 120-129.
73. L. Andronic, and A. Duta, *Mat. Chem. and phys.*, 112, (2008), 3-8.
74. L. Youji, L. Xiaodong, L. Junwen, and J. Yin, *Water research*, (2006), 40-46.
75. R. Andreozzi, R. Marotta, *Water Res.* 38, (2004), 1225–1236.
76. Qingzheng Cheng, Siqun Wang, Timothy G. Rials and Seung-Hwan Lee *Cellulose*, 14, (2007), 593-602.
77. GMAP, http://www.gmap-gelatin.com/about_gelatin_phys.html Retrieved April 2010.
78. E. I. Ryumtsev, N. P. Evlampieva, O. V. Nazarova, S. N. Bokov and E. F. Panarin *Doklady phys. Chem.* 392, (2005), 231-234

79. P. Calza, V. Sakkas, C. Medana, C. Baiocchi, A. Dimou, E. Pelizzeti, T. Albanis, , *Appl. Catal.:Environ.* 67, (2006), 197–205.
80. M. Carballa, F. Omil, J. Lema, M. Llompert, C. Garcí'a-Jares, I. Rodri'guez, M. Go'mez, T. Ternes, *Water Res.* 38 (12), (2004), 2918–2926.
81. J. Clarke, <http://www.chemguide.co.uk/physical/acidbaseeqia/indicators.html> Retrieved June 2009.
82. Fred Senese, <http://antoine.frostburg.edu/chem/senese/101/index.shtml>. Retrieved April 2010.
83. Jonathan Cluett, *About.com Guide* (2011)
84. L. Andronic, S. Manolache, A. Duta, *J. of nanosci. and nanotech*, 8, (2008), 2-8.
85. <http://www.chemicaland21.com/lifescience/phar/ACETYLSALICYLIC>. Retrieved Dec. 2009.
86. M. N. Rashed, A. A. El-Amin, *Int. J. of Phys. Sc.*, 2, (2007), 073-081.

Chapter 3

Experimental Details

3. Experimental equipments

3.1 Materials and Methods

3.1.1 Materials

Gelatin (Sigma Aldrich), Polyvinyl alcohol (Mol. wt – 26300 - 30000 g.mol⁻¹, Sigma Aldrich), Polyvinyl pyrrolidone (Mol. wt- 2500 - 25000 g.mol⁻¹, Sigma Aldrich), Titanium dioxide Degussa P25 (Sigma Aldrich), Methyl orange (Sigma Aldrich), Aspirin (Sigma Aldrich), Ammonium acetate (Sigma Aldrich), Acetonitrile (Sigma Aldrich), potassium phthalate (Sigma Aldrich), Solar simulator (Science tech Inc., SS-IK), UV lamp (Phillips), High performance liquid chromatography (Agilent technologies, G2175 BA), LC/MS (Shimadzu, 2010 EV), Fourier transform infra red (Bruker,Vector-22), Total organic carbon content (Mandel Scientific Inc., TOC-V), Optical microscopy (VWR), Scanning electron microscopy (Shimadzu), Vernier callipers.

3.1.1.1 Polyvinyl alcohol

Polyvinyl alcohol (synonyms, vinyl alcohol polymer, PVA) is a water-soluble synthetic resin, prepared by the polymerization of vinyl acetate, followed by partial or complete catalyzed hydrolysis. The primary raw material used in the manufacture of polyvinyl alcohol is vinyl acetate monomer. The physical characteristics of polyvinyl alcohol vary depending on the degree of polymerization and hydrolysis. It is also resistant to oil, grease and solvent [1]. It is odourless and nontoxic. It has high tensile strength and flexibility, as well as high oxygen and aroma barrier properties. However these properties are dependent on humidity, in other words, with higher humidity more water is absorbed. The water, which acts as a plasticiser, will then reduce its tensile strength, but increase its elongation and tear strength. PVA is fully degradable and is a quick dissolver. PVA has a

melting point of 230°C and 180 – 190°C for the fully hydrolysed and partially hydrolysed grades, respectively. It decomposes rapidly above 200°C as it can undergo pyrolysis at high temperatures. PVA is an atactic material but exhibits crystalline nature, as the hydroxyl groups are small enough to fit into the lattice without disrupting it. FDA has approved this polymer as additives in food and drugs.

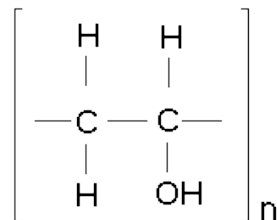


Figure 3.1: Structure of polyvinyl alcohol [2]

Polyvinyl alcohol is classified into grades of partially and fully hydrolysed polymers with different intended functional uses. Polyvinyl alcohol has a history of use in cosmetic, food packaging materials, pharmaceutical and medical applications. Polyvinyl alcohol is used as a coating, binder, sealing and surface finishing agent in food products such as dairy-based desserts, confectionery and cereal products and dietary supplement tablets. Used in eye drops and hard contact lens solution as a lubricant. Used as a fixative for specimen collection, especially stool samples. When doped with iodine, PVA can be used to polarize light.

3.1.1.2 Gelatin

Gelatin is a protein produced by partial hydrolysis of collagen extracted from the boiled bones, connective tissues, organs and some intestines of animals such as domesticated cattle, pigs, and horses. The natural molecular bonds between individual collagen strands are broken down into a form that rearranges more easily. Together with water, it forms a semi-solid colloid gel. Gelatin forms a solution of high viscosity in water and its chemical composition is, in many respects, closely similar to that of its parent collagen. Gelatin solutions show viscoelastic flow and streaming birefringence. If gelatin is put into contact with cold water, some of the material dissolves. Gelatin is also soluble in most

polar solvents. Gelatin gels exist over only a small temperature range, the upper limit being the melting point of the gel, which depends on gelatin grade and concentration and the lower limit, the freezing point at which ice crystallizes. The mechanical properties are very sensitive to temperature variations, previous thermal history of the gel, and time.

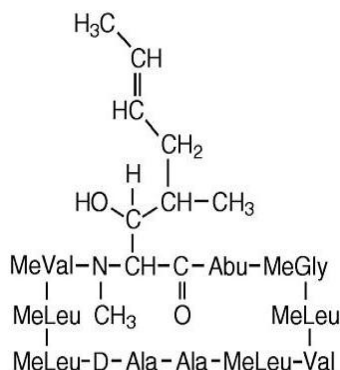


Figure 3.2: Structure of Gelatin [3]

known as a gelling agent in cooking, different types and grades of gelatin are used in a wide range of food and non-food products: Common examples of foods that contain gelatin are gelatin desserts, trifles, aspic, marshmallows, candy corn, and confectioneries such as Peeps, gummy bears and jelly babies. Gelatin may be used as a stabilizer, thickener, or texturizer in foods such as jams, yoghurt, cream cheese, and margarine. it is used, as well, in fat-reduced foods to simulate the mouth feel of fat and to create volume without adding calories. Gelatin is used for the clarification of juices, such as apple juice, and of vinegar. Isinglass, from the swim bladders of fish, is still used as a fining agent for wine and beer [80].

3.1.1.3 Polyvinyl pyrrolidone

Polyvinylpyrrolidone (PVP), also called Polyvidone, is a water-soluble polymer made from the monomer N-vinylpyrrolidone. PVP is soluble in water and other polar solvents. In polar solvents like butanol, ethanol, methanol etc. the solubility increases. When dry it is a light flaky powder, which readily absorbs up to 40% of its weight in atmospheric

water. In solution, it has excellent wetting properties and readily forms films. This makes it good as a coating or an additive to coatings [4].

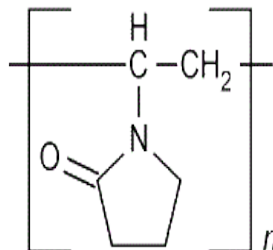


Figure 3.3: Structure of PVP [4]

It is used as a binder in many pharmaceutical tablets; it simply passes through the body when taken orally. PVP added to iodine forms a complex called povidone-iodine that possesses disinfectant properties. This complex is used in various products like solutions, ointment, pessaries, liquid soaps and surgical scrubs. It is known for instance under the trade name Betadine. It is used in pleurodesis (fusion of the pleura because of incessant pleural effusions). For this purpose, povidone iodine is equally effective and safe as talc, and may be preferred because of easy availability and low cost.

3.1.2 Methods

3.1.2.1 Preparation of TiO₂-polymeric film photocatalyst

The photocatalyst film was synthesized in a 500 ml beaker. 24.3 % w/w of PVA and 11% w/w of Gelatin were dissolved properly in distilled water Next, 21.6 % w/w of PVP dissolved in the solution of ethyl alcohol and water (3:1) was added to the gelatin - PVA solution. The resulting solution was reacted for 15 minutes at 45°C, followed by dispersion of 43 % w/w TiO₂ Degussa P25 powder in the mixture. This was followed by physical cross-linking at -2 °C for 5 hours.

3.1.2.2 Photodegradation of Methyl orange

A 121 ml continuous flow reactor in Fig.3.4, containing the methyl orange, was exposed to UV lamp of light intensity 22 mW/cm^2 . The methyl orange solution was pumped from a 250 ml beaker into the reactor by a peristaltic pump at 82 ml/min , being a continuous flow system, the degraded methyl orange solution was pumped out of the reactor into the same beaker, and a magnetic stirrer was employed at the bottom of the beaker for mixing. The pH of the solution was 5.8-6.2. The pH increased with time because of the UV exposure. The polymeric- TiO_2 photocatalyst was coated on the Pyrex glass bottom of the reactor. Following the photodegradation, samples were collected for pH measurement and UV-Vis spectrophotometer analysis. Studies were carried out by varying the flow rates, initial concentrations, pHs, catalyst loadings and light intensities of the experimental set up, to observe their effects on the degradation rate. The optimum light intensity and pH were selected by carrying out studies at different intensity and pH level.

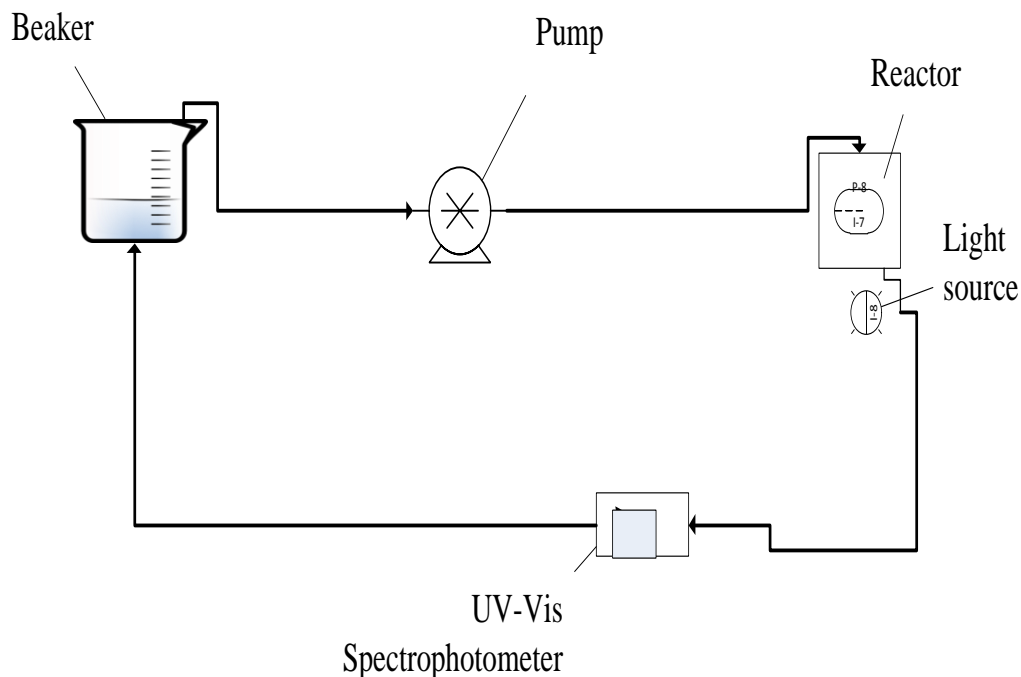


Figure 3.4: Methyl orange photodegradation. Experimental conditions [Continuous flow reactor, light source- UV lamp, and pH-5.8-6.2]

3.1.2.3 Photodegradation of Aspirin

Aspirin solution photodegradation was carried out in a batch reactor of 250 ml, in presence of the film photocatalyst, both under UV lamp and solar simulator. The photodegradation of aspirin was carried out both in the presence of slurry TiO_2 and TiO_2 -Polymeric film. The solution was stirred continuously, by a magnetic stirrer at the bottom of the reactor, during the degradation. The UV lamp was placed under the reactor, while the solar simulator was placed above the reactor. The experiments under the UV lamp was carried out at light intensity of 22 mW/cm^2 , pH – 4.5, TiO_2 loading of 1.5 g/L. On the other hand, the solar light experimentations were carried out at light intensity of 27 mW/cm^2 , pH- 4.5, TiO_2 loading 1.5 g/L. In case, of the degradation studies in presence of TiO_2 /polymeric film, the film thickness was 0.45 mm. The degraded samples were analysed in UV-Vis spectrophotometer. The effects of initial concentration, pH, light intensity, catalyst loading and film thickness on the degradation rate were studied. The optimum pH and light intensity were determined by carrying out experimentations by varying each of the parameters.

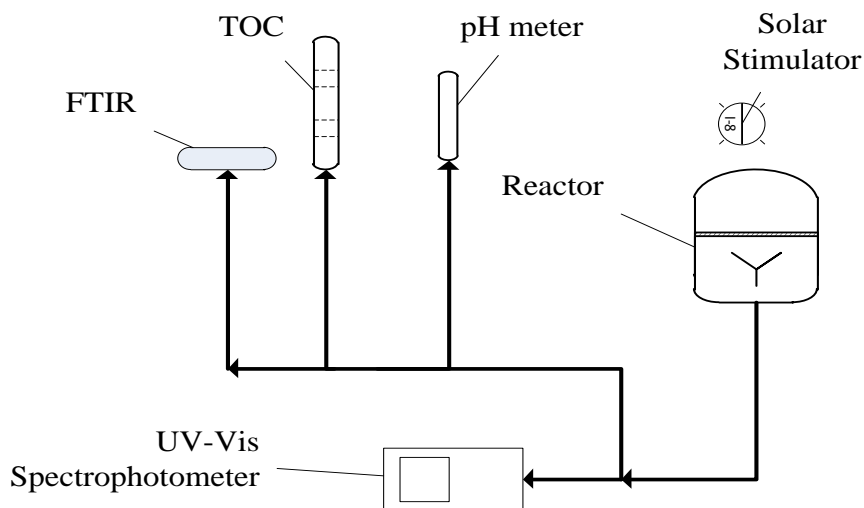


Figure 3.5: Aspirin photodegradation. Experimental conditions [Batch reactor, light source- Solar simulator: $I = 27 \text{ mW/cm}^2$, UV lamp: $I = 22 \text{ mW/cm}^2$, pH-4.5, TiO_2 loading = 1.5 g/L, H = 0.45 mm]

3.1.2.4 Photodegradation of Methyl orange in large scale reactor

Methyl orange was photo degraded under LED lights in a 5 Litres continuous flow reactor shown in the Fig.3.6, which consisted of two concentric cylinders with the LED lights supported on a plastic support hold outside the reactor. The radius of the space between two cylinders was 5 cm and the thickness of the cylindrical wall was 0.45 cm. The methyl orange solution containing 0.00025 cm² pieces of photocatalyst films was pumped by a peristaltic pump from a 7 Litres container into the reactor. After degradation the solution was pumped out of the reactor into another container. The pH of the system was 5.8 throughout the reaction and the light intensity was 4.1 mW/cm². The degraded samples were collected in a container and analysed in UV-Vis spectrophotometer. The effects of initial concentrations and flow rates were studied. Methyl orange solutions of concentration 2, 10, 30, 100, 200 (ppm) were employed for degradation. The flow rate of the solution was varied by the regulating the speed of the peristaltic pump. The degradations were studied at flow rates of 45, 85, 200, 450, 650, 800 ml/min.

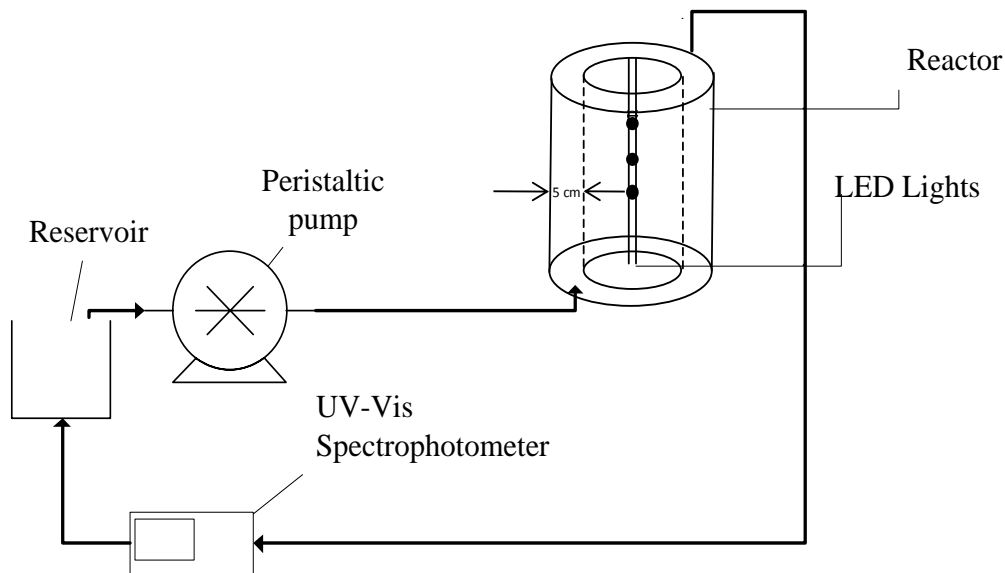


Figure 3.6: Methyl orange photodegradation. Experimental conditions [LED lights, Continuous flow reactor, catalyst-polymeric/TiO₂ film, and pH – 4.1]

3.1.2.5 Reactor setup

Experiments (MeO degradation reactions under UV lamp) were conducted in a semi-batch swirl-flow monolithic-type photoreactor. The reactor consisted of two circular glass plates (each of diameter 0.09m) separated by 0.01m, which were placed between soft padding housed within stainless steel and aluminum casings. Pyrex glass plates were used as it can cut-off UV light below 300 nm thereby eliminating direct photolysis of the organic compounds. The reaction solution, which was circulated by a peristaltic pump, was introduced tangentially between the two glass plates, and exited from the center of the top plate. The tangential introduction of liquid created a swirl-flow, thereby ensuring that the liquid solution was well mixed. A lamp was placed about 0.1 m underneath the bottom glass plate on a holder that could be moved to create a different angle of incidence of light. The light intensity was measured by a digital radiometer (UVP Model number UVX-36). Provision was made for placement of several metal screens of different mesh size between the lamp and the bottom glass plate to obtain variation in light intensity. The lamp and reactor were placed inside a wooden box painted black so that no stray light can enter the reactor. The lamp was constantly cooled by compressed air to protect the lamp from overheating. Teflon tubing was used to connect the reactor and the beaker. The schematic diagram of the setup is shown in Fig. 3.7.

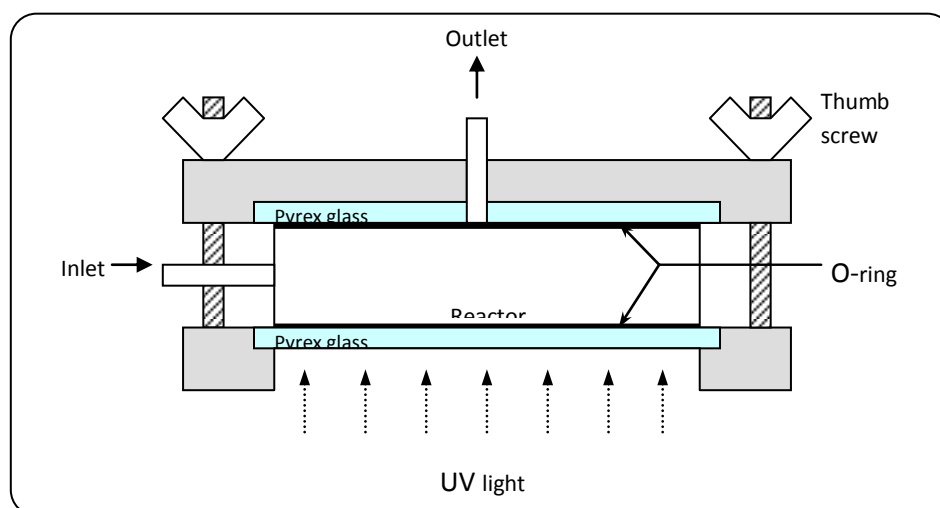


Figure 3.7. Schematic drawing of the monolithic swirl-flow photocatalytic Kinetic reactor.

3.1.2.6. Advantages and disadvantages of reactor types used

Batch reactor – The batch reactor was used for aspirin degradation showed the advantages of small instrumentation cost, flexibility of operation (may be easily shut down). Hence, we may generalize that batch reactor is well suited to produce small amounts of materials. Disadvantages of a batch reactor are poorer quality of product, high handling cost of labours in industries (refill, clean out). Therefore for industrial purpose continuous flow reactor is better.

Continuous flow reactor – This reactor has been used for methyl orange large scale degradation under LED lights. This type of reactor is best for industrial purpose, when large scale quantities are to be processed and when rate of reaction is fairly high. Extremely good quality products can be produced by this reactor.

Semibatch reactor – This reactor was used for MeO degradation under UV lights. This type of reactor is flexible to use but is more difficult to analyze. This reactor may offer good control of reaction speed because the reaction proceeds as reactants added.

3.1.2.7. Instrumental analysis

UV-Vis spectrophotometer was used to analyze the concentration of the degraded samples of pollutants (MeO and aspirin). MeO was analyzed at wavelength of 465 nm, while aspirin analysis was done at wavelength of 298 nm. Total organic carbon content of each of the degraded samples were analyzed, to measure the carbon content before and after the degradation reactions. Fourier Transform Infrared analysis was carried out to detect the functional groups in the MeO and aspirin intermediates. The radiation containing all IR wavelengths ranges from 400 to 5000 cm^{-1} . Results of 32 scans were combined to average out random absorption artifacts, and excellent spectra from very little amount of samples were obtained. High pressure liquid chromatography and Liquid chromatography Mass spectroscopy were carried out in C-18 column, to detect the intermediates formed during the degradation of aspirin molecules. Scanning Electron

Microscopy was carried out to study the topology of the TiO₂-polymeric film photocatalyst produced.

3.2 Nomenclature

MeO – Methyl orange

ASA - Acetyl salicylic acid

TiO₂ - Titanium dioxide

ppm - parts per million

3.3 References

1. Qingzheng Cheng, Siqun Wang, Timothy G. Rials and Seung-Hwan Lee, *Cellulose*,14, (2007), 593-602.
2. GMAP, http://www.gmap-gelatin.com/about_gelatin_phys.html, retrieved June 2010).
3. E. I. Ryumtsev, N. P. Evlampieva, O. V. Nazarova, S. N. Bokov and E. F. Panarin, *Doklady, phys. Chem.* 392, (2005), 231-234.

Chapter 4

Preparation and characterization of the Polymeric-TiO₂ film photocatalyst

4.1 Introduction

Pharmaceuticals in general enter the environment through different pathways, resulting in contamination of waste or fresh water, where bacteria are most likely the primarily affected organisms. Due to high intake of NSAIDs (non steroidal anti-inflammatory drugs), their presence in drinking water has been widely reported [1]. Aspirin belongs to this class of medications called (NSAIDs). NSAIDs are the most frequently prescribed agents to treat fever, pain, arthritis etc. In addition to its effects on pain, fever, and inflammation, aspirin also has an important inhibitory effect on platelets in the blood. This antiplatelet effect is used to prevent blood clot formation inside arteries, particularly in individuals who have atherosclerosis (narrowing of the blood vessels) of their arteries, or are otherwise prone to develop blood clots in their arteries preventing and treating heart attack and strokes.

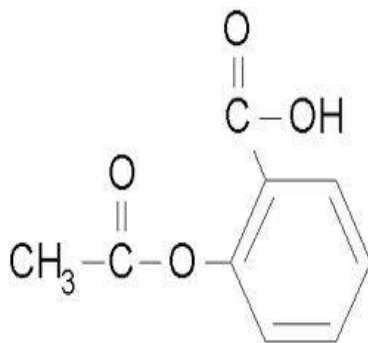


Figure 4.1: Structure of aspirin [2]

In aqueous solutions, they can undergo photochemical transformations with sunlight via direct or indirect photoreactions [2]. Such photochemical degradation can be one of the major transformation processes and one of the factors that control the fate of the organic pollutants in the environment. Various technologies are in use to purify aqueous municipal and industrial effluents containing pharmaceutical substances, before entering

surface waters. Among them, advanced oxidation processes (AOPs) have been the subject of major interest in recent years. As one of the Advance Oxidation Processes (AOPs), TiO₂ photocatalytic oxidation holds much promise to address this issue. TiO₂ is largely used because of its low cost and its photocatalytic efficiency. It is also remarkably active, cheap, non-toxic and chemically stable over a wide pH range. In general, the goal of the application of photocatalysis in water treatment is the transformation, deactivation and finally mineralization of environmentally persistent compounds. The catalyst TiO₂ is chemically stable and non-toxic and able to utilize sunlight and air to produce many reactive species, including the powerful and non-selective oxidant hydroxyl radicals, to destroy organic compounds but it's one of the major drawback is expensive filtration technique needed to remove these slurry TiO₂ from the purified water [3,4]. This problem has resulted in development of several kind of immobilization technique to immobilize the TiO₂ powder which may reduce the post degradation expenses and time. TiO₂ in anatase, Degussa form has been immobilized by following several method. The design and development of an immobilized thin catalyst film makes commercial-scale applications of TiO₂-based photocatalytic processes for water treatment possible. The designs are more likely to be useful in commercial applications because they provide at least three important advantages. First, they eliminate the need for the separation of the catalyst particles from the treated liquid and enable the contaminated water to be treated continuously. Second, the catalyst film is porous and can therefore provide a large surface area for the degradation of contaminant molecules. Third, when a conductive material is used as the support, the catalyst film can be connected to an external potential to remove excited electrons to reduce electron-hole recombination, thereby significantly improving the process efficiency [6]. However, immobilization of TiO₂ on supports also creates its own problems. Several researches have been carried out on immobilization of the TiO₂ [7-9]. Two obvious problems arising from this arrangement: the accessibility of the catalytic surface to the photons and the reactants and a significant influence of the external mass transfer particularly at low fluid flow rate, because of the increasing diffusional length of the reactant from bulk solution to the catalyst surface [10]. Several kinds of film photocatalysts have been formulated by researchers. Among which some researchers have investigated on the characterization and degradation efficiency of TiO₂

loaded carbon fibres [11]. A new modified silicone-TiO₂ polymeric composite has been studied for photodegradation by researchers [12]. Though, these immobilization techniques have been reported to reduce the cost of filtration, all these techniques being expensive their uses have become limited. In our studies, five different polymeric-TiO₂ films were synthesized by varying the cross linking methods. The polymeric film not only acts as a substrate for immobilization of TiO₂ but also, had a synergistic effect on the catalytic efficiency. The morphologies of the films were studied by SEM. The degradation of aspirin solutions were carried out to measure the photocatalytic efficiency of the films. Though film catalysts were able to eliminate filtration process but on the other hand, with immobilization of TiO₂ and increase of the catalyst film thickness, the internal mass transfer may play a dominant role, in decreasing the rate of reactions. All these phenomena, may lead to a lower overall degradation rate when the TiO₂ was immobilized compared with the suspended system. This has also been observed and explained by several other researchers [10, 13].

4.2 Materials and Methods

4.2.1 Materials

Gelatin (Sigma Aldrich), PVA (Sigma Aldrich), PVP (Sigma Aldrich), TiO₂ Degussa P25 (Evonik), UV-Vis Spectrophotometer (Agilent), Beaker (Chemistry store, UWO), pH-meter (Methrom), Magnetic stirrer (Chemistry store, UWO), Conical flask (Chemistry store, UWO).

4.2.2 Methods

4.2.2.1 Preparation of TiO₂-PVP composite

Polyvinylpyrrolidone solution of varying concentrations (33%, 50%, 66.6%, 75%, and 80%) w/w in ethyl alcohol and water (1:2) were prepared. Followed by dispersion of 25% w/w TiO₂. This was followed by drying at 100°C for 1 hour. Experimentations were

carried out by varying the temperature and the duration of drying. Among all of these solutions the 50% PVP solution formed the best coating on glass surface. Therefore, similar studies were carried out by storing the solution at 50°C, 80°C, 90°C, 100°C for (1, 2, 3, 4, 5, 6, 7) hours. It has been observed that drying for 2 hours at 100°C formed the finest quality of coating among all. The film dried for more than 2 hours, formed coatings, which brittle and broke down easily to form powders in water.

4.2.2.2 Preparation of TiO₂-PVP coating

50% w/w of Polyvinylpyrrolidone dissolved in a solution of ethyl alcohol and water (ratio of 1:2) at 35 °C. This was followed by the dispersion of 25 % w/w of TiO₂P25 in the solution.

4.2.2.3 Immobilization

Glass plates of 14 cm² were dipped in the TiO₂/polymer solution and exposed to 100°C in an oven for 1 hour. As PVP degrades above 110°C, therefore the temperature was not raised beyond that limit.



Figure 4.2: TiO₂-PVP photocatalyst immobilized on a glass slide

4.2.2.4 Preparation of polymeric/TiO₂ films

Gelatin, polyvinyl alcohol and polyvinylpyrrolidone were reacted at various ratios by trial and error methods. After, several studies, it has been observed that following percentages of polymers gave rise to a proper and efficient photocatalyst film. It was observed that higher than 11% of gelatin in the formulation made the film more hydrophilic which in turn produced a water soluble photocatalyst. On the other hand the optimum amount of

PVA was observed to be 24.3% w/w. Adding PVA above 24.3% produced a thick film photocatalyst, which in turn attenuated, the light penetration. Though, in our previous formulation 50% w/w PVP was found to be the optimum amount but, after several experimentations, it has been observed that a fine film can be produced by (21.6%) w/w of PVP, in combination with PVA and Gelatin.

24.3 % w/w of PVA and 11 % w/w of Gelatin were dissolved and mixed properly in distilled water to get a transparent solution. Next, 21.6 % w/w of PVP dissolved in the solution of ethyl alcohol and water was mixed with gelatin-PVA solution at 45° C. The solution was reacted for 15 minutes followed by dispersion of 43 % w/w TiO₂ Degussa P25 powder in the mixture. The polymeric solutions with dispersed TiO₂ were cross-linked by several physical and chemical methods.

4.2.2.5 Cross-linking methods

4.2.2.5.1 Freeze-dried (Physical CL)

The polymeric solutions were stored at several low-temperatures ranging from zero-degree to -10 degree centigrade for different time intervals [1, 3, 5, 7, 10, 15, 24 (hours)]. It has been observed that the samples stored for 5 hours shows best results under solar and UV lights. Solutions stored for less than 5 hours showed very soft and flexible films which got partially dissolved in water during the photodegradation reaction. While the one stored for longer period beyond 5 hours though forms mechanically strong catalyst film but shows lower degradation rates than the one at 5 hours. Therefore the freeze-dried film was cross-linked under following conditions:-

The 43 % w/w of TiO₂ dispersed polymeric solution was then physically cross-linked by storing the solution at -2° Centigrade for 5 hours.

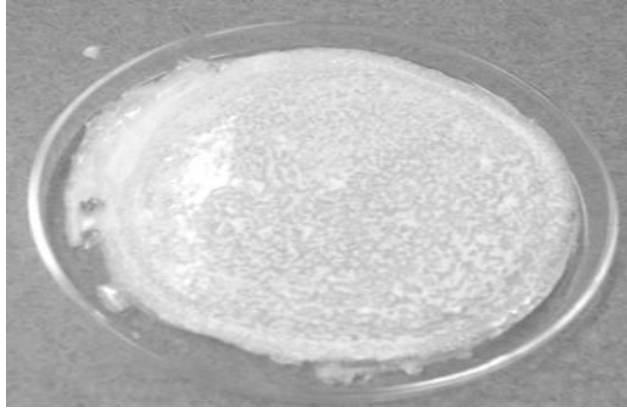


Figure 4.3: Freeze-dried photocatalyst film

4.2.2.5.2 Heat treated (Physical CL)

Following the preparation of the polymeric/TiO₂ solution by above mentioned process, it was cross-linked by heat treatment in an oven for several time intervals ranging from 10 minutes to 120 minutes at several temperatures ranging from 70 degree to 105 °C. As beyond 108 °Centigrade, the polyvinylpyrrolidone starts degrading. Therefore the solution was treated below 108 °C. The solutions were exposed to 108 °C for 120 minutes formed brittle film, while the ones stored at lower temperatures didn't form a consistent catalyst film. It has been observed that the optimum conditions were, heating for 10 minutes at 105 °C. The heat-treated photocatalyst film was prepared by exposing the solution to 105 °C for 10 minutes.



Figure 4.4: Heat-treated film photocatalyst

4.2.2.5.3 Acetaldehyde treated (Chemical CL)

After the polymeric solution was prepared, it was treated with few drops of several percentages of acetaldehyde solutions ranging from 2 %-10 %, at room temperature. The optimum amount of was 2-3 drops of 2% acetaldehyde. The aldehyde cross-linked the polymeric solution and instantly formed a membrane which was dipped in milli Q water for a couple of minutes and washed 3 times to remove the unreacted aldehyde traces.



Figure 4.5: Aldehyde treated photocatalyst film

4.2.2.5.4 UV treated (Chemical CL)

Polymeric solutions with dispersed TiO_2 were exposed of 275 nm wavelength for different time intervals (2min, 5 min, 7min, 10min, 20min, 30 min, and 60 min) to UV light. It has been observed that exposure for 10 min showed best results among all the samples. Samples exposed for 2-7 minutes did not form mechanically strong films, which in turn degrades in the aqueous system during the photodegradation. While the catalyst films formed by exposure of 20-60 minutes though formed mechanically strong films but due to high cross-linking effects, the TiO_2 particles got intertangled within polymer matrices, which in turn made photodegradation difficult. The polymeric solution was prepared following same method as mentioned above and was exposed to UV lamp of 275 nm wavelength for 10 mints to cure the polymeric membrane.

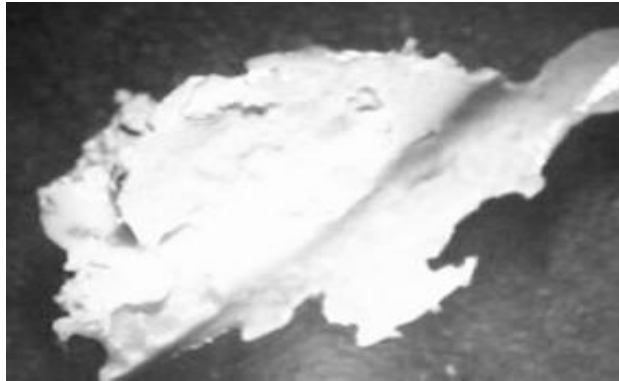


Figure 4.6: UV treated film

4.2.2.5.5 Freeze-dried and UV treated (Physico-chemical CL)

The polymeric solution was prepared following same method as mentioned above and was kept at -2°C for 5 hours and then exposed to UV lamp of light intensity 4 mW/cm^2 for 10 mints to cure the polymeric membrane.

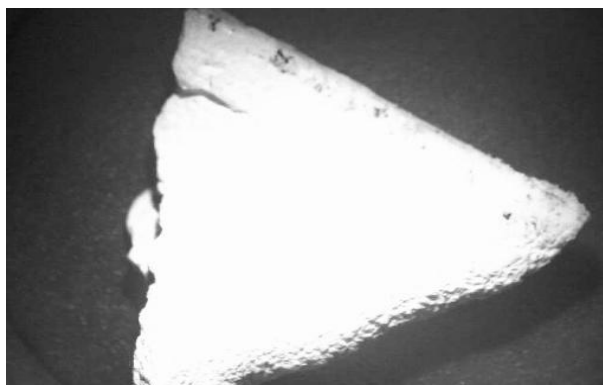


Figure 4.7: Freeze dried and UV treated

4.2.2.5.6 Characterization of film catalyst

Catalyst films were characterized by analysing under optical microscopy and scanning electron microscopy. For verification of a uniform topology of the dried membranes, photocatalyst films were exposed to scanning electron microscope (Hitachi F-4000). SEM studies of the film photocatalysts revealed the specific pore size and pore density. The measuring scale was 2.5 μm .

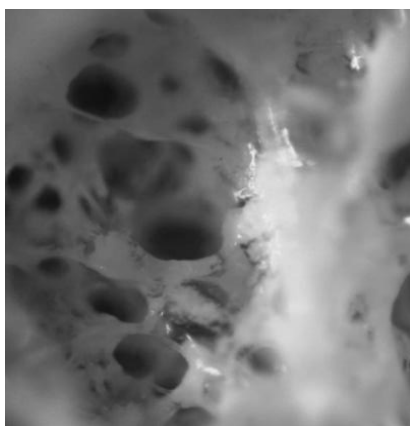
4.2.2.5.7 Analysis of photocatalytic efficiency

The photodegradation reaction was carried out in batch reactors in presence of both solar and UV light with five different kinds of polymeric-TiO₂ catalyst films. Degradation reactions were carried out in batch reactors of 250 ml containing aspirin solution under UV lamp of intensity 22 mW/cm^2 and the solar stimulator of light intensity 27 mW/cm^2 . The concentrations of the degraded aspirin solution were analysed in UV-Vis spectrophotometer Agilent at 298 nm.

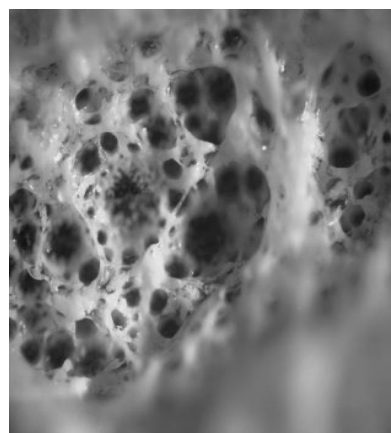
4.3 Results and Discussions

4.3.1 Analysis of optical microscopy

The films were subjected to optical microscopy, to observe the porous structure. Fig. 4.8 showed different topologies of the films. The freeze-dried film showed a spongy porous structure. While the heat treated films were observed to have a highly porous 3 D structure which makes the film to remain buoyant. The aldehyde and UV treated ones were solid matrices with very few pores. The UV-Freeze-dried treated showed a spongy structure similar to freeze-dried but with fewer number of pores.



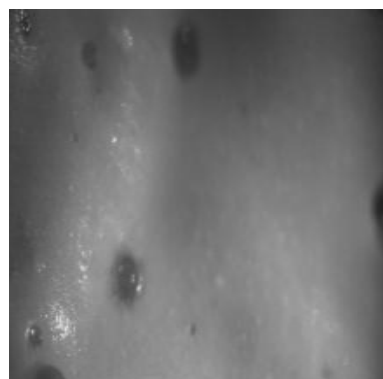
[a]



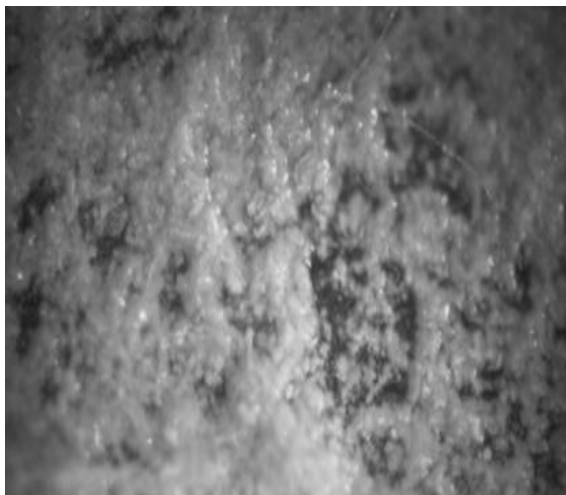
[b]



[c]



[d]



[e]

Figure 4.8 : Optical microscopy of a) Freeze-drying film b) Heat treated film c) UV treated film d) UV-freeze-dried film e) Aldehyde treated film

4.3.2 Analysis of scanning electron microscopy

The film photocatalyst thickness ranges from 0.45 mm to 2mm in thickness. The cross-section micrographs taken by scanning electron microscopy revealed a three-dimensional network structure which is typical for a porous material. In the Fig. 4.9 to Fig. 4.13, the porous structures of the films have been depicted. From the figure with the highest magnification in particular, it can be seen that the freeze-dried membrane is built up homogeneously, interspersed with pores of various diameters ranging from 50 μm to 300 μm . The average pore area was found to be 2078 μm^2 . The pore density ranged from 7-10 pores per square mm for freeze-drying film. While for heat dried 12-15 pores per square mm, were found. The aldehyde and UV treated showed almost no pores and the freeze-dried- UV treated film showed 3-5 pores per sq mm.

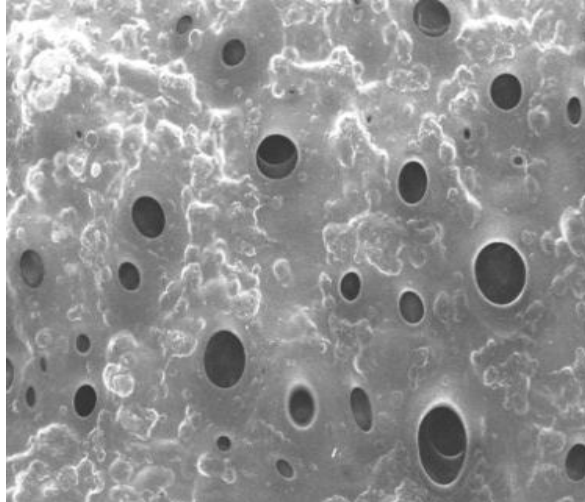


Figure 4.9: SEM of freeze-dried film (measuring scale 2.5 μm)

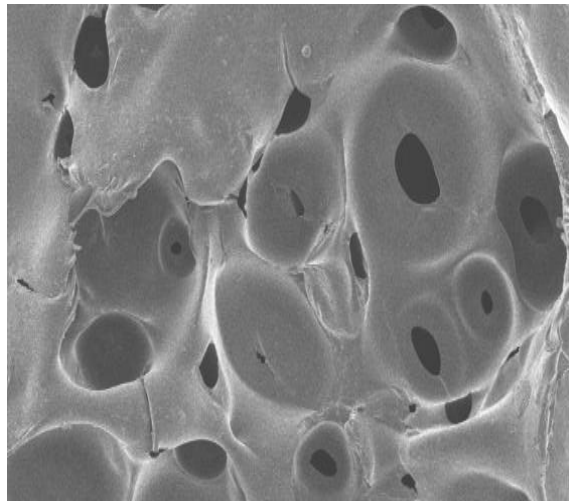


Figure 4.10: SEM of heat treated film (measuring scale- 2.5 μm)

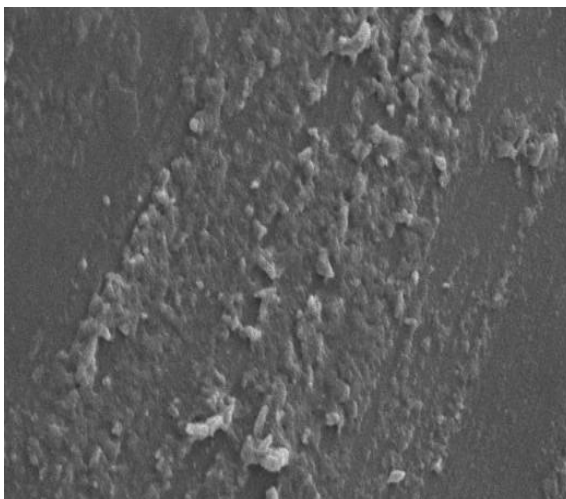


Figure 4.11: SEM of UV treated film (measuring scale- 2.5 μm)

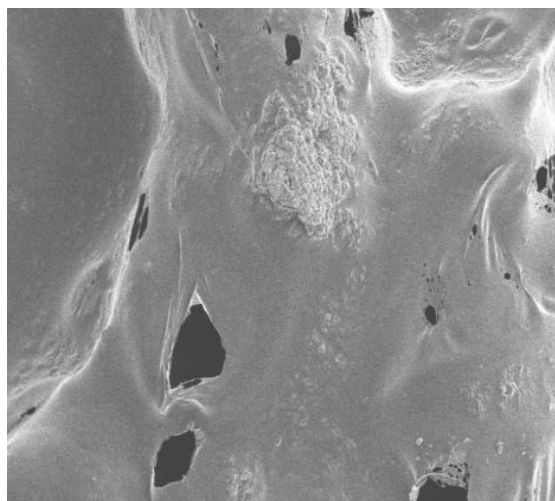


Figure 4.12: SEM of UV treated/freeze-dried film (measuring scale- 2.5 μm)

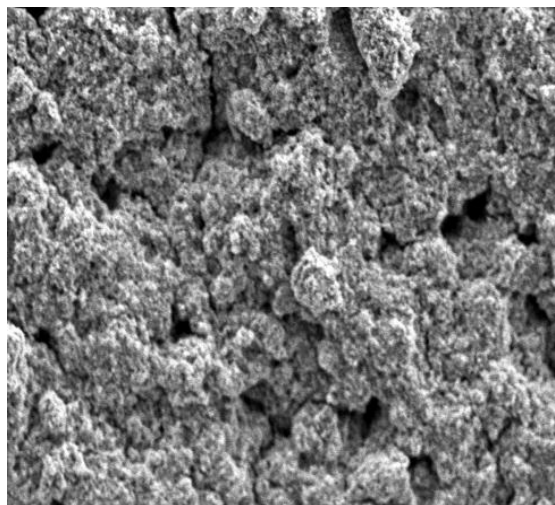


Figure 4.13: SEM of aldehyde treated composite membrane (measuring scale- 2.5 μm)

4.3.3 Degradation of Acetylsalicylic acid

Degradation of aspirin was carried out in batch reactors (250 ml) both under UV and solar lights, to observe the effect of cross-linkages on degradation rate. In the Fig. 4.14 and Fig. 4.15, the rate constants of each degradation reactions were calculated to compare the efficiencies of the film photocatalysts. These k (rate constants) values, were calculated from the initial degradation of aspirin solutions. The degradation rate in presence of slurry was observed to decrease in presence of solar light. While in the presence of freeze-dried film the degradation rate under the solar light was observed to be better than under the UV. Under the solar light freeze-dried film and slurry both showed almost similar degradation rate. The heat and UV treated films were discarded due to quite low degradation rates in comparison with freeze-dried. It has been observed that the freeze-dried catalyst was more efficient in degrading aspirin than the heat treated, UV treated, UV treated - freeze-dried and aldehyde treated catalyst in presence of solar light. Under UV light the efficiency of freeze-dried catalyst was observed to decrease with time.

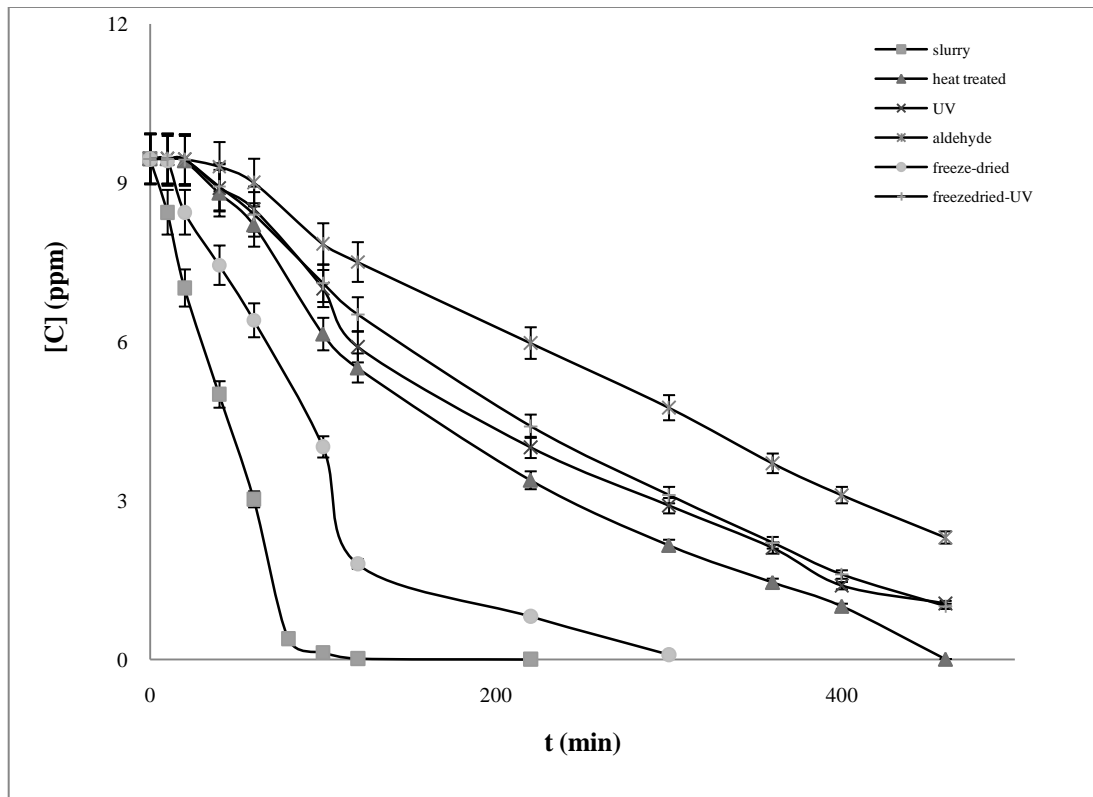


Figure 4.14: Effect of cross-linking methods on degradation of aspirin under UV light. Experimental conditions [$C_0 = 2$ ppm, $I = 22$ mW/cm², pH = 4.5]

The rate constants obtained are: $k_{sl} = 0.099$, $k_{f/d} = 0.05$, $k_h = 0.019$, $k_{uv} = 0.017$, $k_{al} = 0.015$, $k_{f/d-UV} = 0.024$ (mg/L/min)

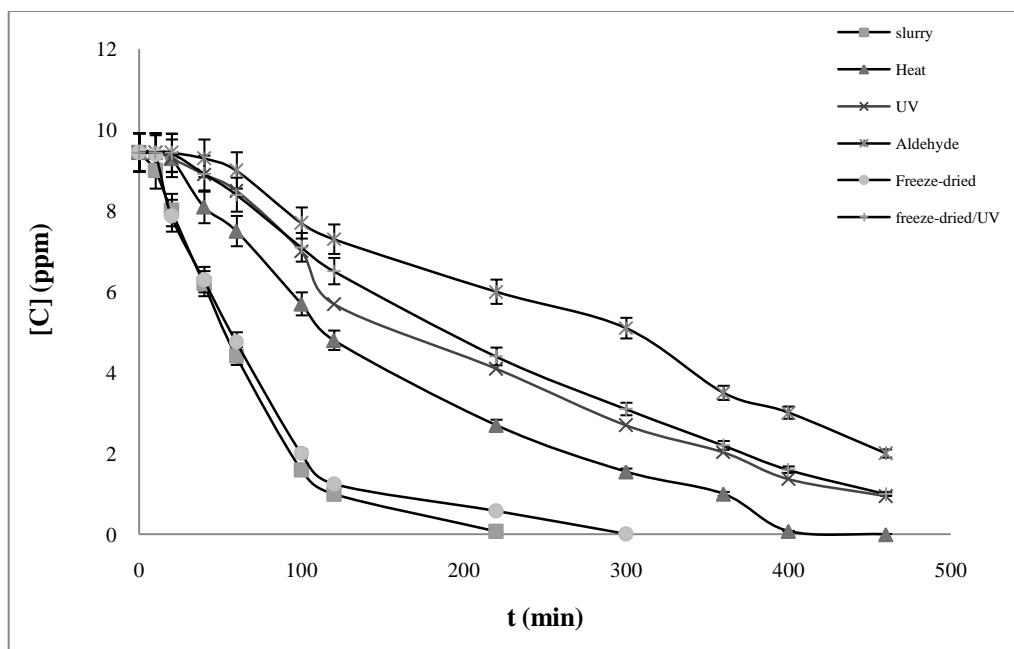


Figure 4.15: Effect of cross-linking methods on degradation of aspirin under solar light. Experimental conditions [$C_0 = 2$ ppm, $I = 27$ mW/cm², pH = 4.5]

The rate constants obtained are: $k_{sl} = 0.08$, $k_{f-d/uv} = 0.027$, $k_{f-d} = 0.079$, $k_{ald} = 0.017$, $k_{uv} = 0.019$, $k_h = 0.022$

This phenomenon can be explained because of cross-linkage formation of the membrane by UV light. After few minutes of UV light exposure during the photodegradation of aspirin the films got cured making more TiO₂ active sites unavailable for the photoreaction, which in turn decreased the reaction rate gradually with time. While on the other hand, though the heat treated catalyst was buoyant and did not show curing effects under UV lights, but the degradation rate of organic pollutants in presence of this film, was lower in comparison to the slurry TiO₂ and freeze-dried catalyst films. The aldehyde treated catalyst was found to remain in submerged condition in the water during the reaction and also showed lower degradation rates as of heat treated catalysts. The UV treated catalyst film showed same morphological characteristics as that of UV-freeze-dried catalyst and both the catalysts were observed to follow almost same rate of degradation in presence of solar light and UV light.

4.4 Conclusions

From this study, it can be concluded that the freeze-dried catalyst was observed to have highest efficiency compared to heat treated, aldehyde treated, UV treated and UV-freeze-dried photocatalysts. The freeze-dried membranes being highly porous showed better adsorption of the pollutants, in comparison with other film photocatalysts. The spongy 3D structure of the catalysts made it capable of adsorbing organic pollutants on its surface, thereby increasing the degradation rate of the catalysts. From the degradation rate constant values obtained, ($k_{f-d} = 0.05$ mg/L/min) under UV and ($k_{f-d} = 0.079$ mg/L/min) under the solar lamp, it can be concluded that, the freeze-dried films were more efficient under the solar light. This was due to the powerful cross-linking effects of the UV light on the polymeric film, which decreased the active sites availability for photo reaction. The UV treated and freeze-dried/UV treated, catalyst films showed very few or almost no pore from the SEM study and therefore showed lower degradation efficiency. Also, due to strong cross-linkages formation by UV light and heat treatment, covalent and ionic bonds were formed between polymer fibres and the TiO_2 . These strong bonds made interstitial TiO_2 particles partially unavailable for photocatalysis. Therefore, these films had fewer active sites available for interacting with the photons. The toxic nature of acetaldehyde reduced the chances of using aldehyde treated catalyst films for drinking water purification. Thus, freeze-dried film catalyst being able to remove the ultra-filtration step and efficient under solar light, it can be concluded that this film photo catalyst holds the potential of an economical and convenient water treatment process.

4.5 Nomenclature

PVA - Polyvinyl alcohol

PVP - Polyvinyl pyrrolidone

TiO₂ P25 - Titanium dioxide Degussa P25

SEM - Scanning Electron Microscopy

CL - Cross link

4.6 References

1. Jeff Don, Martha Mendoza and Justin Pritchard, Associated Press,(2011).
2. http://www.usatoday.com/news/nation/2008-03-10-drugs-tap-water_N.htm. Retrieved May 2010.
3. M. Wilson, <http://www.aspirin-foundation.com/what/chemistry.html>. Retrieved March 2010
4. L.Andronic, S.Manolache, A. Duta, J. of nanosci. And nanotech, 8, (2008), 2-8.
5. P.S. Mukherjee, A.K.Ray, Chem. Eng. Technol., 22, (1999), 253–260.
6. Taicheng An, Jiaxin Chen, Guiying Li , Xuejun Ding , Guoying Sheng, Jiamo Fu, Bixian Mai, Kevin E. O’Shea, Catalysis Today, 139, (2008), 69–76.
7. Gerrit K. Boschloo, Albert Goossens, J. Phys. Chem.,100, (1996), 19489–19494
8. M. N. Rashed, A. A. El-Amin, International J. of Phys. Sc., 2 , (2007), 073-081.
9. R.W. Matthews, J. of Phys. Chem., 91, (1987), 3328–3333.
10. D.W. Chen, F.M. Li, A.K. Ray, AIChE J. 46, (2000), 1034–1045.
11. Shuhua Zhou and Ajay K. Ray, Ind. Eng. Chem. Res. 42, (2003), 6020-6033.
12. A. Baba, M.K. Park, R. C. Advincula, W. Knoll, Langmuir, 18, (2002), 4648-4655.
13. Li-Huei Lin, Hsun-Tsing Lee, J. of Applied Polymer Science, 102, (2006), 3341–3344.
14. R.W. Matthews , Photoxidation of organic impurities in water using thin films of titanium dioxide. J. Phys. Chem. 91, (1987), 3328–3333.

Chapter 5

Degradation of methyl orange by TiO₂/polymeric film catalyst under UV lamp

5.1 Introduction

According to the World Health Organization more than 1 billion people in the world are suffering from the lack of access to clean potable water. Waterborne infections account for 80 percent of all infectious diseases in the world [1]. Disinfection power of ultraviolet light has opened a new era in water treatment and application of doped/composite titania (TiO₂) has expanded the spectrum of light to visible light enhancing the efficiency of the operation. Removal of the non-biodegradable organic chemicals in water is of immense interest in recent years. Pharmaceutical compounds, pesticides and dyes are important groups of synthetic organic compounds which are being released in waste water on a daily basis. Release of these organic compounds in wastewater is a serious threat to the environment. These compounds though present in very minute level but may affect human health on daily consumption. Among several synthetic dyes, methyl orange has been employed in many experiments due to its several side effects and unique properties. Methyl orange is one such dye, which is toxic and carcinogenic to human health. If consumed may cause nausea, vomiting, gastrointestinal irritation. Due to its complex aromatic structure conventional water treatment technologies are ineffective in removing these organic dyes completely from the wastewaters [1, 2]. Therefore, the so called Advanced Oxidation Processes (AOPs) have been proposed as the alternative methods for water purification.

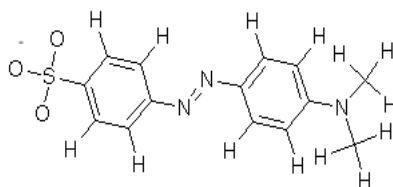


Figure 5.1: Structure of Methyl orange (red form) [3]

Advanced oxidation processes (AOPs) show the potential to become a preferred future treatment technology, attributed to its capability of completely degrading almost all organic pollutants into the ultimate products (carbon-dioxide and water). Currently the main disadvantage of AOPs is their high cost among all AOPs, photo catalysis has been observed to be the most promising and emerging technology. Photocatalytic degradation offers certain advantages over the traditional water treatment technologies. TiO₂ Degussa P25 is being widely used as semiconductor photocatalyst because of its non toxic nature, high corrosion resistance, and chemical stability, insolubility in water and excellent optical transparency in visible and infrared lights. Besides, TiO₂ being cheap and effective in removing organic compounds has attracted attention of researchers [2-5]. The only drawback of TiO₂ semiconductor is its band gap lies in the near-UV of electromagnetic spectrum (band gap -3.2 eV). TiO₂ requires UV-A light of wavelength < 388 nm for photo excitation giving rise to electrons and holes in the conduction and valence band respectively. The valence band holes are powerful oxidants (+1.0 to +3.5V), while the conduction band electrons are good reductants (+0.5 to -1.5V). Most organic photo degeneration reactions utilize the oxidizing power of the holes either directly or indirectly. When TiO₂ is illuminated by UV light, electrons are promoted from the valence band to the conduction band to give electron-hole pairs. The holes in TiO₂ will react with water molecules or hydroxide ions and produce hydroxyl radicals. The interaction of the Positive holes or the negative electrons with the absorbed organic pollutants can give rise to unstable intermediates which are further attacked by hydroxyl or peroxy species occasioning a carbon-carbon bond rupture (or aromatic ring opening) with concomitant release of low molecular weight products which may in turn be further oxidized to CO₂. The attacking hydroxyl radical presumably comes from the photo splitting of water by photo generated hole. Alternatively, the peroxy radical may come from the protonation of a superoxide anion, O₂⁻ produced from electron uptake of dissolved O₂. Oxygen is usually supplied as an electron acceptor to prolong the recombination of electron-hole pairs during photocatalytic oxidation. The hydroxyl radical is a powerful oxidizing agent and attacks organic pollutants present at or near the surface of TiO₂. It causes photooxidation of pollutants according to the following reactions [6-8].



Several researches have been carried out to develop the properties of TiO_2 as photocatalyst by doping methods or by complexing with polymers. Recently, doping TiO_2 with nonmetal atoms has received a lot of attention [9]. Researchers have reported that doping TiO_2 with nitrogen or carbon can lower its band gap and shift its optical response to the visible region [10]. Narrowing the band gap helps TiO_2 to act under light of longer wave length or under visible light. A polymer–metal complex is composed of synthetic polymers and metal ions bound to the polymer ligand by a ionic bond. A polymer ligand contains anchoring sites like nitrogen, oxygen or sulphur obtained either by the polymerization of monomer possessing the coordinating site or by a chemical reaction between a polymer and a low molecular weight compound having the coordinating ability. In addition these TiO_2 -polymer complexes helps in ion selectivity in waste water treatment, recovery of trace metal ions [11]. Researchers investigated the photocatalytic degradation of methyl orange in aqueous TiO_2 under different irradiation sources which showed better decolourization of MeO under solar than UV lamp [12]. Several researchers have studied the degradation of MeO with TiO_2 as slurry under UV lamps. These processes having several disadvantages and requires expensive and time consuming procedures. Although the reaction rate may be high, the slurry systems require the separation of these small catalysts particles from the treated slurry, which has been found to be difficult to accomplish and hence reduce the economical viability [14]. To

avoid the separation problem, photo catalyst particles have been immobilized onto macro supports [15]. So far, most of the researchers carried out immobilisation of catalysts at high temperature which again requires expensive and complex procedures to be followed. Therefore, in our study investigations have been carried out to develop a novel composite for more efficient degradation of MeO in aqueous solution under UV lamp. Polyvinylpyrrolidone has been introduced in the preparation of the composite to make the composite act as a storage house of energy source over a long period of time and polyvinyl alcohol forms a strong film preventing crack formations on the photocatalyst composite. These polymers have been physically cross-linked to form a sponge like structure, which can be more efficient as a photocatalyst than TiO_2 alone. Besides the catalyst immobilisation procedure has been carried out at very low temperature to avoid the disadvantages of high temperature processes. Also, the effects of initial dye concentration, flow rate, pH of methyl orange and irradiation time on photocatalytic degradation rate were investigated. Acidic pH has been observed to be more suitable for degradation of MeO by other researchers [16, 17].

5.2 Experimental set up and procedure

5.2.1 Materials and equipment

The materials used in this study include; TiO_2 Degussa P25 (Evonik), Polyvinyl alcohol and Polyvinylpyrrolidone (Sigma Aldrich), Methyl orange (VWR), Beaker (Chemistry store, UWO), UV-Vis spectrophotometer (Shimadzu), UV lamp (Phillips) and Methrom pH meter has been used to analyse the pH of the solutions.

5.2.2 Preparation of TiO_2 -polymeric composite

The polymers used to prepare the catalyst have been considered non-toxic by WHO and also have been proved to by toxicology researches [18, 19, and 20]. 24.3 % w/w of PVA and 11% w/w of Gelatin were dissolved and mixed properly in distilled water and to get a

transparent solution. Next, 21.6 % w/w of PVP dissolved in the solution of ethyl alcohol and water (1: 2) at 45° C. The solution was reacted for 15 minutes followed by dispersion of 43 % w/w TiO₂ Degussa P25 powder in the mixture.

5.2.3 Preparation of immobilized catalyst

The support used in this research was a circular sand blast glass plate of 99 sq. cm areas. The TiO₂/polymeric solution was poured on the sand blast side of glass plate and stored around -2 °C for 5 hours. The total mass of catalyst deposited per unit area was determined by weighing the glass plate before and after the catalyst coating.

5.2.4 Photocatalyst composite activity test

The TiO₂-polymeric composite coated glass slide was dipped in an aqueous solution of 0.1M AgNO₃ and 10% C₂H₅OH. Next, the glass slide was illuminated by UV light. The Photo catalyst coating was found to change colour (turns brownish black) immediately due to formation of AgO [18]. This proved that the photocatalyst was effective under the UV light.

5.2.5 Methyl orange photodegradation and analysis

The photo reactor consists of one circular quartz glass plate placed in a stainless steel casing held between two steel plates. The TiO₂-polymeric composite catalyst was immobilised on the glass plate. The reactor consisted of a single inlet and outlet system. The UV lamp (Philips) was placed under the reactor inside a wooden box with a small opening. The radiation intensity of the lamp was 275 nm. The lamp was constantly cooled by air circulation through a fan fitted to the wooden box. The whole system was covered by a box so that no stray light can enter the reactor.

The methyl orange solution was kept in a conical flask connected to a peristaltic pump from which the solution was pumped into the reactor. After photodegradation the solution was pumped out of the reactor into the same conical flask which was continuously stirred by a magnetic stirrer. The concentration change of the solutions were continuously examined in UV-Vis spectrophotometer at ($\lambda = 465$ nm). Also, arrangements have been made to measure the pH of the solutions directly after the photo degradation before reaching the original solution in the conical flask. To study the role of light intensity in degradation of the pollutant, wire mesh was placed between the lamp and the bottom plate of the reactor. In this experiment the t_r (residence time) of methyl orange in the reactor has been calculated. This residence time in the reactor was plotted against the concentration to measure the removal rate of the pollutant.

5.3 Results and Discussions

5.3.1 SEM analysis of the photocatalyst

The Scanning electron microscopy was carried out to study the topographical morphology of the TiO₂-PVA composite. For verification of a uniform structure micrographs of the dried membrane were taken using a scanning electron microscope (Hitachi F-4000).

From SEM image in Fig. 5.2, it was observed that the TiO₂-polymeric catalyst film have porous sponge like surface which in turn may helped to adsorb many organic compounds. Also the SEM study revealed the specific pore volume and pore density. SEM image of the morphology of the photocatalyst films have been shown in the following Figures. With the highest magnification in particular, the freeze-dried film has been observed to be homogenously interspersed with pores of various diameters ranging from 50 μm to 300 μm . The average pore area was found to be 572 μm^2 . The pore density ranged from 7-10 pores per square mm.

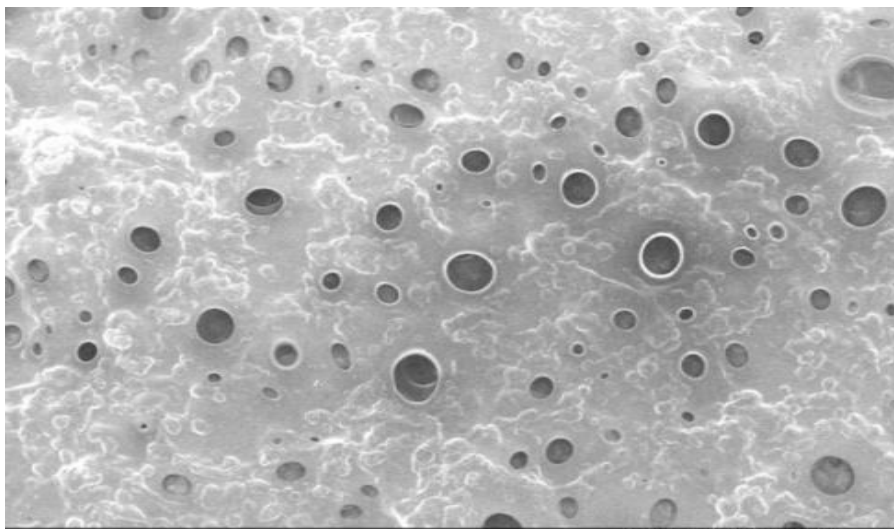


Figure 5.2: SEM image of TiO₂/polymeric film

5.3.2 Blank experiment

Dark reaction was carried out to saturate the catalyst surface by dye adsorption so that during the reaction under UV light no more adsorption of dye occurs. This experiment was carried out with photo catalyst but no illumination. Dark reaction was carried out with different concentrations of methyl orange solutions (100 ppm, 50 ppm, 30 ppm, 15 ppm and 5 ppm), and changes were observed in UV- Visible spectrophotometer. The changes in concentrations observed, proved adsorption of methyl orange on the catalyst surfaces.

Adsorption equilibrium constants were determined from both dark reaction and UV reaction. The small change in concentration of methyl orange in absence of light (dark reaction) in presence of a catalyst composite can be attributed to the adsorption of methyl orange onto the surface of the TiO₂-polymeric composite. The concentration of MeO adsorbed on the catalyst was calculated from the difference between the initial and equilibrium concentrations. Having prepared the plot of $1/q_e$ Vs $1/C_0$ (Fig.5.3), where q_e is the amount of dye adsorbed on the catalyst surface and C_0 is the initial concentration, q_m and K were obtained. This reaction appeared to follow Langmuir adsorption isotherm:

$$q_e = q_m K C_0 / (1 + K C_0) \quad (7)$$

q_m and K are the saturation and adsorption equilibrium values respectively.

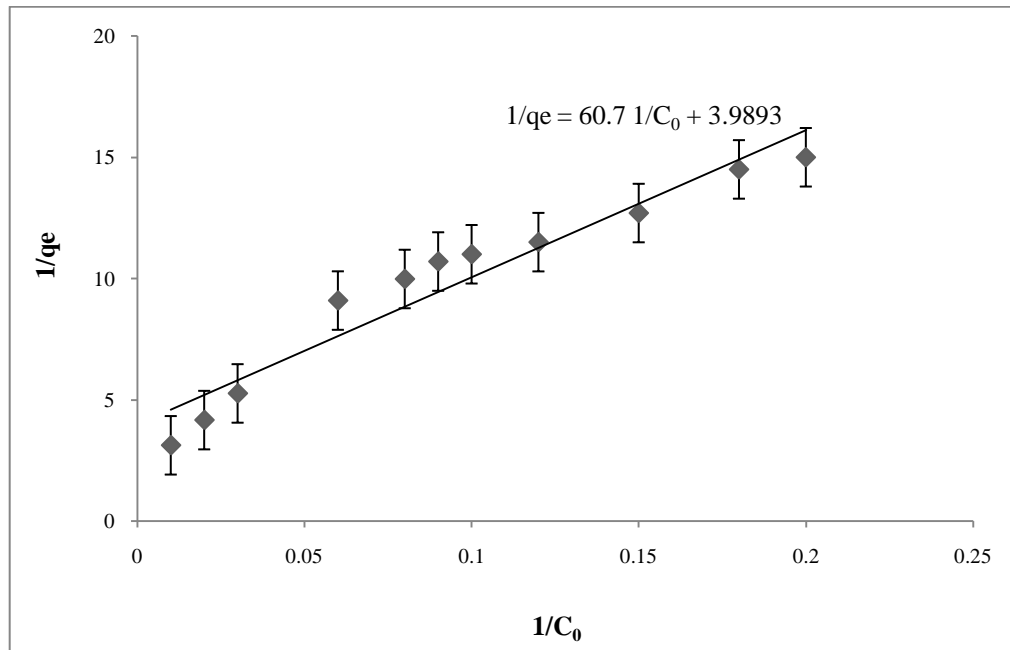


Figure 5.3: Dark reaction of MeO degradation in presence of TiO_2 -polymeric photocatalyst. Experimental conditions [$I = 22 \text{ mW/cm}^2$, $pH = 5.8 - 6.2$]

From the plot in Fig.5.3, the value of K obtained was 0.065 L/mg and q_m was obtained to be 0.25 mg/L . Here q_m is the maximum amount of dye adsorbed and K is the adsorption constant.

5.3.3 Effects of flow rates on the photodegradation of methyl orange

Experiments were carried out at several flow rates (25 ml/min, 42 ml/min, 85ml/min and 100 ml/min). In Fig. 5.4 the effects of different flow rates on the removal percentage of dye have been shown. From the figure it has been revealed that with the increase of flow rate the rate of removal of dye increased. Higher removal efficiency was observed at higher flow rate due to induced mixing and turbulence which reduced mass transfer

resistances. Therefore the flow rate of 85 ml/min was chosen as the optimum flow rate for the rest of the experiments.

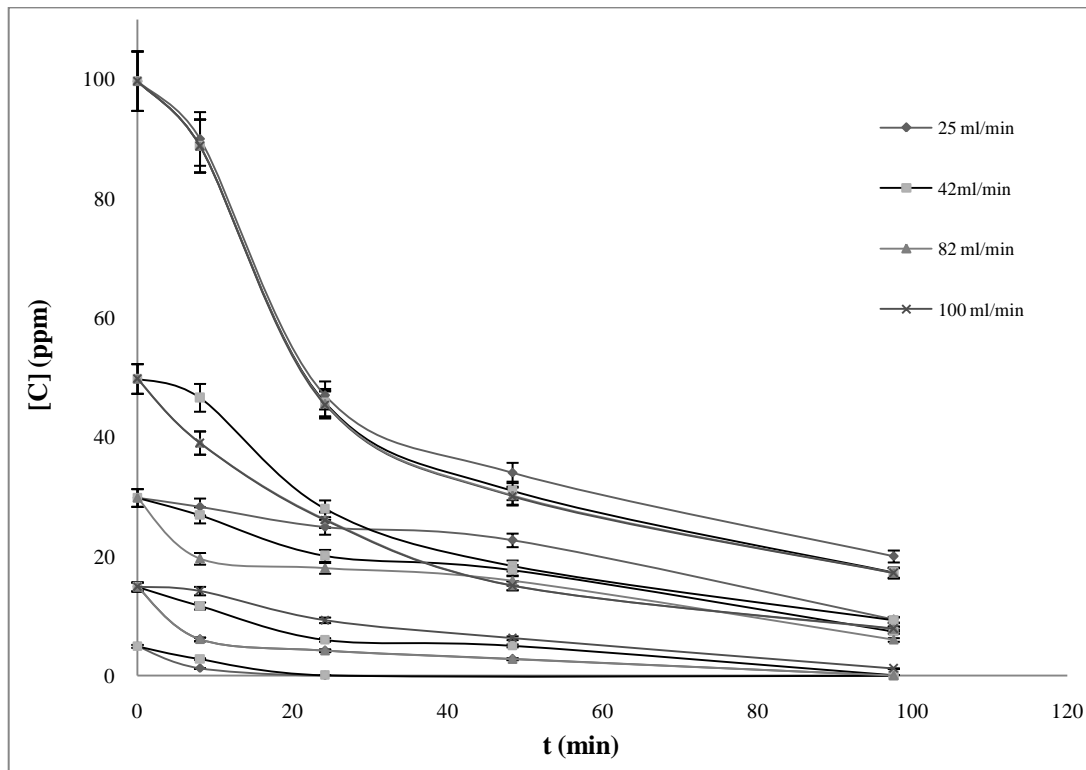


Figure 5.4: Effects of flow rates on the photo degradation of MeO. Experimental conditions [I = 22 mW/cm², pH = 5.8-6.2]

It was also been observed that the effect of the increase of flow rate on the degradation rates was less for the higher concentrated solutions than for the low concentrated ones. This can be explained as at high concentration, the rate of degradation was independent of the mass transfer effects while the reverse for low concentrated solutions.

5.3.4 Photodegradation of MeO

For methyl orange solution (100 ppm), the photo degradation reaction was continued till 140 minutes ($t_r = 112.9$ min) (the residence time). The photo degraded samples were collected for spectrophotometric observations at very small intervals of time both at the beginning and also towards the end of the reaction.

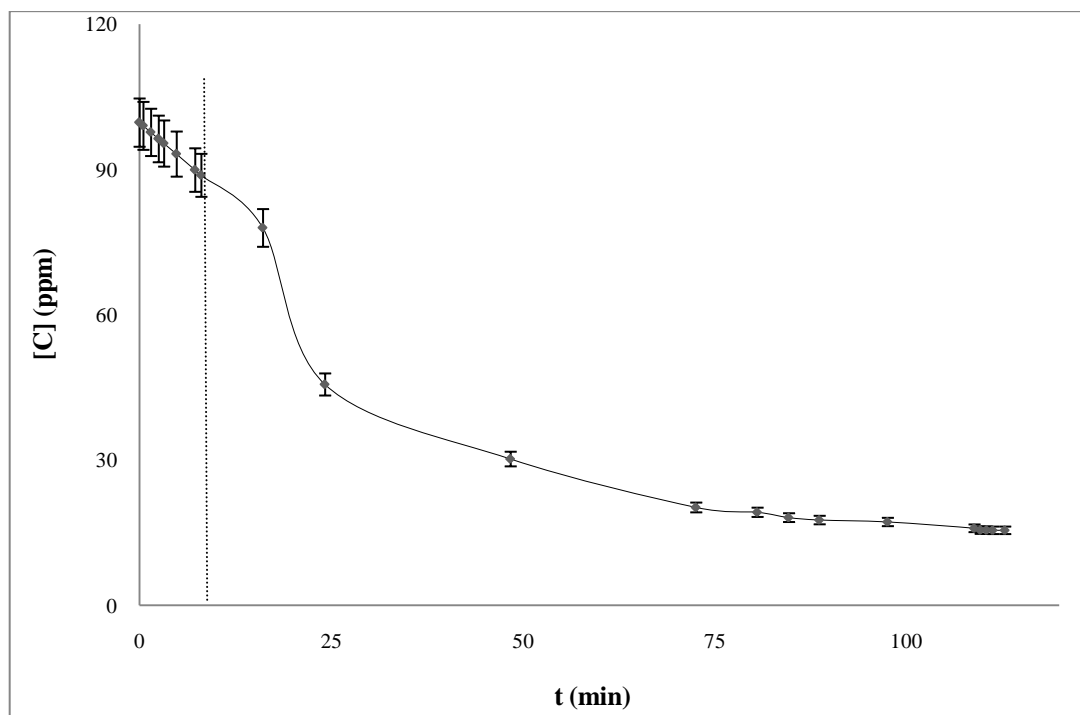


Figure 5.5: Photodegradation of MeO. Experimental conditions [$C_0 = 100$ ppm, $I = 22\text{mW/cm}^2$, pH - 5.8 -6.2, Flow rate - 85 ml/min]

From the Figure 5.5 rate constant of the photocatalysis has been calculated, from the initial degradation of 100 ppm MeO solution. The rate constant was calculated to be 1.34 mg/L/min. It was also observed that degradation rate was independent of the mass transfer effects at very high concentrations. It was found that TiO_2 -polymeric composite catalyst degraded 85% of the methyl orange under the UV light in 140 minutes.

$$\epsilon\% = (C_0 - C)/C_0 \times 100 = 85\% \quad (5.8)$$

Although 90 - 95% decolourisation of methyl orange under different irradiations had been reported [12] it should be noted that methyl orange is light sensitive and decolouration does not necessarily mean carbon content reduction. Buffer solution was used to maintain pH at acidic level and higher degradation rates were observed.

5.3.5 Effects of initial concentration

The initial MeO concentration in the solution affects the photo degradation rate. Short time was necessary to study initial concentration effect and therefore every experiment was carried out for 8 minutes. The experiments were carried out to calculate the intrinsic rate constant, which was independent of extrinsic and intrinsic mass transfer resistances. The organic dye concentrations in waste water usually range from 0.01- 0.05 g/dm³ [19]. Therefore, methyl orange solutions of different concentrations were used (100ppm, 50 ppm, 30 ppm, 15 ppm, 5 ppm). The solutions were subjected to photo degradation at pH 5.8 - 6.2 under UV lamp of 175 Watt and wavelength ($\lambda = 275$ nm) for 8 minutes to observe the initial degradation rate. The reactions were carried out at pH 5.8 - 6.2, without the addition of buffers. The graph of concentration vs. time shown in the Fig. 5.6 explains that the degradation of MeO followed the model of Langmuir-Hinshelwood. It was observed that the degradation rate decreased with the decrease of initial concentration. With the increase of the initial concentration the probability of reaction between dye molecules and the photocatalyst also increased, which led to an enhancement in the degradation rate.

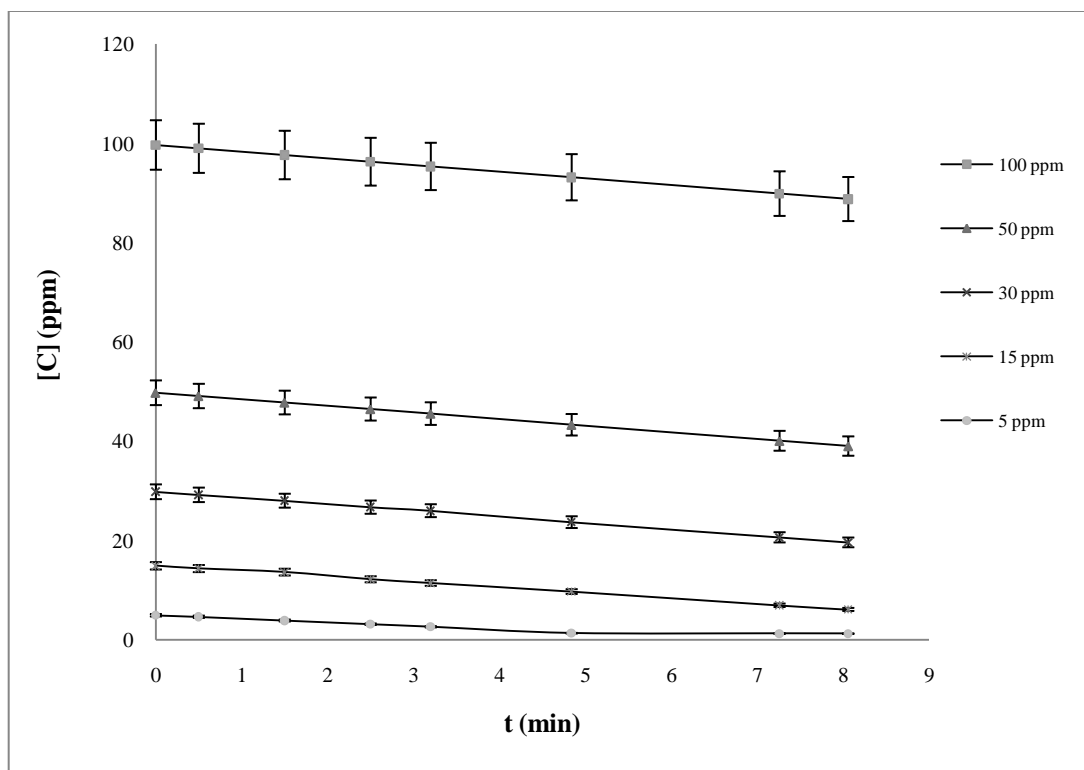


Figure 5.6: Effects of initial concentrations on the photocatalytic degradation of MeO. Experimental conditions [I = 22 mW/cm², pH - 5.8-6.2, Flow rate - 85 ml/min]

Interestingly, also in some other studies [20, 21] the photocatalytic degradation rate was shown to decrease with the increase of initial concentration. The decrease was claimed to be due to the increasing number of photon absorption by the catalyst in lower concentration. While a researcher has reported that degradation rate increased with the increase of dye concentration (upto 100 ppm) to a certain limit and further increase lead to a decrease in degradation rate, which is due to the reduction in generation of OH radicals on the catalyst surface [20]. Our studies also showed that the degradation increased with the increase of dye concentration up to 100 ppm. This was due to the effect of mass transfer resistances at lower concentration, which decreased the rate of degradation. While at higher concentration, the degradation rate remained independent of the mass transfer effects. Also, with the increase of concentration, the probability of reaction between pollutant molecules and the catalyst increased, thereby increasing the rate of reaction. Besides, high concentrated MeO solutions are more acidic than at lower concentrated ones and the UV exposure, also contributed in shifting the pH from acidic to

alkaline. Therefore, degradation rate was found to decrease with decrease of concentration. Thus combined effects of UV light and initial concentration decreased the degradation rate with time.

5.3.6 Kinetics of photodegradation

TiO₂-PVA catalyst was observed to be efficient in degrading MeO solution. The degradation kinetics of methyl orange followed the Langmuir-Hinshelwood (L-H) model.

$$r = -dC/dt = kKC_t/(1 + KC_t) \quad (5.9)$$

r is the photo catalytic degradation rate, k is the L-H rate constant, K is the Langmuir adsorption constant of the methyl orange in the photo catalytic degradation reaction. A linear plot of r_0^{-1} Vs C_0^{-1} is often obtained to estimate as the L-H rate constant and K as the Langmuir adsorption constant for methyl orange in the photo catalytic degradation reaction.

$$r_0 = kKC_0/(1+KC_0) \quad (5.10)$$

The equation is further expressed in a linear form

$$1/r_0 = 1/(kKC_0) + 1/k \quad (5.11)$$

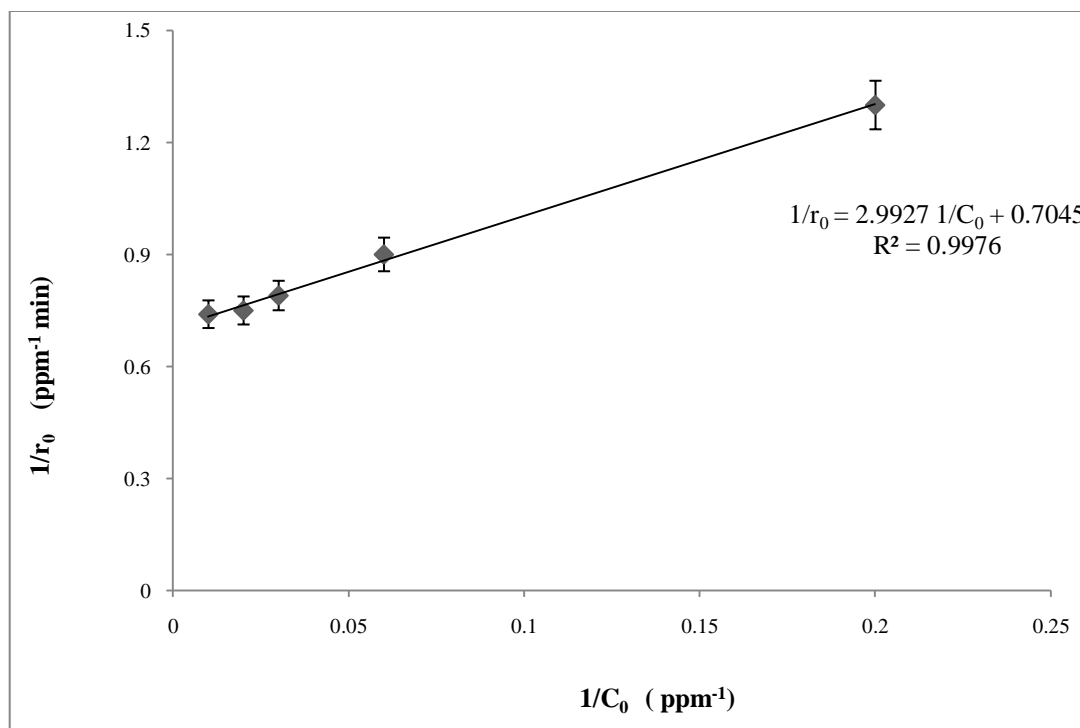


Figure 5.7: Photodegradation of MeO with TiO₂-polymeric catalyst. Experimental conditions [I = 22 mW/cm², pH = 5.8-6.2, Flow rate = 85 ml/min]

The rate constant was found from Fig. 5.7, to be $k = 1.42$ mg/L/min, which is close to that obtained from the degradation of 100 ppm MeO (the $k = 1.34$ mg/L/min). K was found to be 0.23 Lmg⁻¹.

The degradation rate was observed to decrease with the decrease of concentration. This was due to the combined effect of mass transfer resistances and the pH shift during the reaction changed the degradation rate. The shift from acidic pH to alkaline lowered the degradation rate. At very high concentration the MeO showed acidic pH which changed towards alkalinity with time due to UV exposure, so the interaction between the TiO₂ surface and MeO molecules changed due to change in surface charges. The pH changed the surface charge on TiO₂ particles which in turn varies the attraction force between TiO₂ particles and methyl orange molecules. Also, with the progress of experiment the catalyst gets cross-linked by the UV light which also affected the degradation rate.

Several researches have been carried out on photo degradation of organic dyes under UV lights in presence of immobilized TiO₂ coatings or slurry, reporting the rate constants *k* and its dependence on different factors [12, 15, 20, and 21]. Our results cannot be compared with the rate constant datas reported by other researchers, mainly due to the differences in the nature of the photocatalysts and the light sources used but in our research it has been observed that the immobilised TiO₂-polymeric film was able to degrade MeO under UV lamp at a rate of 1.42 mg/L min⁻¹.

5.3.7 Total organic carbon measurement

The total organic carbon content was measured after the degradation of methyl orange under UV lamp in presence of the TiO₂-polymeric photocatalyst. After photodegradation the total organic carbon content of methyl orange was observed to decrease with time. The decrease of carbon content signifies the degradation of the methyl orange into nontoxic decomposition compounds. Table 5.1., showed the decrease of TOC level after photodegradation reaction, at different time intervals.

Table 5.1: Total organic carbon content measurement

Time	Carbon content (mg/L)
0	1428
10	952
20	713
30	522
60	319
90	230
120	90
140	7.2

5.3.8 Effects of pH on the degradation of methyl orange

It is well known that pH value has an influence on the rate of degradation of some organic compounds in photocatalytic processes [16, 17]. The photodegradation of methyl orange was studied at three different pH values (4, 5.8, and 7.8). The pH was adjusted by the addition of 0.1 M potassium hydrogen phthalate (100 mls) + 0.1 M HCl (0.2 ml) at

varied ratio for acidic pH 4 and 5.8. For alkaline pH 7.8, 0.1 M KH_2PO_4 (100 ml) + 0.1 M NaOH (7.2 ml) were used. The pH value is a complex parameter since it is related to the state of the photocatalyst surface, which affects the adsorption of MeO on the photocatalyst [20]. The pH shifted more towards alkalinity with time. Therefore, experiments have been carried out at different pH level, controlled by buffers. Methyl orange of different concentrations (100ppm, 50 ppm, 30 ppm, 15ppm, 5 ppm) were treated with acidic and alkaline buffer solutions and thereafter photo degradation were carried out at pH 4, pH 5.8 and pH 7.8. From the Fig. 5.8- Fig. 5.12, it was observed that the effect of pHs on the degradation of the pollutants were variable. Several researches have been carried out to explain the effects of pH on photodegradation of dyes. Our studies have been carried out at pH 4 - pH 7.8. This pH test has been performed to explain why and how the degradation rate decreases with time. The results indicated that the pH value of the pollutant was a key factor in dye degradation and changing the surface charge of the catalyst also influenced the photocatalytic reaction. pH changed the adsorption of dye molecules onto the TiO_2 surface. For TiO_2 P25 the pzc is around pH 6.2 [22]. So, when pH was less than 6 a strong adsorption of MeO on the TiO_2 particles was observed as a result of electrostatic attraction of the positively charged TiO_2 with the dye. At alkaline pH the MeO molecules are negatively charged and their adsorption was also expected to vary due to columbic repulsion. Some researchers [12, 15] have shown at acidic pH the degradation rates vary from depending upon the concentration. In this experiment at acidic pH of 4 the degradation rate was observed to be $2.6 \text{ mg/L/min}^{-1}$, while at uncontrolled pH, the rate was 1.1 mg/L/min .

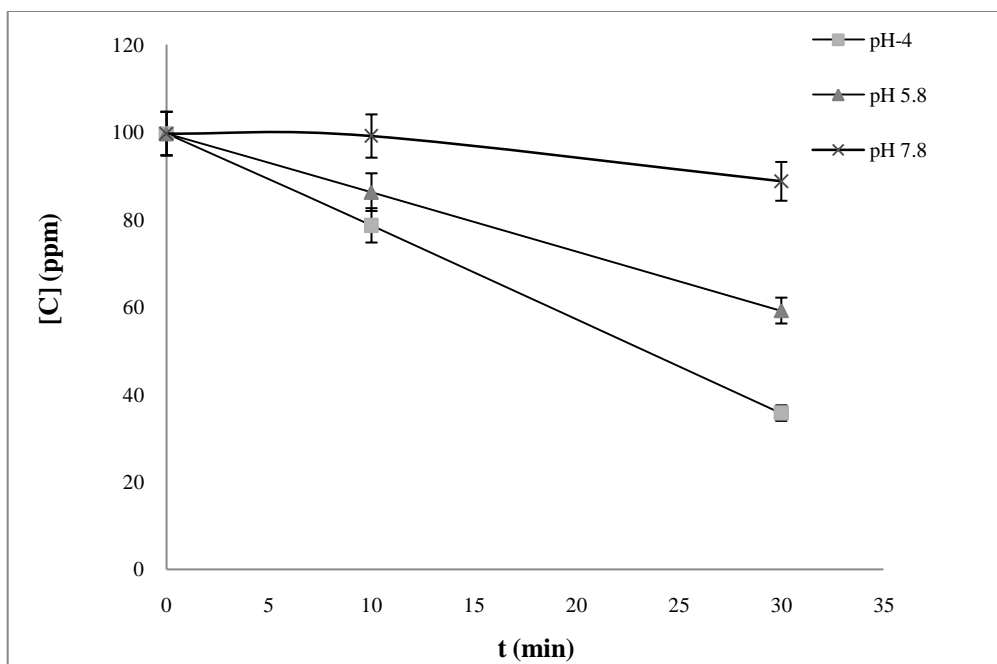


Figure 5.8: Photodegradation of MeO with TiO₂-polymeric catalyst. Experimental conditions [C₀ = 100 ppm, I = 22 mW/cm², Flow rate = 85 ml/min]

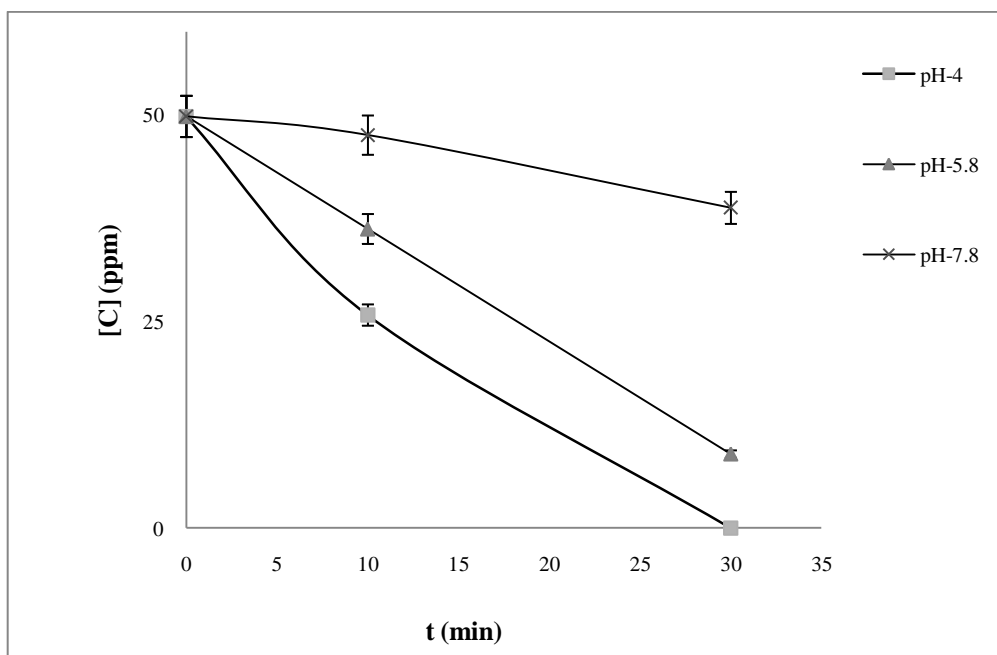


Figure 5.9: Photodegradation of MeO with TiO₂-polymeric catalyst. Experimental conditions [C₀ = 50 ppm, I = 22 mW/cm², Flow rate = 85 ml/min]

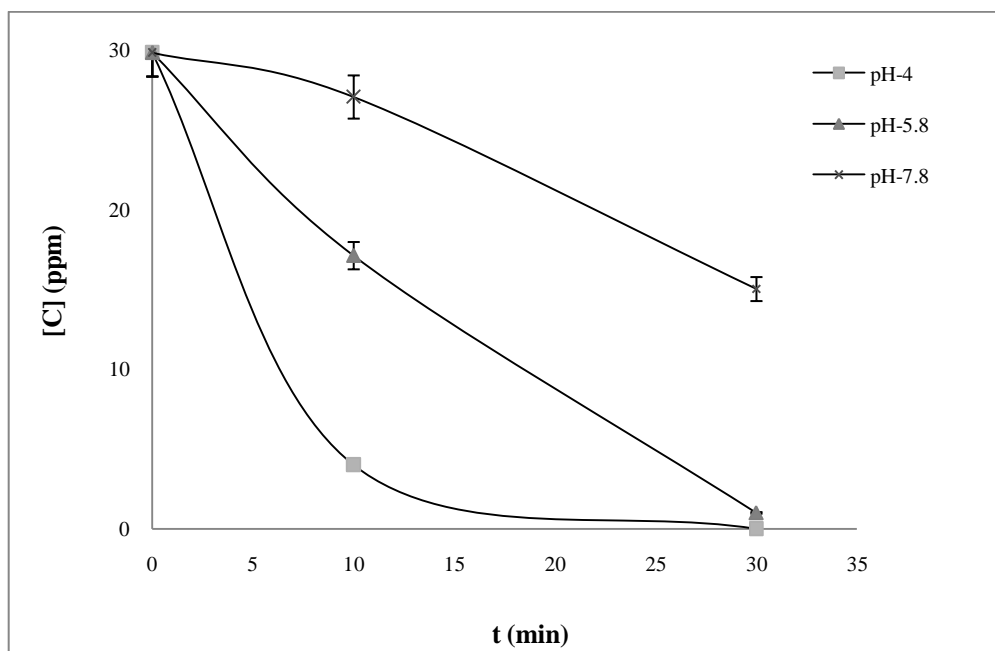


Figure 5.10: Photodegradation of MeO with TiO₂-polymeric catalyst. Experimental conditions [C₀ = 30 ppm, I = 22 mW/cm², Flow rate = 85 ml/min]

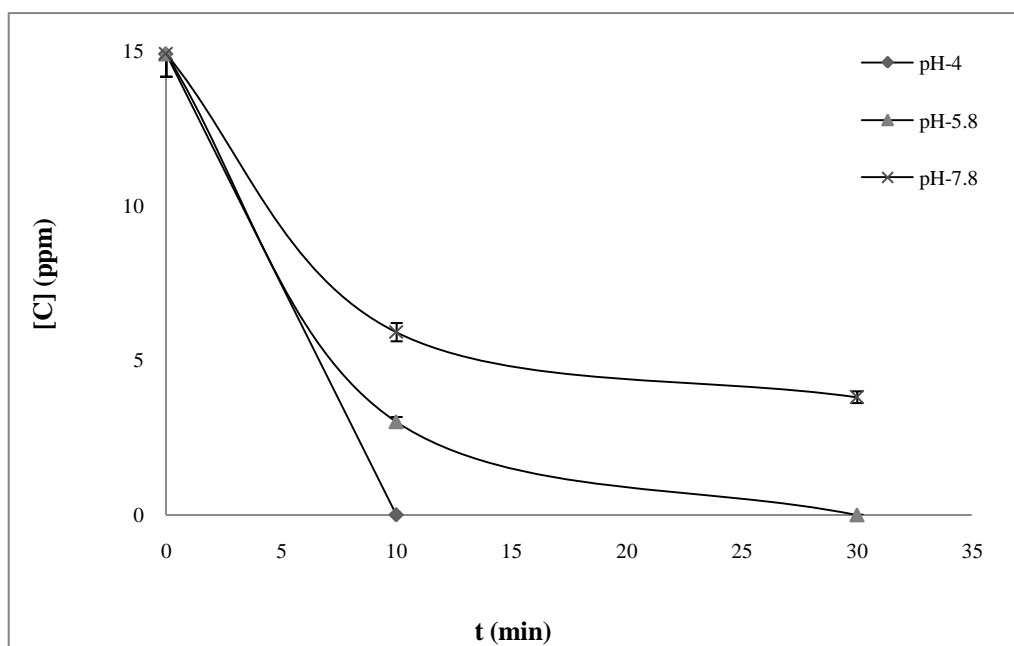


Figure 5.11: Photodegradation of MeO with TiO₂-polymeric catalyst. Experimental conditions [C₀ = 15 ppm, I = 22 mW/cm², Flow rate = 85 ml/min]

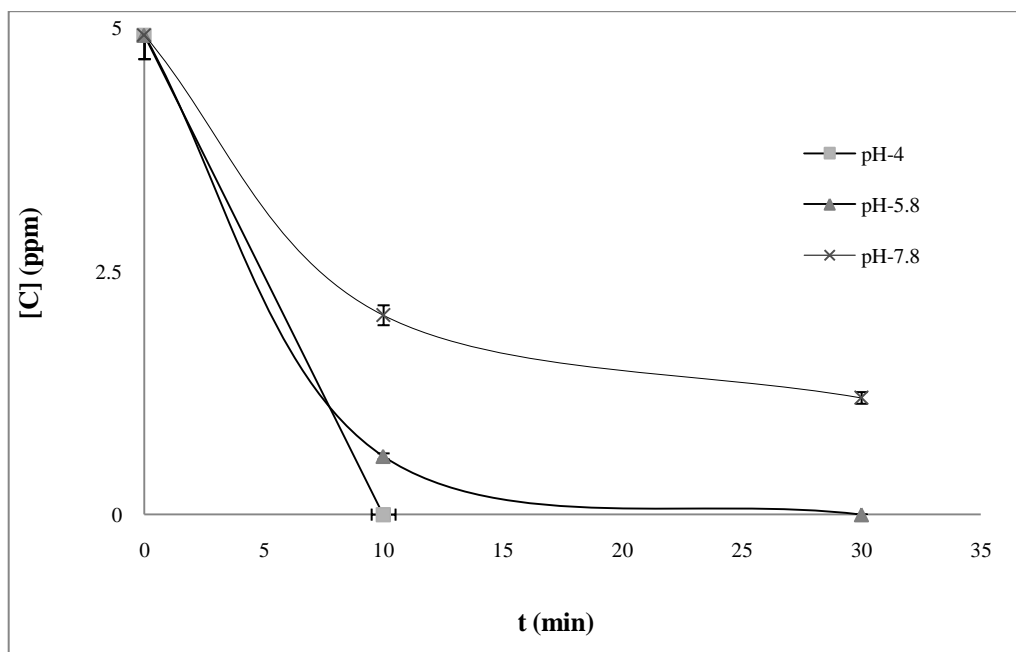


Figure 5.12: Photodegradation of MeO with TiO₂-polymeric catalyst. Experimental conditions [C₀ = 5 ppm, I = 22 mW/cm², Flow rate = 85 ml/min]

5.3.9 The effects of light intensity on the degradation of Methyl orange

Light intensity plays a major role in photodegradation. To study the effect of light intensity on the degradation of MeO, the experiments were conducted at varying light intensity. MeO solutions of various concentrations were subjected to light intensity study, after dark reaction phenomenon was carried out. The intensity of the light was varied by placing different mesh screens between lamp and the reactor plate. From the Fig. 5.13- Fig. 5-16, it can be explained that at lower intensities the rate increases linearly with the increase in light intensity. While at higher intensities, the rate remained unaffected. This reveals at higher intensities the rate is independent of light intensity. This phenomenon occurred due to electron hole recombination competitiveness on catalyst composite surface with varying light intensity [13]. Here, the k values are obtained from this equation:- $(1 + kC)/kC (-dc/dt)$

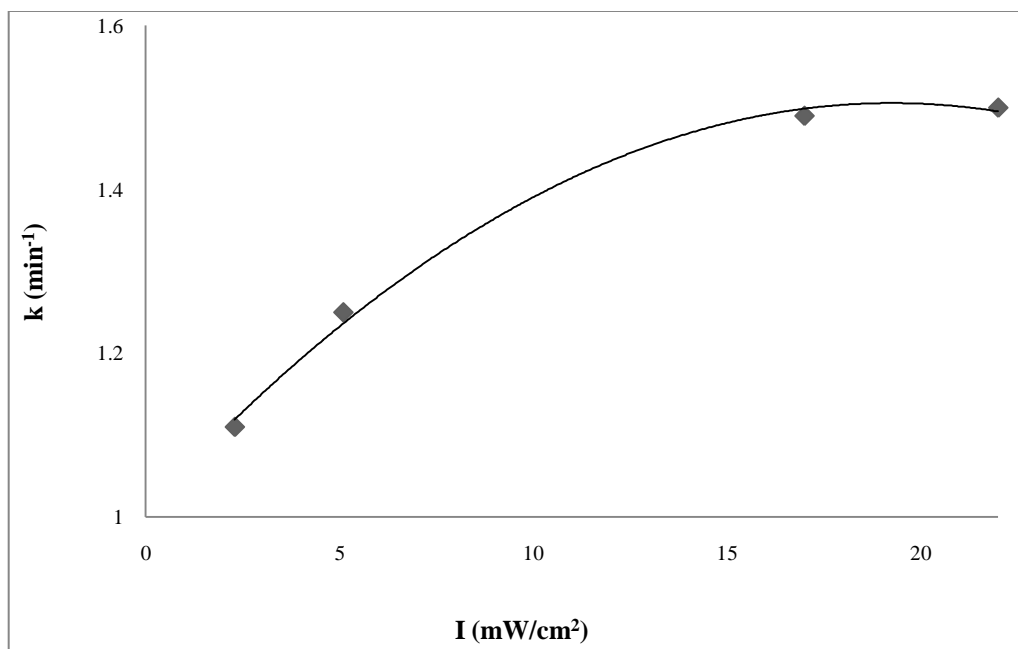


Figure 5.13: Photodegradation of MeO with TiO₂-polymeric catalyst. Experimental conditions [C₀ = 100 ppm, Flow rate = 85 ml/min, pH – 5.8-6.2]

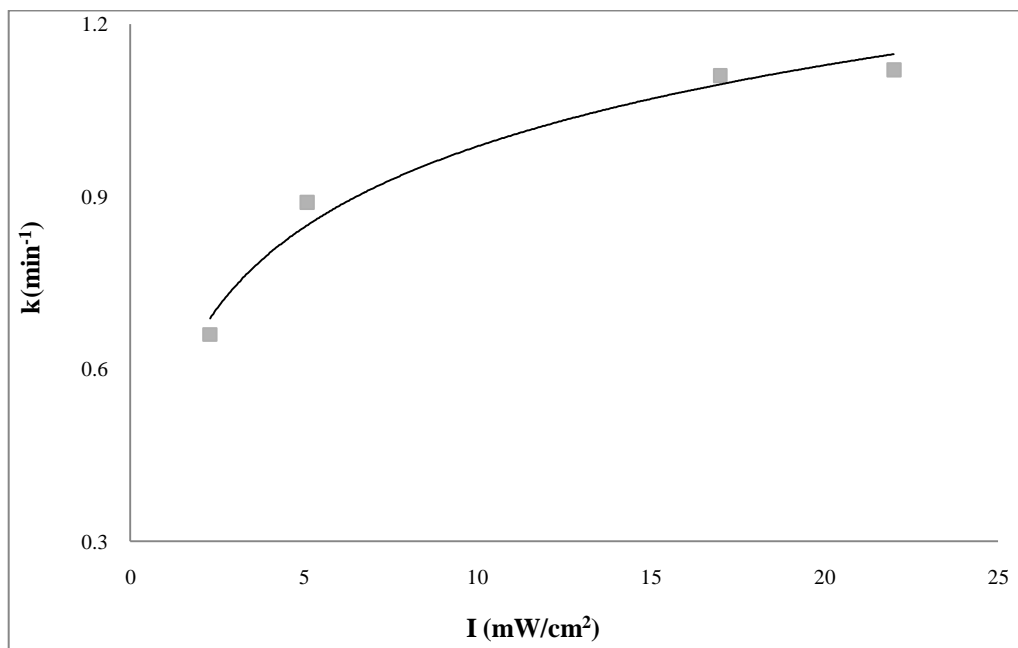


Figure 5.14: Photodegradation of MeO with TiO₂-polymeric catalyst. Experimental conditions [C₀ = 50 ppm, Flow rate = 85 ml/min, pH – 5.8-6.2]

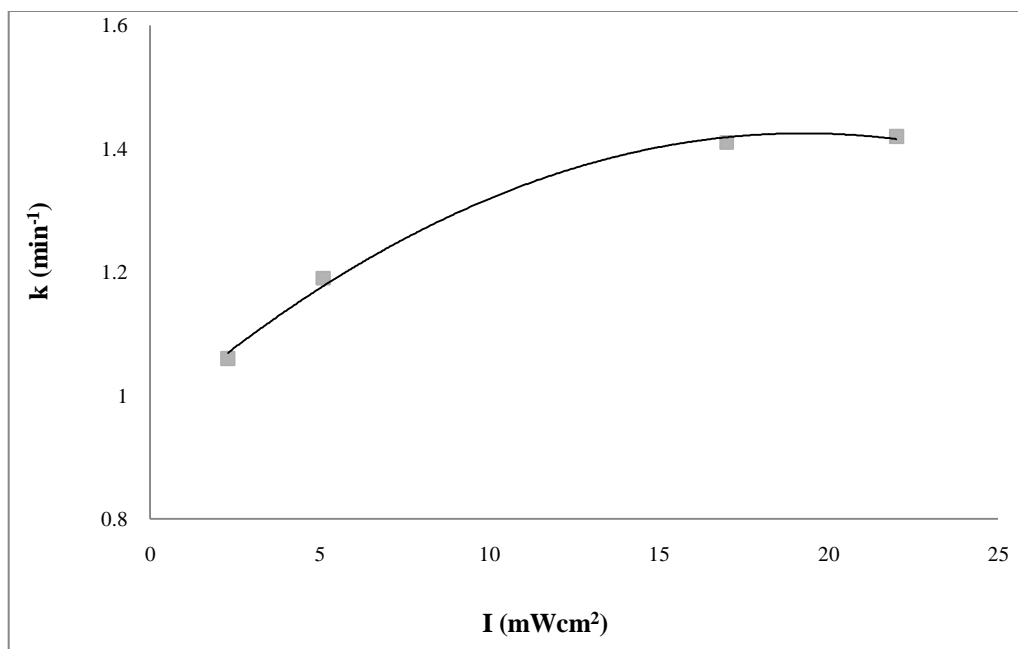


Figure 5.15: Photodegradation of MeO with TiO₂-polymeric catalyst. Experimental conditions [$C_0 = 15$ ppm, Flow rate = 85 ml/min, pH – 5.8-6.2]

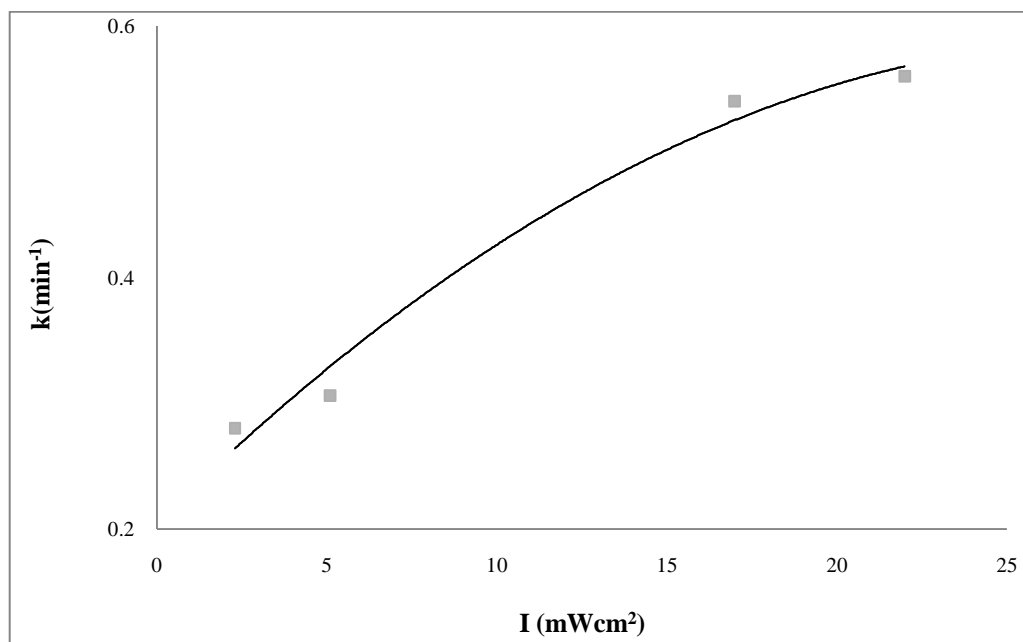


Figure 5.16: Photodegradation of MeO with TiO₂-polymeric catalyst. Experimental conditions [$C_0 = 100$ ppm, Flow rate = 85 ml/min, pH – 5.8-6.2]

5.4 Conclusions

The TiO₂/polymeric composite catalyst developed in this experiment was observed to degrade MeO under solar rays and UV lamp. The degradation kinetics fitted into Langmuir-Hinshelwood model. The porous TiO₂-polymeric catalyst coating was found to be efficient in degrading methyl orange under UV lamp. Also, the development of the porous sponge like nature of the catalyst composite contributed in the purification process by adsorption. In this experiment TiO₂ has been incorporated in the network of polymers. PVA formed the matrix and also played a role to form smooth coating. Also, due to its economical preparation procedure and the non-toxic nature of its formulation ingredients, it can be concluded that the TiO₂/polymeric film catalyst has high potential in photocatalysis field. Several other physical and chemical factors monitor the degradation rate which have been studied and discussed in this thesis. Besides, from the flow rate experiment results, it can be concluded that at higher flow rate the degradation was observed to be faster which can be attributed to external mass transfer resistance minimization. The degradation rates changed with the change of UV light intensities which proved the effect of light intensities on the degradation. At lower intensity, the degradation was proportional to light intensity. While at higher intensities the degradation rate remained unaffected. This was due to low light intensity reactions involving electron-hole formation are predominant and electron-hole recombination was negligible. However, at increased light intensity electron-hole pair separation competed with recombination, thereby causing lower effect on the reaction rate. The kinetics study revealed that methyl orange degradation followed L-H model. The degradation rate was observed to decrease with time, which can be explained as the combined effects of the UV cross-linking on the polymer matrix and the pH shift towards alkalinity with UV exposure. The TOC measurement showed the photodegradation reduced the carbon content of the methyl orange.

5.5 Nomenclature

TiO₂ - Titanium Dioxide

SEM - Scanning Electron Microscopy

TOC - Total Organic Carbon content

PVA - Poly Vinyl Alcohol

PVP - Poly Vinyl Pyrrolidone

MeO - Methyl Orange

5.6 References

1. Peter Vikeshland, Krista L Rule, <http://www.innovationmagazine.com/innovation/>. Retrieved May 2010
2. C.C. Liu, Y.H. Hsieh, P.F. Lai, C.H. Li, C.L. Kao, *Dyes and Pigments*, 68, (2008), 2-6.
3. Beata Zieli ska, Joanna Grzechulska and Antoni W. Morawski, *J. of Photochemistry and Photobiology A: Chemistry*, 157, (2003), 65-70.
4. Fujishima, K. Honda, *Nature*, 238, (1972), 37-38.
5. L. Andronic, and A. Duta, *Mat. Chem. and phys.*, 112, (2008), 3-8.
6. Tang J, Durrant JR, Klug DR., *J. Am Chem Soc.*, 130, (2008), 13885-91.
7. J.Wong, <http://www.peakpureair.com/tio2-photocatalytic.htm>. Retrieved Jan. 2009.
8. A.A. Fujishima, T.N. Rao and D.A. Tryk, *J. of Photochem. and Photobio. C.Photochemistry Reviews*, (2000).
9. Rocío Silveyra, Luis De La Torre Sáenz, Wilber Antúnez Flores, V. Collins Martínez, A. Aguilar, Elguézabal, *Catalysis Today*, 107, (2005), 602-605.
10. Bitao Sua, b, Xiuhui Liub, Xiaoxia Pengb, Tai Xiaob and Zhixing Su., *Materials Sc. and Engg.* 349, (2003), 59-62.
11. L.Andronic, S.Manolache , and A. Duta, *J. of nanosci. and nanotech*, 8, (2008), 2-8.
12. M.N. Rashed, A.A.El-Amin, *Int. J. of Physical Sciences*, 2, (2007), 131-145.
13. P.S. Mukherjee, A.K.Ray, *Chem. Eng. Technol.* 22, (1999), 253–260
14. D. Chen, A.K.Ray, *Applied Catalysis B: Environmental*, 23, (1999), 143-147.
15. Dingwang Chen, Fengmei Li, and Ajay K. Ray, *J. of AIChE*, 46, (2000), 846-1100.
16. Vincenzo Augugliaro, Claudio Baiocchi, Alessandra Bianco Prevot, Elisa García-López, Vittorio, *Annali di Chimica, Società Chimica Italiana*, 93, (2003), 639-644.
17. Loddo Sixto Malato, Giuseppe Marci, Leonardo Palmisano, Marco Pazzi and Edmondo Pramauro, *Chemosphere*, 149, (2002), 1223-1230.
18. Nikolai Kislov, Jayeeta Lahiri, Himanshu Verma, D. Yogi Goswami, Elias Stefanakos, Matthias Batzill, *Langmuir*, 25, (2009), 3310–3315
19. Hae Keun Yoo, Dong Seok Seo and Jong Kook Lee, *J. of Ceramic Processing*

Research, 5, (2010), 150-161.

20. S. K. Kansal, G. Kaur, S. Singh, Reaction Kinetics and Catalysis Letters, 98, (2009), 177-186.
21. S.B. Sakthivela, M.V. Neppolianb, B. Shankarb, M. Arabindoob, V. Palanichamyb, V. Murugesanb, Sol. Energy Mater. Sol. Cells, 77, (2003), 65-82.
22. Priti Bansal, Dhiraj Sud, Desalination, 267, (2011), 244-249.
23. Jung-Chuan Chou, Lan Pin Liao, Thin Solid Films, 476, (2005), 157-161.

Chapter 6

Photodegradation of aspirin under both solar and UV light in presence of slurry TiO₂

6.1 Introduction

Heterogeneous photocatalysis has received considerable attention in recent years as a viable treatment technology for handling industrial effluents and contaminated drinking water. The process couples low-energy ultraviolet light with semiconductors acting as photocatalysts. In this process, electron-hole pairs that are generated by the band-gap excitation carry out in situ degradation of toxic pollutants. The holes act as powerful oxidants to oxidize toxic organic compounds, while electrons can reduce toxic metal ions to metals, which can subsequently be recovered by solvent extraction [1]. Photocatalytic degradation offers certain advantages over traditional water treatment methods. Complete destruction of most contaminants is possible without the need of additional oxidizing chemicals such as hydrogen peroxide or ozone. Degussa P25 TiO₂ is widely used as the photocatalyst, which requires UV-A light (*wavelength* < 380 nm) of intensity 1-5 W/m² for photo excitation. The catalyst is cheap and can also be activated with sunlight [2]. TiO₂ catalyst has been used in two forms: freely suspended in an aqueous solution and immobilized onto a rigid inert surface. In the former case, a high ratio of illuminated catalyst surface area to the effective reactor volume can be achieved [3], and almost no mass-transfer limitation exists because the diffusional distance is very small, resulting from the use of ultrafine (< 30 nm) catalyst particles [4]. In large-scale applications, however, the catalyst particles must be filtered prior to the discharge of the treated water, even though TiO₂ is harmless to the environment. Hence, a liquid-solid separator must follow the slurry reactor. The installation and operation of such a separator will raise the cost of the overall process because the separation of the ultrafine catalyst particles is a slow and expensive process. Besides, the penetration depth of the UV light is limited because of the strong absorption by TiO₂ and dissolved organic species, particularly for dyes. All of these disadvantages render the scale-up of a slurry reactor very difficult [5]. The preceding problem can be eliminated by immobilizing the TiO₂ catalyst over suitable

supports [6, 7]. The design and development of an immobilized thin catalyst film makes commercial-scale applications of TiO₂-based photocatalytic processes for water treatment possible [8]. The designs are more likely to be useful in commercial applications because they provide at least three important advantages. First, they eliminate the need for the separation of the catalyst particles from the treated liquid and enable the contaminated water to be treated continuously. Second, the catalyst film is porous and can therefore provide a large surface area for the degradation of contaminant molecules. Third, when a conductive material is used as the support, the catalyst film can be connected to an external potential to remove excited electrons to reduce electron-hole recombination, thereby significantly improving the process efficiency [9]. However, immobilization of TiO₂ on supports also creates its own problems [10, 11]. There were at least two obvious problems arising from this arrangement: the accessibility of the catalytic surface to the photons and the reactants and a significant influence of the external mass transfer particularly at low fluid flow rate, because of the increasing diffusional length of the reactant from bulk solution to the catalyst surface. On the other hand, with an increase of the catalyst film thickness, the internal mass transfer may play a dominant role by limiting the utilization of the catalyst near the support surface. All of these usually lead to a lower overall degradation rate when the catalyst is immobilized compared with the suspended system [12]. In this study Aspirin has been chosen as a model pollutant, as traces of aspirin have been detected in the drinking water of South-Western Ontario [13]. Slurry TiO₂ Degussa P25 has been used as the photocatalyst to degrade aspirin both under UV and solar light. Its physico-chemical characteristics are as follows: BET surface area $55 \pm 15 \text{ m}^2 \text{ g}^{-1}$, average primary particle diameter is around 30 nm, purity above 98% and with anatase to rutile ratio as 80:20 [14]. Experiments are performed to determine the various rate constants. Experiments are also conducted to study the initial concentration, catalyst loading, effect of light intensity on the reaction rate constants for two different sources of lights under similar experimental conditions.

6.2 Materials and Methods

6.2.1 Materials

TiO₂ Degussa P25 (Evonik), Beaker (Chemistry store), magnetic stirrer (Chemistry store), UV-Vis Spectrophotometer (Agilent), pH meter (Methrom), UV lamp (Phillips), Acetylsalicylic acid (Sigma Aldrich).

6.2.2 Methods

6.2.2.1 Blank reaction

Primarily experiments were conducted in the presence of catalyst but in the absence of light (dark reaction), which showed a small decrease in the concentration of aspirin, because of the adsorption onto the catalyst surface, which reached an equilibrium value within 30 minutes. Hence, before the light was turned on, it was always ensured that adsorption equilibrium was reached.

6.2.2.2 Photodegradation of aspirin under UV lamp

After, the dark reaction the solution along with the 1.5 gm of dispersed slurry TiO₂ Degussa P25 was exposed to UV lamp of 275 nm wavelength. A batch reactor of 200 ml was used to photodegrade aspirin solution both under UV and solar light. A magnetic stirrer was placed at the bottom of the reactor for the proper mixing of the solution during the reaction. UV lamp was placed at the bottom of the reactor, inside a wooden box. Provision was made to put different screens in between UV lamp and the bottom of the reactor, to change the light intensities as required. The lamp was kept cool by a compressed fan attached to the box to avoid over-heating of the lamp. The pH was 4.5 throughout the reaction. The change in concentration of the degraded solution was recorded by UV-Vis Spectrophotometer at 298 nm.

6.2.2.3 Degradation under solar simulator

The experiment was carried out in a batch reactor of 200 ml under the solar simulator of light intensity 27 mW/cm^2 . The catalyst employed in this reaction was powdered TiO_2 Degussa P25. The reaction was carried out at pH- 4.5 (without addition of buffer). The light source was placed at the top the reactor. The solar simulator had a fan attached to control the heating of the instrument and systems were there to control the light intensity during the reaction. Samples were analysed at intervals in UV-Vis spectrophotometer at 298 nm.

6.3 Results and Discussions

6.3.1 Photodegradation under UV lights

6.3.1.1 Photodegradation rate constant

Heterogeneous photocatalytic degradations often follow Langmuir–Hinshelwood kinetics:- $r_{xn} = KkC/(1 + kC)$. Here, k is reaction rate constant, K is adsorption constant and C is the concentration of the pollutant.

The degradation of aspirin under UV lamp showed a k value of 0.13 mg/L/min

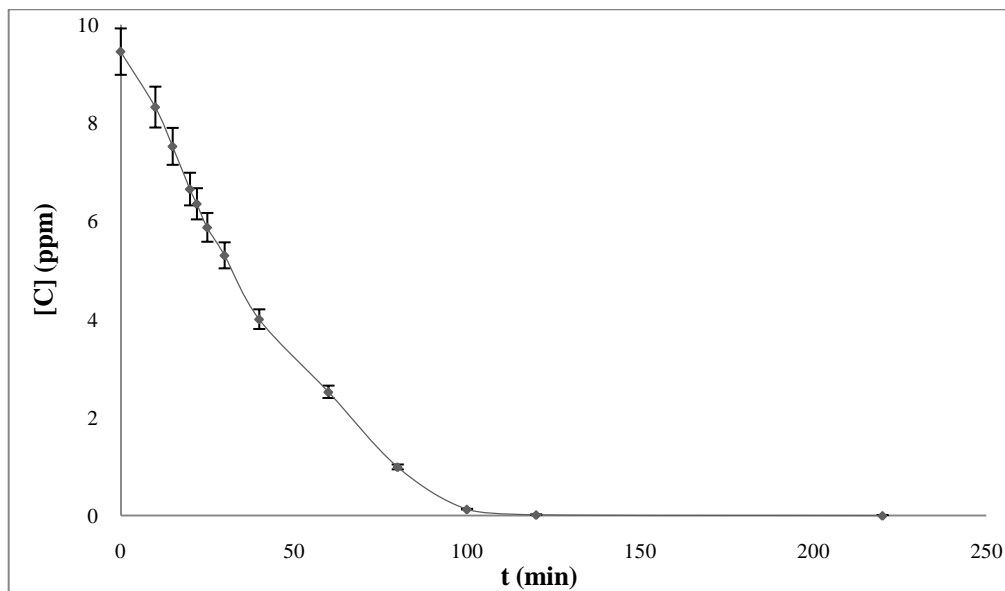


Figure 6.1: Photodegradation of aspirin with TiO_2 slurry. Experimental conditions $[C_0 = 10 \text{ ppm}, \text{pH} = 4.5, I = 22 \text{ mW/cm}^2, H = 0.45 \text{ mm}]$

6.3.1.2 Effect of initial concentration

The initial concentration of the pollutant is always an important parameter in any process water treatment and, therefore, it is essential to examine the effect of the initial concentration. The apparent k value of the reaction increased with the increase of initial concentration, up to certain limit, beyond that concentration k value was observed to decrease. The variation of k value with the variation of initial concentration has been shown in Fig.6.2.

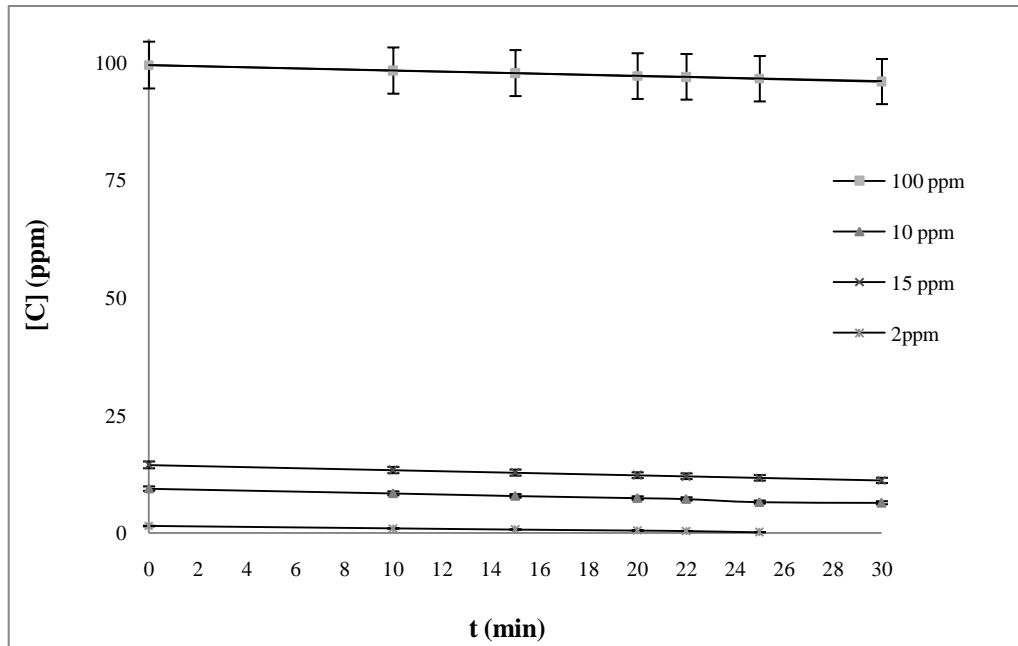


Figure 6.2: Effect of initial concentration. Experimental conditions [$I = 22 \text{ mw/cm}^2$, $\text{pH} = 5.8-6.2$, $H = 0.45 \text{ mm}$]

$k_{100} = 0.14 \text{ ppm/min}$, $k_{15} = 0.11 \text{ ppm/min}$, $k_{10} = 0.096 \text{ ppm/min}$, $k_2 = 0.052 \text{ ppm/min}$

When, Concentration is much high i.e. $KC \gg 1$, then rate was independent of mass transfer effects. While, in case of low concentrations, rate was dependent on mass transfer effects, which decreased the degradation rate. With the increase of the initial concentration of the aspirin the probability of reaction between aspirin molecules and the photocatalyst also increased which led to an enhancement in the degradation rate up to 100 ppm.

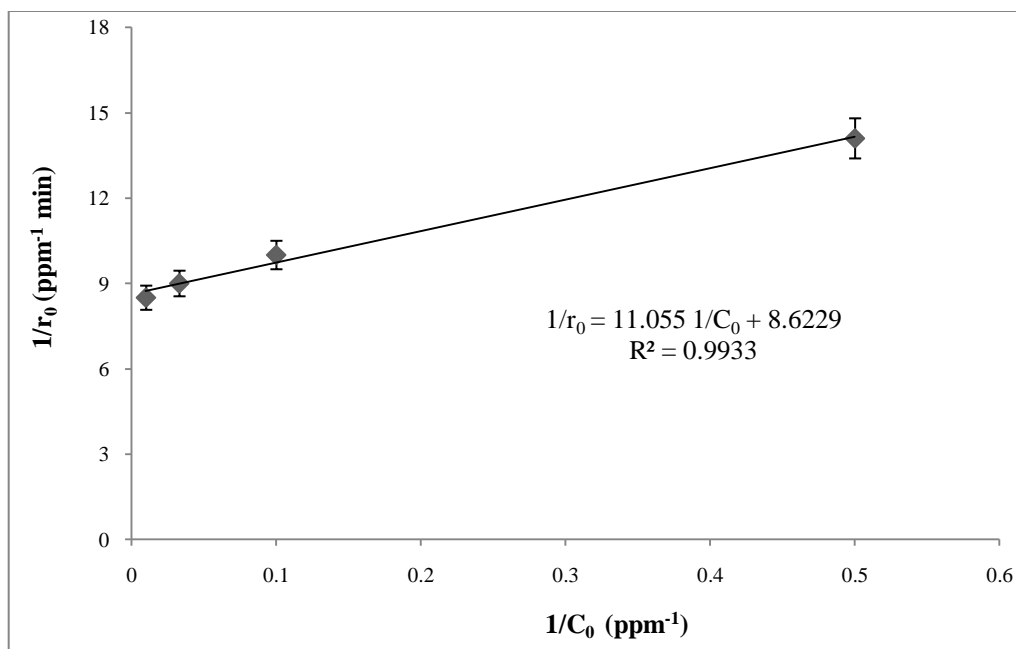


Figure 6.3: Photodegradation of aspirin. Experimental conditions [I = 22 mw/cm², pH - 5.8-6.2, H= 0.45 mm]

The plot of inverse of (initial concentration vs initial rate) $1/C_0$ vs $1/r_0$ showed approximately similar k value as obtained from the plot of concentration vs time for very high concentrated aspirin solution. The rate constant and adsorption constant values obtained from this equation $1/r = 1/kKC + 1/k$, were $k = 0.12$ mg/L/min, $K = 0.7$ Lmg⁻¹

6.3.1.3 Effect of catalyst loading

The variation in degradation rate of aspirin against the TiO₂ amount was determined over the range of 0.5 gm - 3.5 gm/L (Fig. 6.3). The rate constant was found to increase with the increasing amount of TiO₂ and approached a limiting value with further increase, beyond that specific amount. The optimum catalyst loading was 1 gm/L. The limiting amount was observed to be 1.5 gm/L, beyond which the degradation rate decreased because of the following assumed reasons a) the pollutant cannot reach some of the catalyst surface area because of agglomeration of the catalyst particles (internal mass-transfer resistance), (b) light cannot reach some of the catalyst surface area because of

absorption and scattering (shielding effect) of light, (c) light cannot penetrate the agglomerates and activate the inner surfaces.

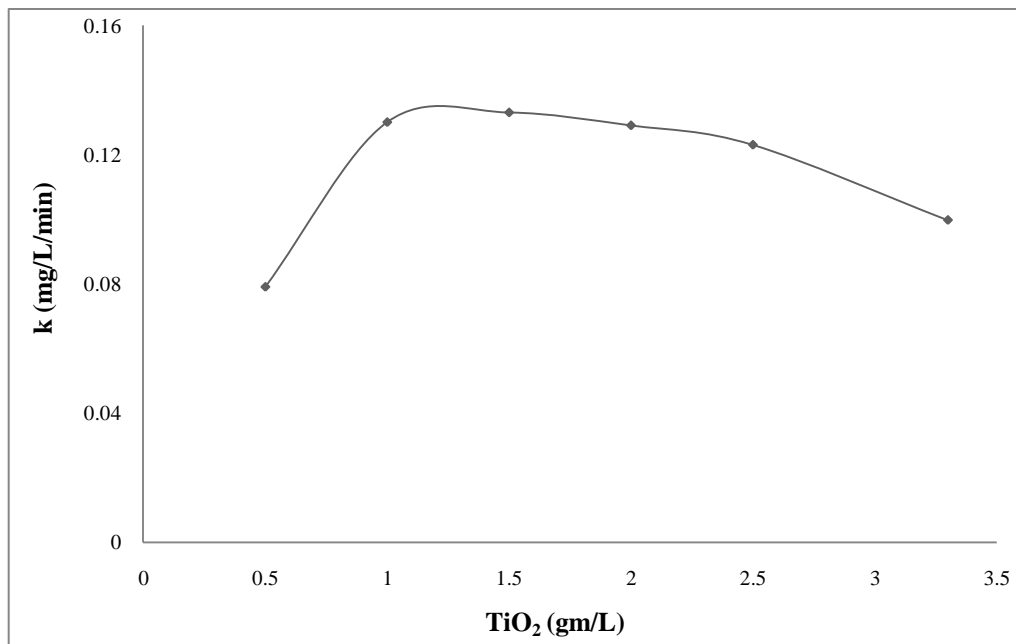


Figure 6.4: Effect of catalyst loading. Experimental conditions [$C_0 = 100$ ppm, $I = 22$ mw/cm², pH - 5.8-6.2]

6.3.2 Photodegradation under solar lights

6.3.2.1 Calculation of rate constant

Degradation of a very high concentrated acetylsalicylic acid solution was carried out under similar conditions as that of UV lights, to determine the degradation and adsorption rate constant. As, at very high concentration, $KC \gg 1$, the degradation rate remained independent of the mass transfer resistance.

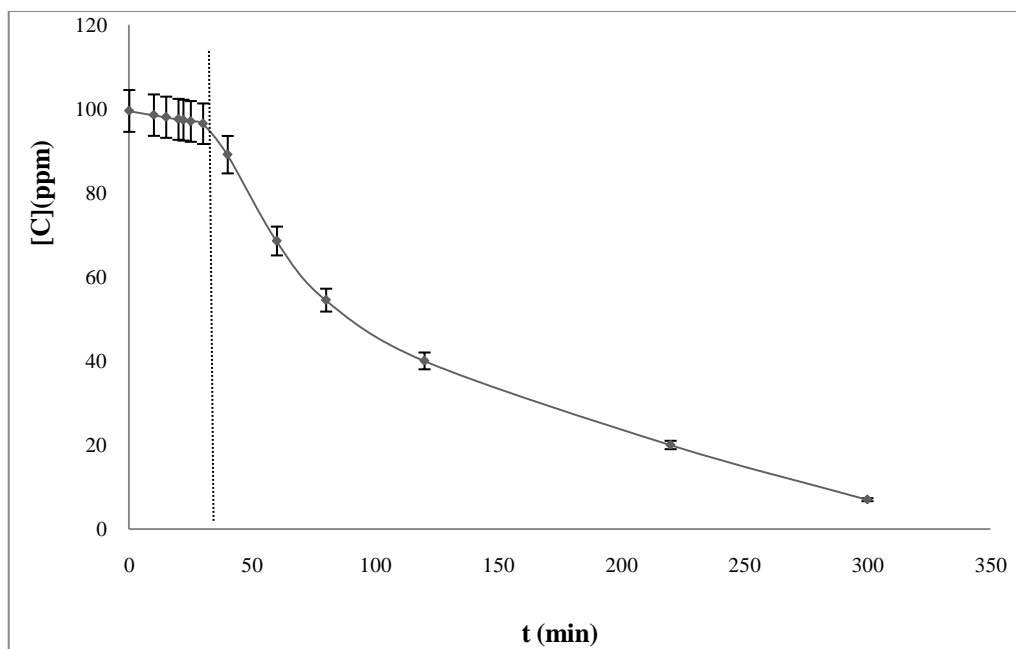


Figure 6.5: Photodegradation of aspirin under solar light in batch reactor. Experimental conditions [$C_0 = 100$ ppm, pH - 4.5, $I = 27$ mW/cm², H=0.45 mm]

The rate constant obtained from the above Fig. 6.5, was $k = 0.1$ mg/L/min

6.3.2.2 Effect of Initial concentration

Degradation rate was observed to increase with the increase of initial concentration of acetylsalicylic acid, in the Fig. 6.6. This can be explained as, at very high concentration, $KC \gg 1$ - rate was independent of mass transfer effects. While at lower concentrations, rate was dependent on mass transfer effects. Also, with the increase of the initial concentrations of the aspirin the probability of reaction between aspirin molecules and the photocatalyst also increased, which led to an enhancement in the degradation rate up to a concentration of 100 ppm. In brief, rate increased with the increase of concentration up to a certain limit, beyond which it decreased due to two reasons i) As a result of decreasing number of photon absorption by the catalyst at higher concentration. ii) Due to the reduction in generation of $\cdot\text{OH}$ radicals on the catalyst surface, as pollutant molecules covered the active sites.

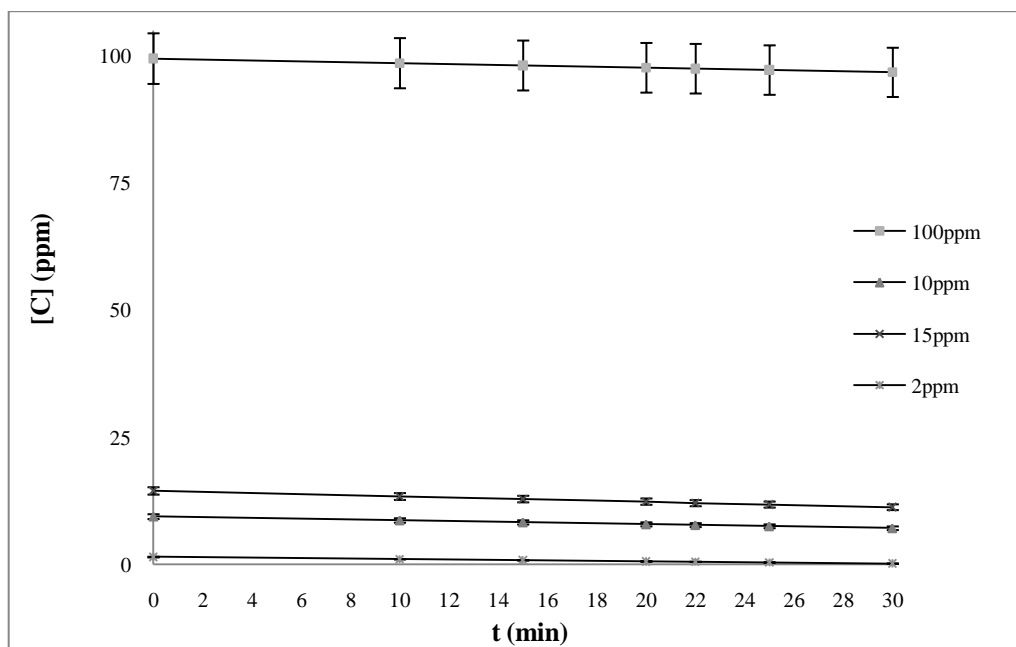


Figure 6.6: Effects of initial concentrations. Experimental conditions [pH - 4.5, I = 27 mW/cm², H=0.45 mm]. $k_{100} = 0.12$ ppm/min, $k_{15} = 0.09$, $k_{10} = 0.063$, $k_2 = 0.042$

6.3.2.3 Kinetic study

A graph of initial rates Vs initial concentration (r_0^{-1} Vs C_0^{-1}) was plot, which showed the k, K values. The rate constant value was observed to be approximately the same as that of the value obtained from the very high concentrated initial degradation rate in Fig. 6.5.

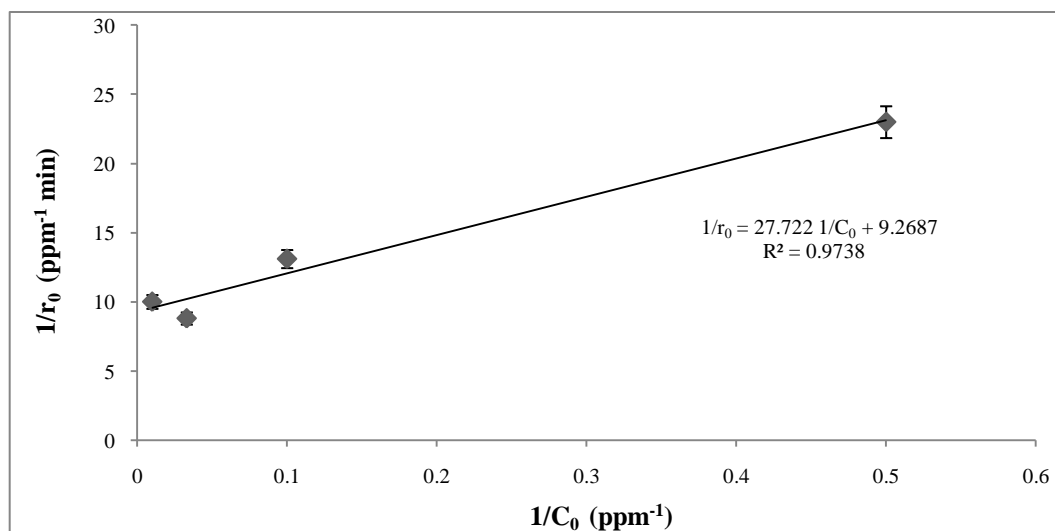


Figure 6.7: A plot of $1/r_0$ Vs $1/C_0$

The adsorption constant and the reaction rate constants calculated from the inverse rate vs inverse concentration plot were: $-K = 0.3 \text{ L/mg}$, $k = 0.107 \text{ mg/L/min}$

6.3.2.4 Effect of catalyst loading

The rate constant was found to increase with the increase of the amount of TiO_2 . The optimum catalyst loading was 1 gm/L , as observed in Fig 6.8. The limiting amount was observed to be 2 gm/L , beyond which the degradation rate decreased, because of the following reasons: i) the pollutant could not reach some of the catalyst surface area because of agglomeration of the catalyst particles (internal mass-transfer resistance). ii) light was not reachable to some of the catalyst surface areas because of absorption and scattering (shielding effect) of light. iii) light was unable to penetrate and activate the agglomerates.

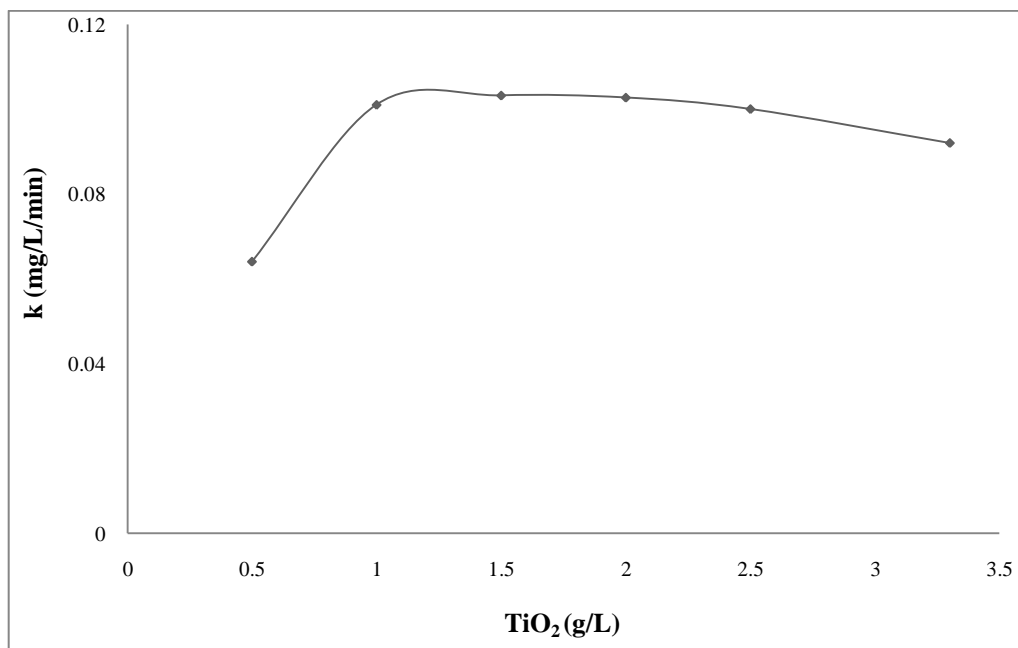


Figure 6.8: Effect of catalyst loading on photodegradation of acetylsalicylic acid. Experimental conditions [$C_0 = 100 \text{ ppm}$, $\text{pH} = 4.5$, $I = 27 \text{ mW/cm}^2$]

6.4 Conclusions

It was observed that the rate of degradation under the solar light was lower than that under the UV light, in presence of TiO_2 slurry. This, was because the slurry form of TiO_2 has already been proved to have more efficiency under UV light as the band gap of TiO_2 is 3.2 eV. Therefore, the electrons in the valence band can only be excited by wavelength below 388 nm. Though, the solar lights contain that wavelength but since the percentage was less, therefore the degradation rate was lower than that under the UV illumination. The effects of initial concentration of aspirin, showed similar results in both cases (under solar and UV light). The increase, in rate with increase of concentration, can be concluded as, the combined effect of minimization of mass transfer, OH radical producibility and proton absorption. It was observed that though the increase of TiO_2 concentration, increased the degradation rate initially but beyond the optimum amount (TiO_2), the rate decreased. This, study showed similar results both under UV and solar lamp, as the catalyst agglomeration occurred in each case and the light shielding phenomenon took place due to this agglomeration of TiO_2 particles. Thus, it can be concluded that slurry form of TiO_2 can be more efficient as photocatalyst under UV light than under the solar.

6.5 Nomenclature

ASA – Acetylsalicylic acid

T - Time

[C] - Concentrations

6.6 References

1. Shuhua Zhou, Ajay K. Ray, *Ind. Eng. Chem. Res.* 42, (2003), 6020-6033.
2. Fujishima, K. Honda, *Nature*, 238, (1972), 37-38.
3. P.S. Mukherjee, A.K.Ray, *Chem. Eng. Technol.* 22, (1999), 253–260
4. D. Chen, A.K.Ray, *Applied Catalysis B: Environmental*, 23, (1999), 143-147
5. Dingwang Chen, Fengmei Li, and Ajay K. Ray, *J. of AIChE*, 46, (2000), 846-1100.
6. L.Andronic, S.Manolache , and A. Duta, *J. of nanosci. and nanotech*,8,(2009), 64-71.
7. Kanheya Mehrotra, Gregory S. Yablonsky, Ajay K. Ray, *Chemosphere*, 60, (2005), 1427-1435.
8. Chen, D.W., Li, F.M., Ray, A.K., *AIChE J.*, 46, (2000), 1034–1045.
9. Camila M. Maroneze, Rita C. S. Luz, Richard Landers ,Yoshitaka Gushikem, *J. of solid state electrochem.*, 14, (2010), 115-121.
10. Sabate, J. Anderson, M. A. Kikkawa, H. Edwards, M., Hill, C. G., *J. Catal.* 127, (1991), 167-177.
11. Alberici, R. M., Jardim, W. F. *Water Res.*, 28, (1994), 1845-1853.
12. Naskar S. S., Pillay A., Chanda M., *J. Photochem.Photobiol. A*,113, (1998), 257-265.
13. <http://www.ene.gov.on.ca/environment/en/category/water/index.htm>. Retrieved April 2009.
14. G. Cerrato, L. Marchese, C. Morterra, *Applied Surface Science*, 70-71, (1993), 200-205.

Chapter 7

Photodegradation of Aspirin under both UV and solar light in presence of polymeric-TiO₂ film

7.1 Introduction

A vast array of pharmaceuticals including antibiotics, anti-convulsants, mood stabilizers and pain killers have been found in drinking water supplies, all over the world. Though, these have been detected in ppm and ppb level but long term consumption on a daily basis could be harmful [1]. Aspirin is one such drug which has been detected in the drinking water of south-western, Ontario. Aspirin, also known as acetylsalicylic acid (ASA), is an ester of salicylic acid. Aspirin is a commonly used Non-steroidal anti-inflammatory drug (NSAIDs) to relieve minor aches and pains. It is also used as an antipyretic to reduce fever and as an anti-inflammatory medication. ASA can also be used during a heart attack to reduce the death risk. The main undesirable side effects of aspirin are gastrointestinal ulcers, stomach bleeding, and tinnitus, especially in higher doses [2, 3]. In commercial aspirin products, a small amount of ASA (300 to 400 mg) is bound together with a starch binder and sometimes caffeine and buffers to make a tablet [4]. The basic conditions in the small intestine break down the ASA to yield salicylic acid, which is absorbed into the bloodstream [5]. The addition of a buffer reduces the irritation caused by the carboxylic acid group of the aspirin molecule. Aspirin degrades in aqueous medium [6]. Hydrolysis of the ester, generates acetic acid and salicylic acid, which further converts into several toxic intermediates causing environmental pollution and affect human health in several ways [7]. Researchers have carried out degradation of salicylic acid in presence of H₂O₂/O₂/UV light and Pt/graphite as photocatalysts [8]. Acetic acid degradation has also been studied by several researchers in presence of TiO₂-Pt nanoparticle under UV light [9].

In this study, a comparison between solar and UV lamp photodegradation has been depicted. Photodegradation was carried out in a batch reactor by TiO₂-polymeric film photocatalyst. Effects of initial concentration, pH, light intensity and catalyst loading were studied. To the best of our knowledge, degradation kinetics of aspirin has not been

carried out in details, yet. Therefore, aspirin which has been detected in trace amounts in the drinking water of S-W Ontario has been taken up as a model compound [10].

7.2 Materials and Methods

7.2.1 Materials

250 ml batch reactor (Chemistry store, UWO), UV lamp (175watt, Phillips), Solar simulator, UV-Vis Spectrophotometer (Agilent), 250 ml beaker (Sigma Aldrich), Beaker, magnetic stirrer and conical flask (Chemistry store, UWO), Gelatin, PVA and PVP (Sigma Aldrich), ethyl alcohol (Chemistry store, UWO).

7.2.2 Methods

7.2.2.1 Photocatalyst preparation

The polymers used to prepare the catalyst have been considered non-toxic by WHO [18, 19, and 20]. 24.3 % w/w of PVA and 11% w/w of Gelatin were dissolved and mixed properly in distilled water to get a transparent solution. Next, 21.6 % w/w of PVP dissolved in the solution of ethyl alcohol and water (1:2) at 45° C. The solution was mixed properly, followed by dispersion of 43 % w/w TiO₂ Degussa P25 powder in the mixture and crosslinked at -2°C.

7.2.2.2 Experimentation under UV lamp

A batch reactor (250 ml) containing 150 ml of acetylsalicylic acid solution was used. The UV lamp (Philips) was placed under the reactor inside a wooden box with a small opening. The radiation intensity of the lamp used for photodegradation was 275 nm. The lamp was constantly cooled by air circulation by a fan fitted in the wooden box. The whole system was covered by a box so that no stray light can enter the reactor. After

photodegradation the concentrations of the solutions were continuously examined in UV-Vis spectrophotometer at ($\lambda = 298$ nm). Also, arrangements were made to measure the pH of the solutions. To study the role of light intensity in degradation of the pollutant, a wire mesh was placed between the lamp and the bottom plate of the reactor.

7.2.2.3 Experimentation under solar simulator

A 250 ml batch reactor containing 150 ml of aspirin solution was exposed to solar simulator. A magnetic stirrer was introduced at the bottom of the reactor. This system had liquid-catalyst type of illumination. The degraded samples were analysed by UV-Vis spectrophotometer at 298 nm. TOC analysis was also carried out to measure the carbon content.

7.3 Results and Discussions

7.3.1 Photodegradation under UV lamp

7.3.1.1 Effects of initial concentration

Photodegradation of aspirin was carried out at different initial concentrations. From Fig.7.1, it was observed that the degradation rate increased with the increase of concentration. This can be explained as, at very high concentration, the degradation rate was independent of external mass transfer effects, so the rate increased at higher concentrations. The decrease of degradation rate with the decrease of concentration was, due to the mass transfer effects, which was more predominant at lower concentrations.

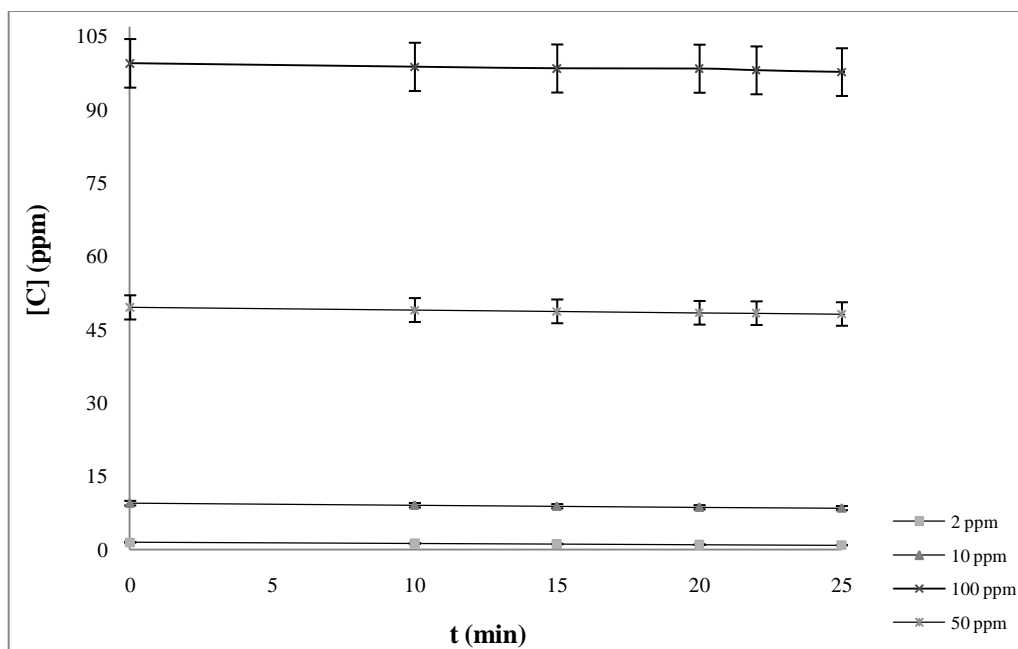


Figure 7.1: Photodegradation of MeO. Experimental conditions [I = 22 mW/cm², pH 4.5, H= 0.45 mm]

$k_{100} = 0.076$ ppm/min, $k_{50} = 0.05$ ppm/min, $k_{10} = 0.032$ ppm/min, $k_2 = 0.025$

Also, with the increase of the concentration, the probability of reaction between pollutant molecules and the photocatalyst increased. Therefore, increased the degradation rate.

7.3.1.2 Kinetic study

Photodegradation of a very high concentrated aspirin solution was carried out under the UV lamp, to calculate the rate constant which was independent of mass transfer effects. The initial rate constant value from this study was observed to be $k = 0.068$ mg/L/min.

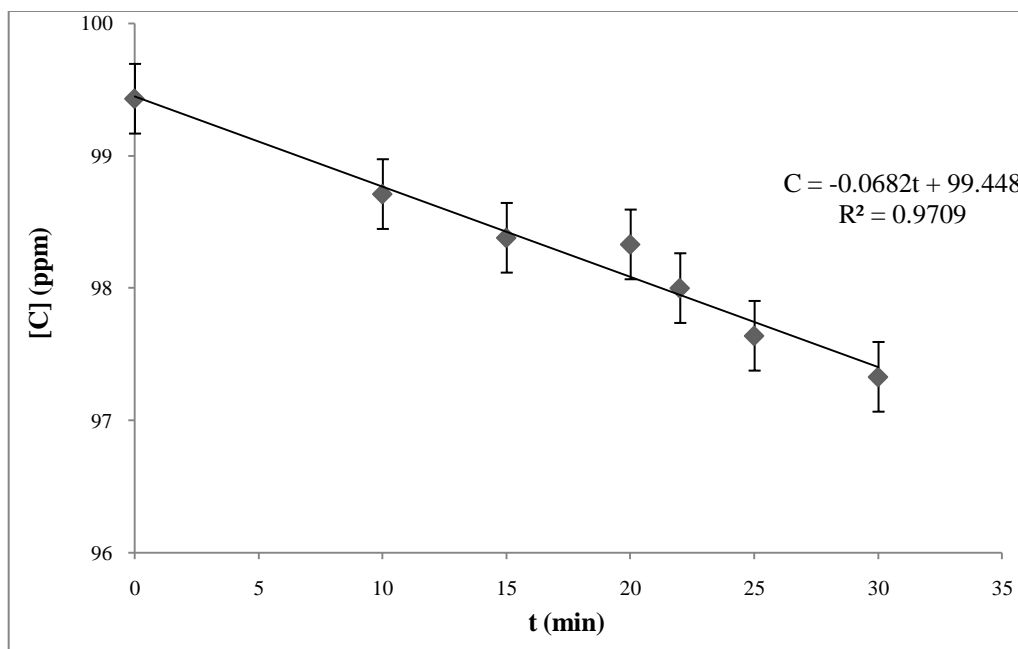


Figure 7.2: Photodegradation of aspirin under UV lamp. Experimental conditions [$C_0 = 100$ ppm, pH - 4.5, $I = 22$ mW/cm²]

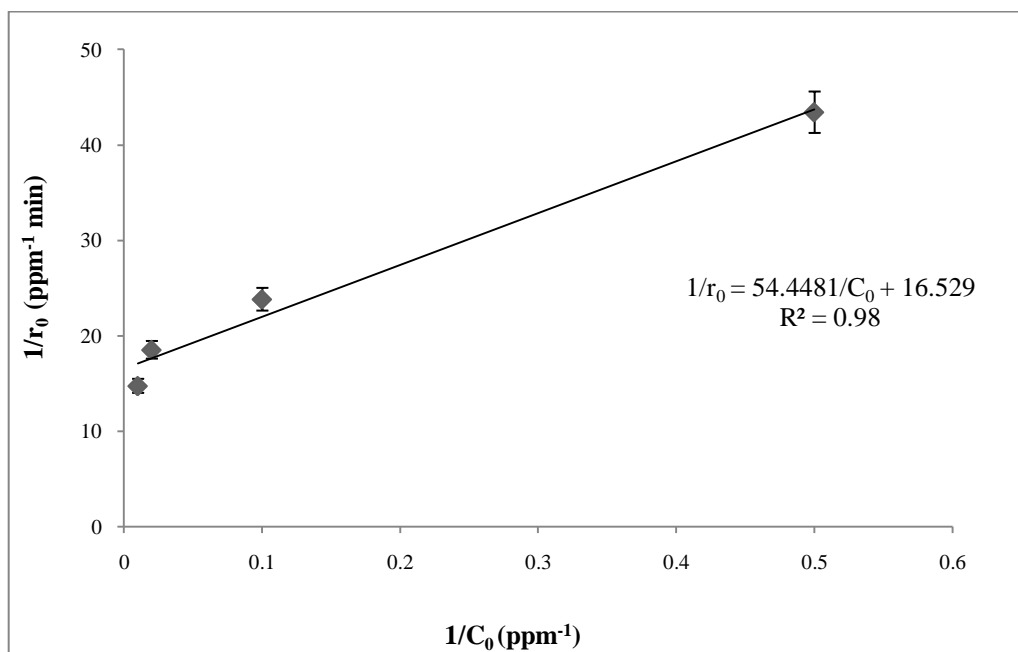


Figure 7.3: Plot of r_0^{-1} vs C_0^{-1} .

$K = 0.3$ Lmg⁻¹, $k = 0.06$ mg/L/min (obtained from $1/r_0$ vs $1/C_0$)

A graph of inverse of initial rate vs initial concentration was plot to calculate the rate constant and adsorption constant values. The k and K values obtained from this plot were observed to be approximately the same as that obtained from very high concentrated aspirin solution degradation. High concentration of Aspirin obeyed Langmuir-Hinshelwood kinetics while at low concentration first order kinetics was followed.

7.2.1.3 Effects of light intensities

At low intensities degradation rate was observed to be quite low, however it increased with the increase of light intensity gradually. It was observed that degradation rate was proportional to the light intensities at lower intensity of light but at higher intensities, the degradation rate remained almost unaffected by variation of the light intensity. This can be explained as the electron, holes formation increased with increase of light intensity at lower light intensities and the recombination phenomenon was negligible while at higher intensities, the electron hole recombination competes with electron hole separation. Therefore the effect of light on the degradation rate, decreased.

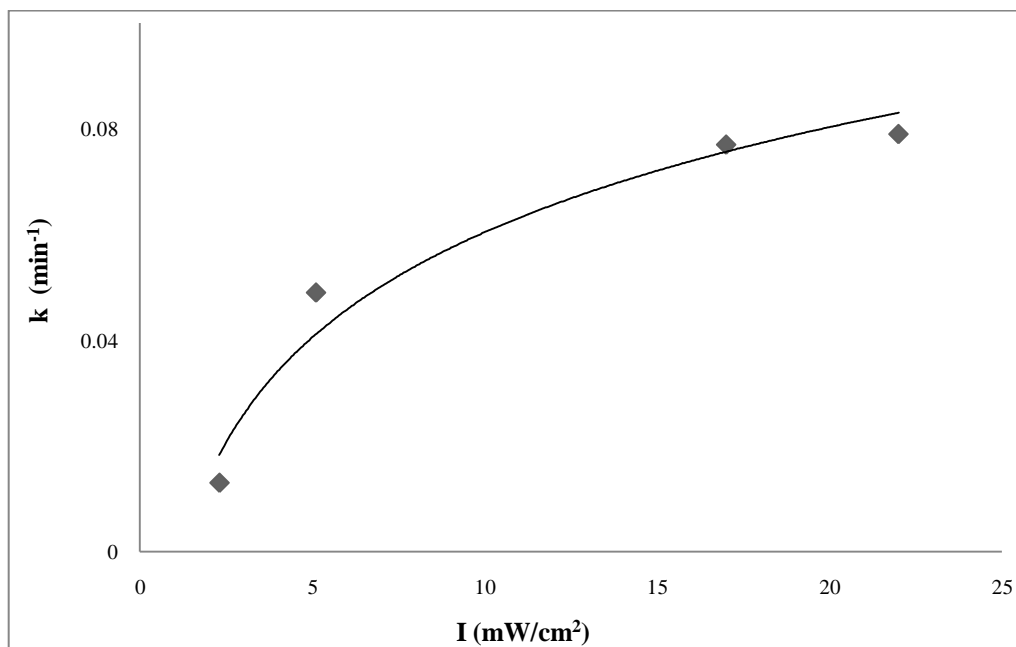


Figure 7.4: Effect of light intensity on degradation rate. Experimental conditions [Light source = UV lamp, pH-4.5, $C_0 = 100$ ppm]

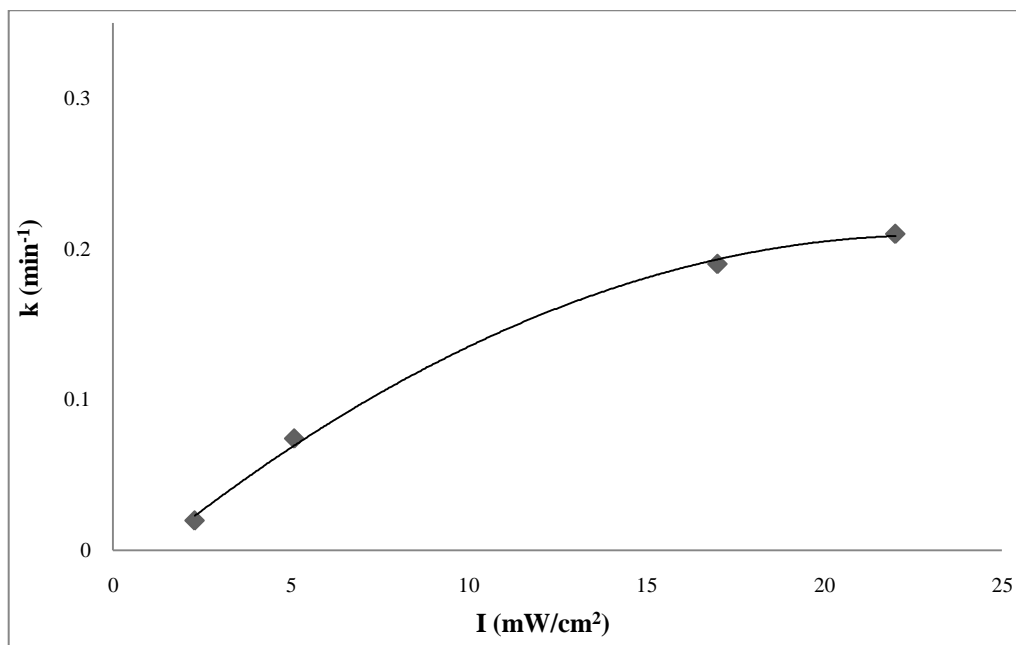


Figure 7.5: Effect of light intensity on degradation rate. Experimental conditions [Light source= UV lamp, pH-4.5, $C_0 = 2$ ppm]

7.2.1.4 Effect of catalyst loading

Photodegradation of aspirin solutions were carried out at different concentration of TiO_2 , (in the polymeric film) to study the effect of TiO_2 concentration on the degradation rate. With the increase of the catalyst loading, the catalyst active sites increased, increasing the degradation rate. On further increase of TiO_2 amount, the degradation remained constant due to the unchanged diffusional length across the grain boundary. Beyond 2.5 g/L of TiO_2 , decrease in degradation rate observed. This was because, the increased amount of TiO_2 , contributed to increase the thickness of the film which increased the probability of charge recombination due to increased diffusional length through the grain boundaries.

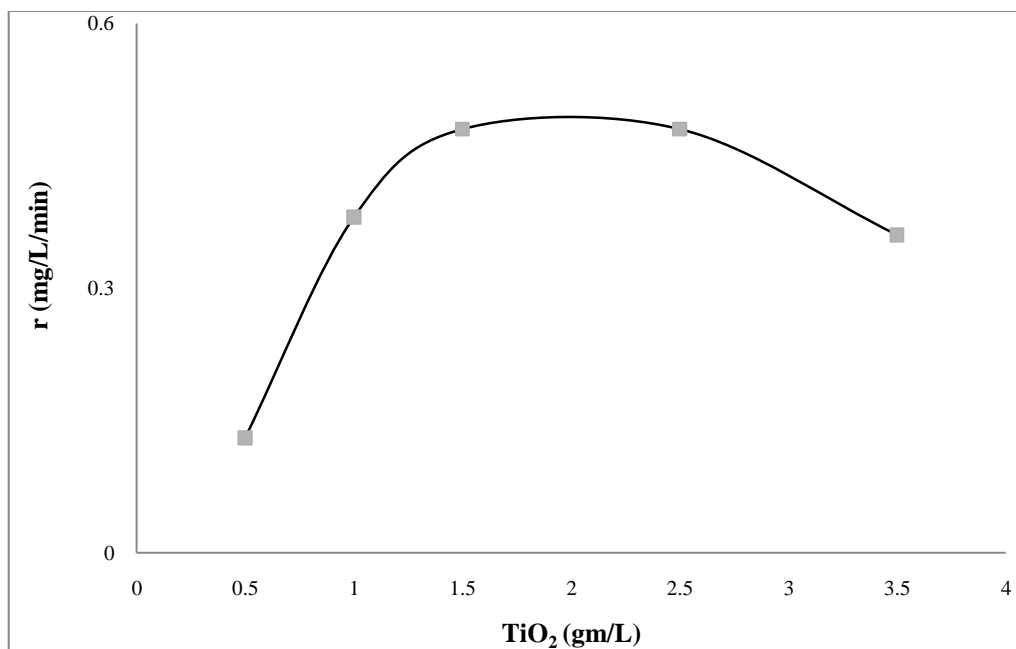


Figure 7.6: Photodegradation of aspirin under UV light with TiO₂/polymeric film. Experimental conditions [$C_0 = 100$ ppm, pH – 4.5, $I = 22$ mW/cm²]

7.2.1.5 Effect of film thickness

A degradation study was carried out by varying the thickness of the catalyst film, ranging from 0.45 mm to 2.5 mm. In this case amount of TiO₂ was kept constant. While, the amount of polymeric constituents were varied. It was observed in Fig. 7.7, that film thickness played an important role in the degradation of aspirin molecules.

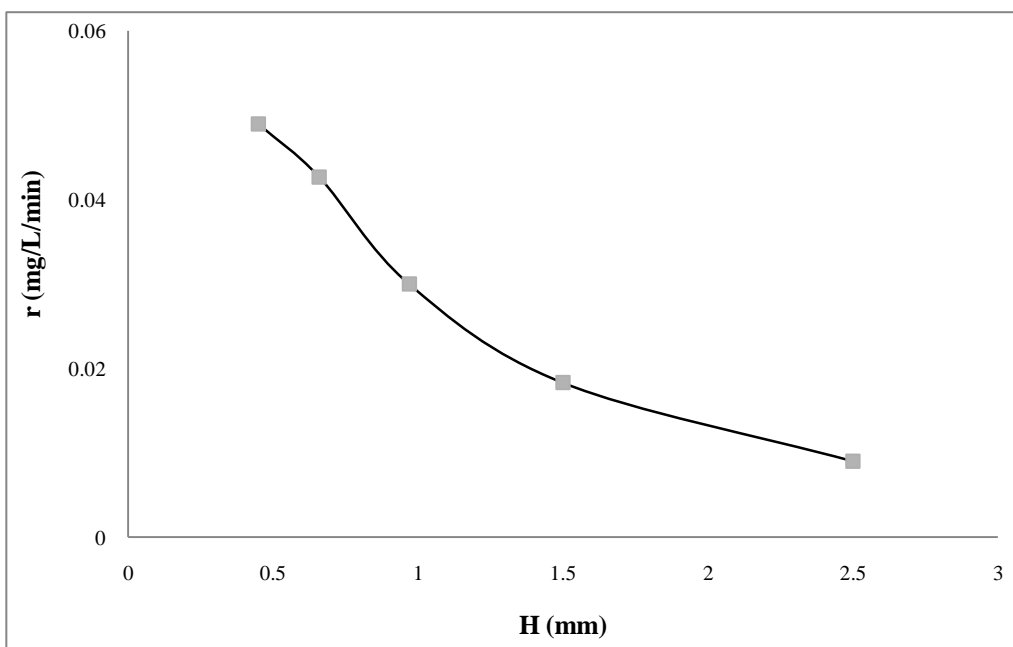


Figure 7.7: Photodegradation of aspirin under UV light with TiO₂/polymeric film. Experimental conditions [C₀ = 100 ppm, pH – 4.5, I = 22 mW/cm², TiO₂ loading 1.5 g/L]

It was observed that with the increase in film thickness the photocatalytic reaction rate decreased. The increase of the catalyst loading though should increase the degradation rate, due to more available catalyst surface sites but at the same time there were two other factors within the catalyst films that restricted the presence of charge carriers at the interface. One of the reasons, was attenuation of light due to absorption by the catalyst, and the other was the increased probability of charge recombination due to the increased diffusional lengths through the grain boundaries and constrictions within the micro-porous film.

7.3.2 Photodegradation under solar light

7.3.2.1 Effects of initial concentrations of acetylsalicylic acid on degradation

Photodegradation of aspirin was carried out at different the initial concentrations. The initial concentrations ranged from 2 ppm to 100 ppm.

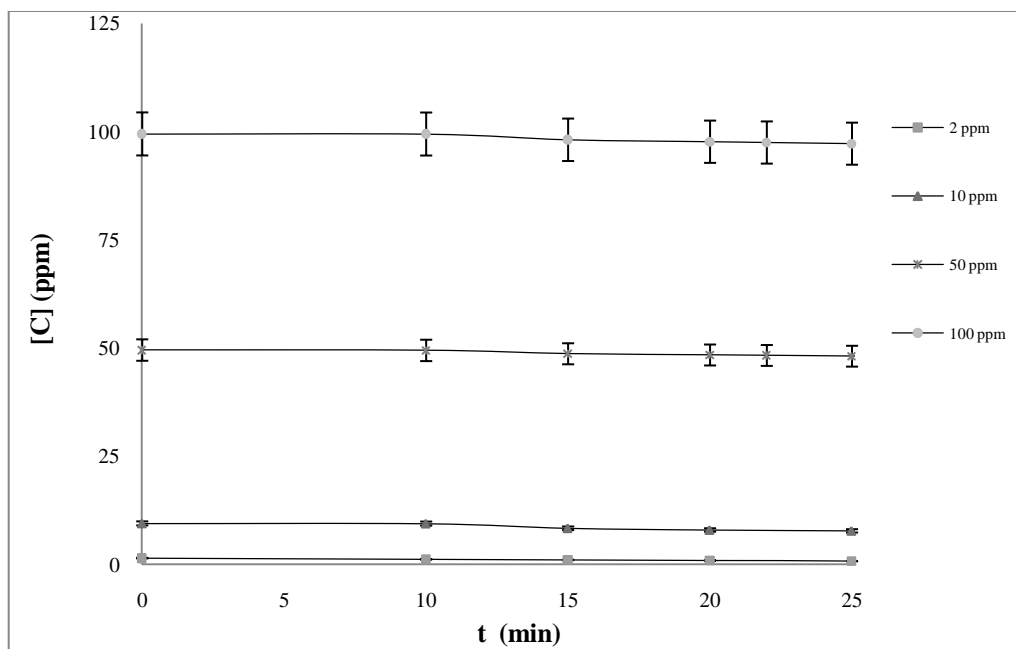


Figure 7.8: Photodegradation of aspirin under solar light with TiO₂-polymeric film. Experimental conditions [I = 27 mW/cm², pH - 4.5, H= 0.45 mm]

$k_{100} = 0.09$ ppm/min, $k_{50} = 0.06$ ppm/min, $k_{10} = 0.05$ ppm/min, $k_2 = 0.028$ ppm/min

At very high concentration, $KC \gg 1$ - rate remained independent of mass transfer effects. Therefore, higher degradation rates were observed with the increase of concentration up to 100 ppm. At lower concentrations, rates were dependent on mass transfer effects. Also, with the increase of the initial concentrations of the aspirin the probability of reaction between aspirin molecules and the photocatalyst also increased which leads to an enhancement in the degradation rate up to 100 ppm.

It can be observed from the above rate constants values, that the degradation rates under the solar light were higher than under the UV lamp. This can be explained due to the crosslinking effect of UV light on the polymer matrix, which made some TiO₂ particles unavailable for photocatalysis.

7.3.2.2 Kinetic study

Photodegradation of very high concentrated aspirin solution was, independent of mass transfer effects. Therefore, to obtain the intrinsic kinetic parameter, k value was calculated from a very high concentrated solution. The rate constant value obtained from the Fig. 7.9 was compared to the one obtained from Fig. 7.10.

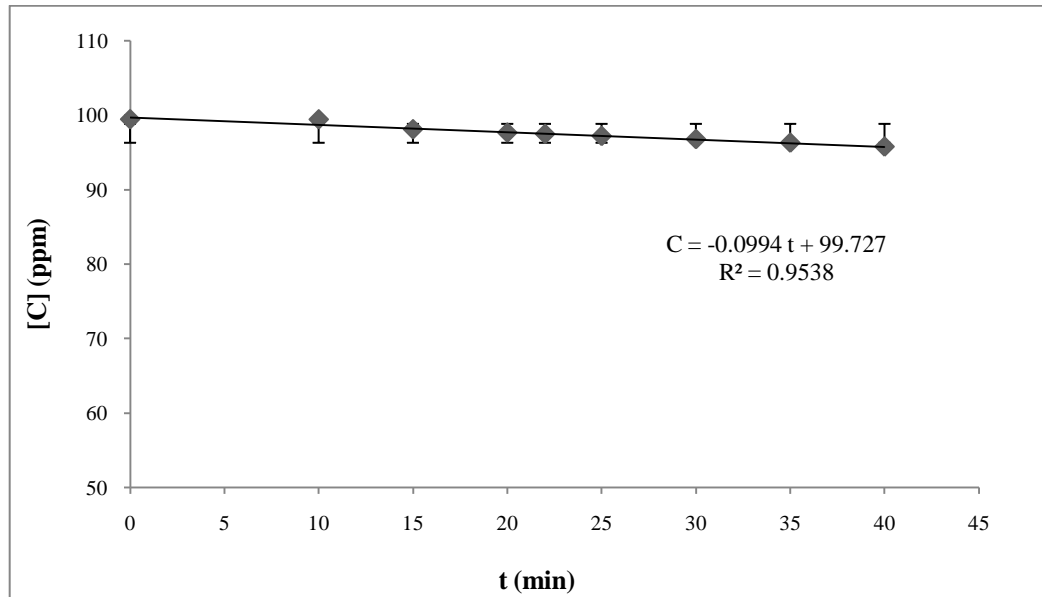


Figure 7.9: Photodegradation of aspirin under solar light with TiO₂/polymeric film. Experimental conditions [C₀ = 100 ppm, pH = 4.5, I = 27 mW/cm²]

This reaction fitted into L-H kinetic model. The rate constant was 0.099 mg/L/min.

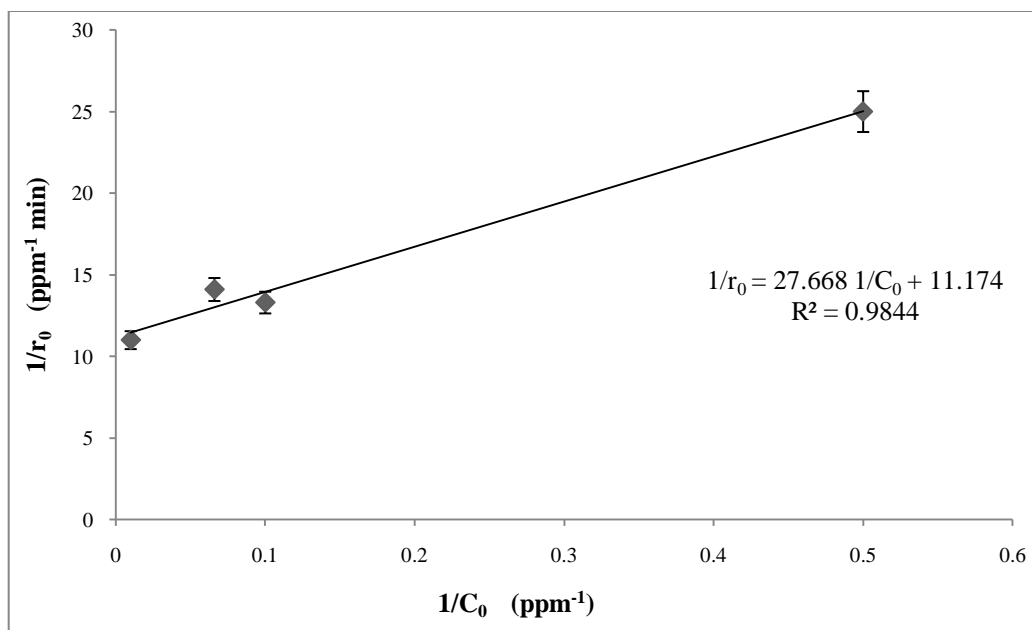


Figure 7.10: Photodegradation of aspirin under solar light [initial rate Vs initial concentration]

k values (0.099 mg/L/min) obtained from 100 ppm solution degradation was approximately the same as the one obtained (0.089 mg/L/min) from the plot of $1/r_0$ vs $1/C_0$. Adsorption constant was $K_{ads} = 0.4 \text{ Lmg}^{-1}$

7.3.2.3 Effect of catalyst loading

Initially with the increase of the amount of TiO_2 , the degradation rate was observed to increase up to a certain extent but on further increase, the degradation rate became constant up to certain extent and beyond that amount, the rate decreased. This was due to three following reasons: i) With the increase of the catalyst loading, the catalyst active sites increased, increasing the degradation rate. ii) On further increase of TiO_2 amount, the degradation rate remained constant due to the unchanged diffusional length across the grain boundary. iii) Beyond 2.5 g/L of TiO_2 , increase of TiO_2 amount increased the thickness of the film which increased the probability of charge recombination due to increased diffusional length through the grain boundaries of the catalyst film.

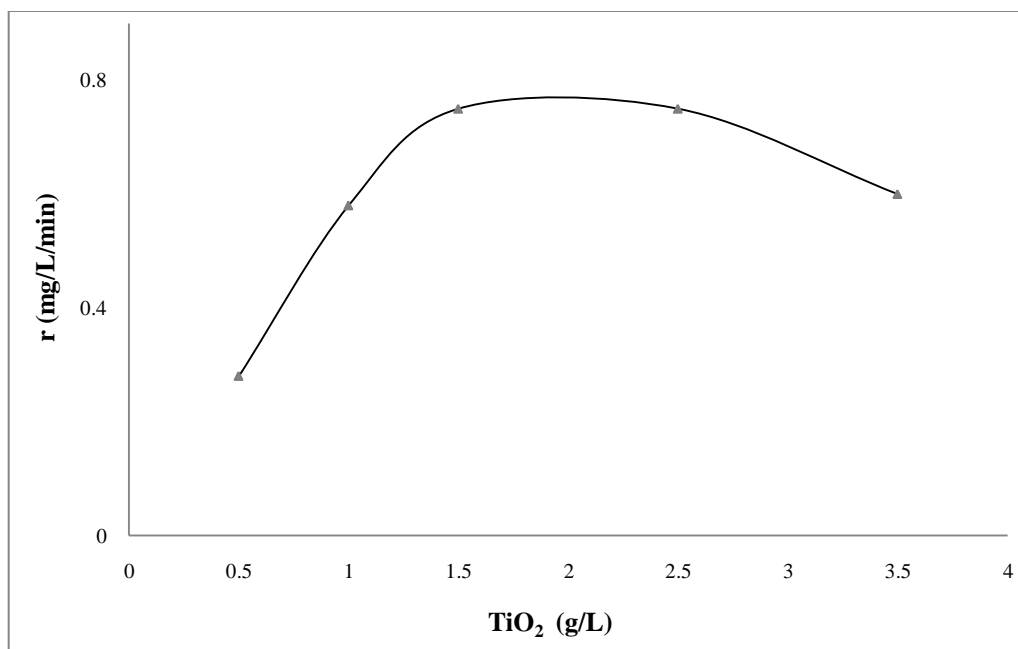


Figure 7.11: Photodegradation of aspirin under solar light with TiO_2 /polymeric film. Experimental conditions [$C_0 = 100$ ppm, pH – 4.5, $I = 27$ mW/cm²]

7.3.2.4 Effect of film thickness

Studies were carried out by varying the thickness of the TiO_2 -polymeric film. It was observed in Fig. 7.12 that with the increase in film thickness the decreased the photocatalytic degradation rate.

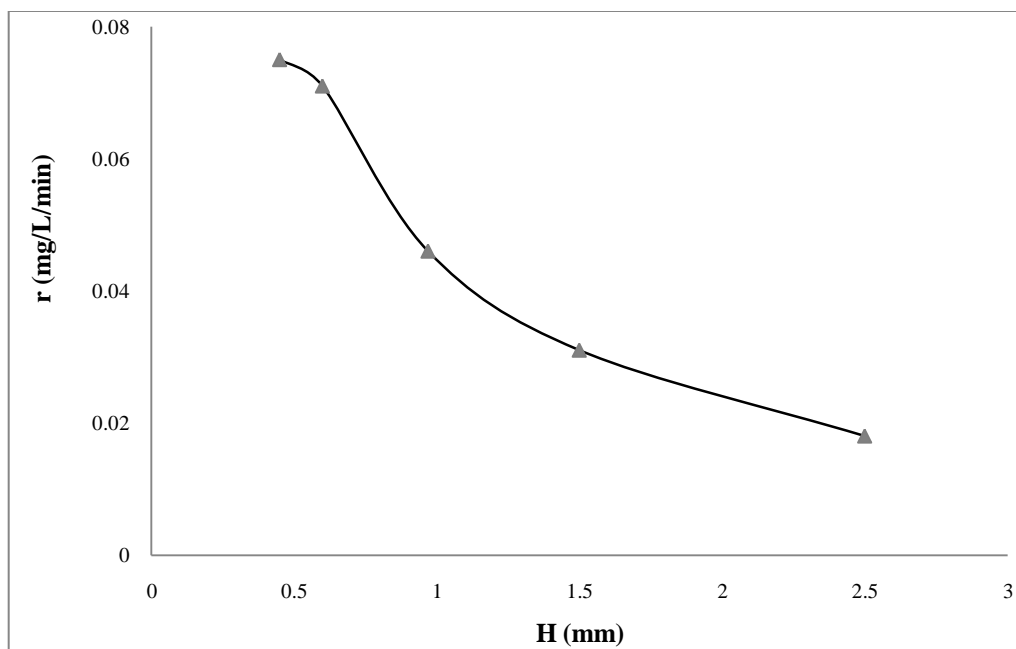


Figure 7.12: Photodegradation of aspirin under solar light with TiO₂/polymeric film. Experimental conditions [$C_0 = 100$ ppm, pH – 4.5, $I = 27$ mW/cm², TiO₂ loading 1.5 g/L]

There were two counteracting affects, which resulted in this decrease of rate. The increase of the catalyst loading though should increase the degradation rate, due to more available catalyst surface sites but at the same time there are two factors within the catalyst films that had restricted the presence of charge carriers at the interface. One was attenuation of light due to absorption by the catalyst, and the other was the increased probability of charge carrier recombination due to the increased diffusional lengths through the grain boundaries and constrictions within the micro-porous film.

7.3.2.5 Effects of pH

Studies were carried out at two different pHs- 3.2 and 9.1. Degradation rates at these two pHs were observed as, the TiO₂ surface charges remain positive from pH 3.1- 6.2. While, beyond 6.2 it possess negative charge. At the lower concentrations, pHs had a substantial effects on the degradation rate of aspirin. While, on the other hand, at higher

concentrations level, differences in degradation rates with changing pH values were not as intense. These experiments also show that decreasing acetylsalicylic acid concentration increased the photodegradation at low values of pH, while an opposite trend was observed at high pH values.

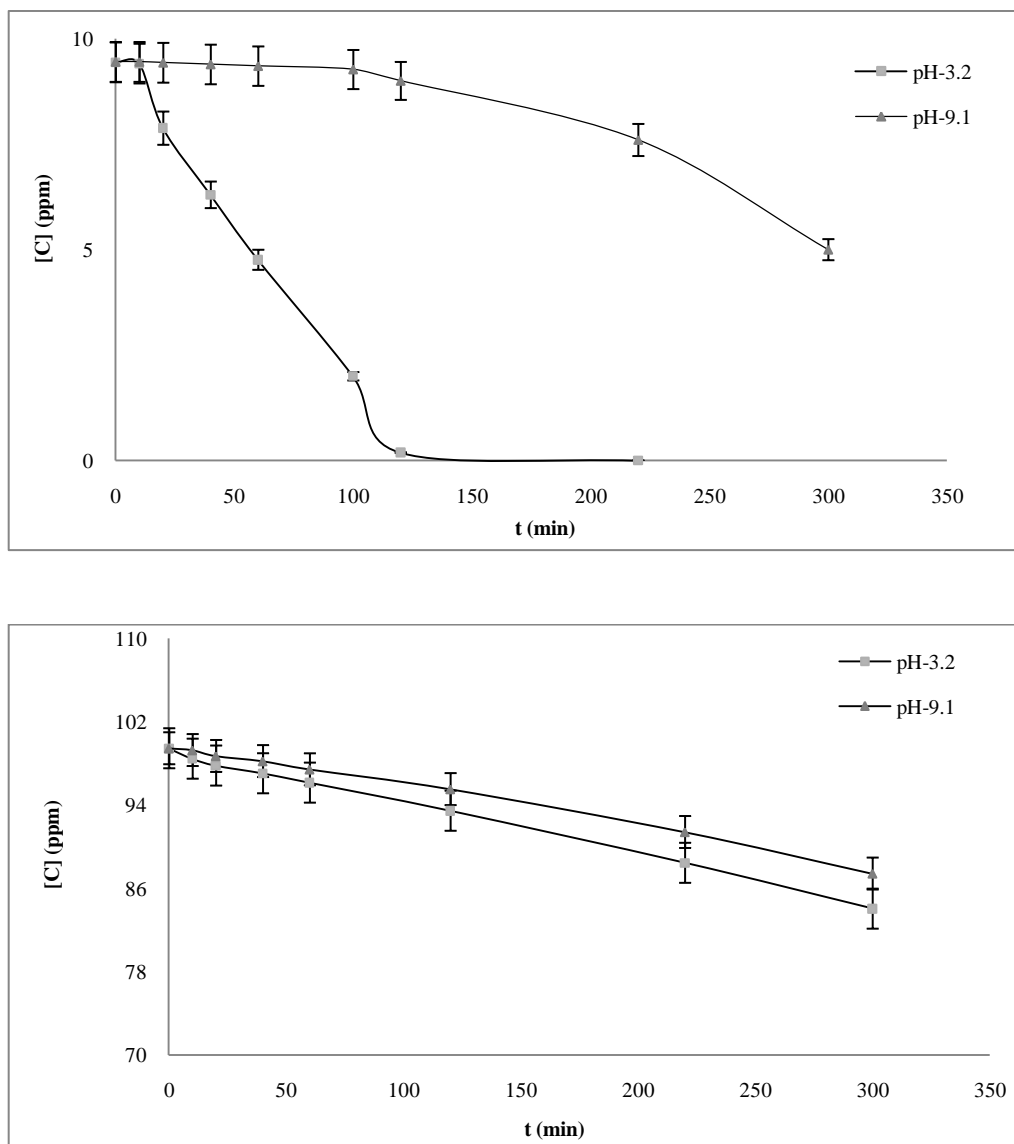


Figure 7.13: Photodegradation of Aspirin under solar light. Experimental conditions [C₀ = 100 ppm, 10 ppm, pH – 3.2, 9.1, I = 27 mW/cm²]

The decrease in acetylsalicylate degradation rate with increasing pH can be interpreted by considering, two different reaction pathways that took place under conditions of varying

pHs. It can be explained as the electron transfer and indirect hydroxyl radical attack were the predominant reaction mechanisms at low and high pH, respectively. At low pH, the positively charged titanium hydroxide offered a suitable surface for acetylsalicylate chemisorptions. This bond had a relatively high covalent character, and the oxygen atoms of the salicylate ions formed from break down of aspirin, being relatively strong electron donors, were able to directly interact with valence band holes. Increasing the pH reduced the adsorption and gradually increased the electrostatic repulsion between the acetylsalicylate anion ($pK_a = 2.914$) and the catalyst surface [8]. The increased distance between the two reactants no longer allowed direct charge transfer. With only limited acetylsalicylate adsorption occurring, most of the decomposition was probably mediated by $\cdot OH$ radicals formed at semiconductor surface sites. The decrease in photodecomposition rates at pH 9.1 was probably due to Coulombic repulsion between the organic anions and the highly negatively charged oxide surface. Decomposition would thus depend on diffusion of surface-generated $\cdot OH$ radicals to the low concentration of anion in the double layer, a slower process than direct charge transfer. Photodegradation experiments conducted at different initial acetylsalicylate concentrations also appeared to confirm that different reaction mechanisms control the photodegradation under different conditions than those observed with varying pH. Increasing the initial acetylsalicylate concentration produced opposite trends. At low pH, the initially photodegradation rate decreased compared to that of low concentrated solution degradation at same pH. While it increased at high pH. At low pH, the higher acetylsalicylate surface coverage led to displacement of $\cdot OH$ and water ligands at the titanium centers, thus reducing the rate of photo formation of $\cdot OH$ radicals. Slower degradation of non adsorbing species would have resulted due to above mentioned phenomenon. The decomposition of chemisorbing species would be affected as well at higher concentrations, because these species also compete at the catalyst surface with the initial reagent for the same active sites. Similar results have been observed by other researchers in case of photodegradation of other NSAIDs with TiO_2 [8, 11].

7.3.2.6 Effect of light intensity

At low light intensities, the degradation rate was observed to be quite low which increased with the increase of light intensity gradually. It was observed that the rate was proportional to the light intensities at lower intensity of light but at higher intensities, the degradation rate remained almost unaffected by variation of the light intensity. This can be explained as the electron, holes formation increased with increase of light intensity at lower light intensities and the recombination phenomenon was negligible, while at higher intensities the electron hole recombination competes with electron hole separation.

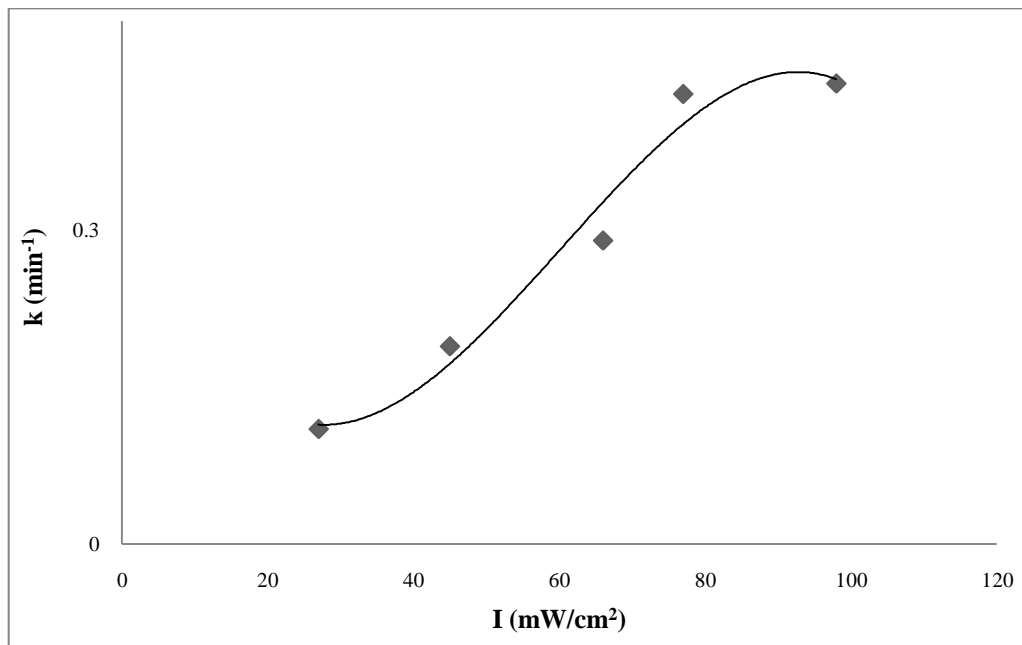


Figure 7.14: Effect of light on degradation rate. Experimental conditions [Light source = Solar simulator, pH - 4.5, C = 100 ppm]

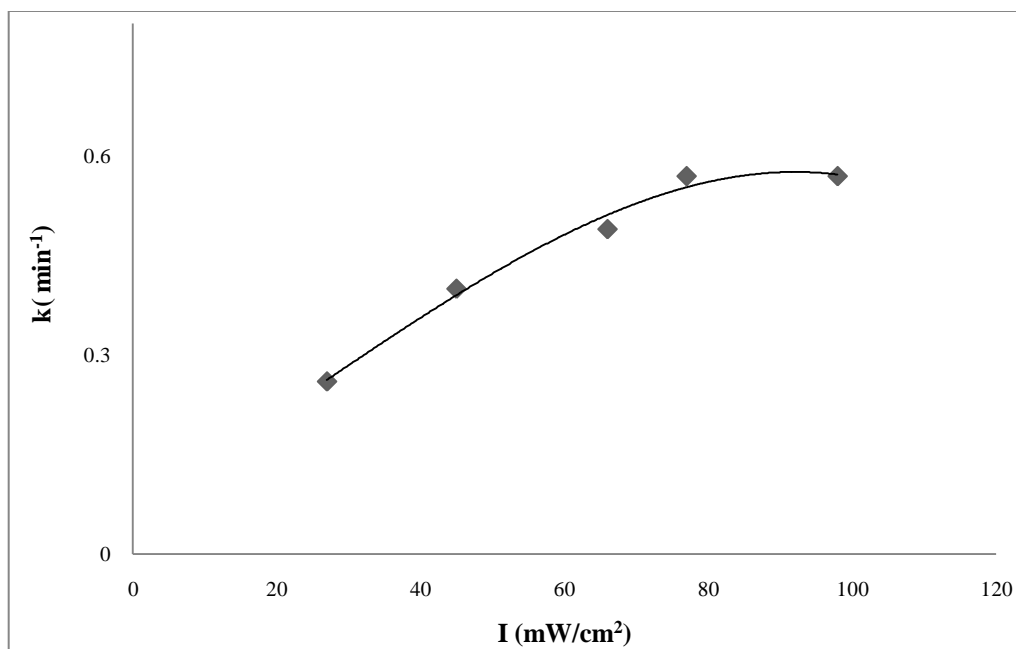


Figure 7.15: Effect of light on degradation rate. Experimental conditions [Light source = Solar simulator, pH-4.5, C = 2 ppm]

Incase of the effect of light intensity, similar trends were observed under the UV lamp, excepting that the rates were lower than under the solar lights.

7.4 Conclusion

It can be concluded that the TiO₂-polymeric film was more efficient under solar light than the UV lamp. This can be explained due to the cross linking effect of UV lamp on the polymeric film. Though solar light consist of 4% UV band but its intensity being lower did not show similar effects. When direct charge transfer occurs at low pH, the degradation was more efficient than the one at high pH. In this case, however, degradation rates decreased as the increase of adsorbate concentration, decreased OH radical production. At higher pH values, less chemisorptions occurred and indirect charge transfer predominated, thus decreased the rates. Initial concentrations were observed to

play an important role on the degradation rate. The degradation rate was observed to increase with the increasing concentration of aspirin. The increase of photocatalyst film thickness, decreased the degradation rates. This was because of the light attenuation. Also, the probability of charge carrier recombination increased due to the increased diffusional lengths through the grain boundaries within micro porous film. Besides, the increased diffusional length for diffusion of pollutants from bulk to catalyst surface even contributed in this decreasing degradation rate phenomenon. While the varying TiO₂ loading shows a different trend. Increase of TiO₂ amount, increased the degradation rate initially. As, the active sites for photoreaction increased, therefore the rate of reaction increased initially but further increase, showed constant degradation rate. This was due to the diffusional length of charge carrier to catalyst-liquid interface remained unchanged. Beyond this certain thickness, the degradation rate decreased as the charge carriers generated relatively far from the liquid-catalyst interface, and consequently more susceptible to recombination loss. With the increase of light intensity, increase of photodegradation rate was observed at lower values of light intensities. While at very higher intensity level, the effect of light intensities on degradation rate was observed to be minimum. This was because, at low light intensities reactions involving electron-hole formation are predominant and electron-hole recombination was negligible. However, at increased light intensity electron-hole pair separation competed with recombination, thereby causing lower effect on the reaction rate.

7.5 Nomenclature

TiO₂ – Titanium Dioxide

ASA – Acetylsalicylic acid

[C] – Concentration

ppm – Parts per million

mW – milli Watt

7.6 References

1. Peter J Vikeshland, Krista L Rule, <http://www.innovationmagazine.com/innovation/> Retrieved Aug. 2009.
2. Mike Adams, <http://www.naturalnews.com/001891.html>, Retrieved May 2010.
3. <http://www.chemicaland21.com/lifescience/phar/ACETYLSALICYLIC.htm>, Retrieved Nov. 2010.
4. Whittle B.J., Makki K.A., Grady J.D., *Gut*, 22, (1981), 798-803.
5. Nathan Wei, <http://www.arthritis-treatment-and-relief.com/aspirin-side-effects.html>, Retrieved Dec. 2009.
6. http://www.pharmpedia.com/Stability_Of_Drugs:Mechanisms_Of_Degradation.html Retrieved Oct. 2010.
7. <http://web.uvic.ca/~pmarrs/chem463/465e35aspirinhydrolysis.pdf>. Retrieved May 2010.
8. Christoph K. Scheck, Fritz Frimmel, *Wat. Res.* 29, (1995), 2346-2352.
9. Muggli, S.D., Falconer, J. *Catalysis*, 187, (1999), 230-237.
10. <http://www.ene.gov.on.ca/environment/en/category/water/index.htm>, Retrieved May 2009.
11. Zheng X.Z., Wei L.F., Zhang Z.H., Jiang Q.J., Wei Y.J., Xie B., Wei M.B., *Int. J. of hydrogen energy*, 34, (2009), 9033-9041.

Chapter 8

Mechanism of aspirin degradation under solar light in presence of a TiO₂/polymeric film

8.1 Introduction

Aspirin, known as acetylsalicylic acid (ASA), is a commonly used Non-steroidal anti-inflammatory drug (NSAIDs) to relieve minor aches and pains. It is also used as an antipyretic to reduce fever and as an anti-inflammatory medication. ASA can also be used during a heart attack to reduce the death risk. The main undesirable side effects of aspirin are gastrointestinal ulcers, stomach bleeding, and tinnitus, especially in higher doses [1, 2]. Aspirin degrades in aqueous medium into several toxic intermediates causing environmental pollution and affect human health in several ways. Removal of these organic compounds by traditional techniques (charcoal adsorption, ozonization) is challenging and costly. These methods usually generate concentrated effluent streams, which are harmful to environment [3, 4]. Recent advanced technologies in photocatalytic oxidation of organic materials can be safely employed in treatment of organic wastes as the final products are mostly carbon dioxide and water. Titanium dioxide (TiO₂) has been employed in photocatalytic oxidation processes due to its capability of producing hydroxyl radical ($\cdot\text{OH}$) when exposed to ultraviolet/solar light.

Upon illumination of TiO₂ by UV light, electrons are promoted from the valence band to the conduction band to give electron-hole pairs. The holes in TiO₂ react with water molecules or hydroxide ions and produce hydroxyl radicals. The interaction of the positive holes or the negative electrons with the absorbed organic pollutants provide unstable intermediates, which are further attacked by hydroxyl or peroxy species occasioning a carbon-carbon bond rupture (or aromatic ring opening) with concomitant release of low molecular weight products which may in turn be further oxidized to CO₂. Contradictory results have been reported for the contribution of TiO₂ in degradation of organic materials. It was shown that at low pH the positive holes are considered as the major oxidizing species, whereas hydroxyl radicals are considered as the predominant species at neutral or high pH levels [4]. Interestingly it was claimed in another report that

holes are the major oxidizing species at pH=3, while below and above this pH the hydroxyl radicals are the major degrading agents [5]. Such a discrepancy is most probably due to the nature of the organic compounds and operating conditions. Therefore it can be concluded that aspirin undergoes the following reactions when exposed to the catalyst illuminated by solar light;



Several mechanisms have been proposed to account for the initial steps of semiconductor-mediated photodegradation of aliphatic and aromatic organics. The heterogeneous reaction mechanisms proposed are similar to their homogeneous counterparts [5-8]. These mechanisms can be summarized as;

- (i) Direct charge transfer from the semiconductor to the dissolved molecule.
- (ii) Generation of radicals from water decomposition, which then attack the aromatic ring.

Most of the studies on photocatalytic degradation of several drugs include a detailed examination of the so-called primary processes under different working conditions, while little information is available on the reaction mechanisms involved in the degradation process.

In this study, degradation of aspirin in the presence of polymeric TiO₂ under solar light was investigated. The most probable reactions and the mechanisms were suggested based on the qualitative and quantitative measurement of intermediates and final products.

8.2 Materials and Method

8.2.1 Materials

TiO₂-Degussa P25 (Evonik), LC/MS (Shimadzu) FTIR (Bruker, V22), HPLC (Agilent, Polymeric/TiO₂ membrane (Sigma Aldrich), polyvinyl alcohol, (Sigma Aldrich) polyvinyl pyrrolidone (Sigma Aldrich), solar simulator, pH meter (Mehstrom).

8.2.2 Methods

8.2.2.1 Photocatalyst preparation

The catalyst was prepared by dissolving and mixing 24.3% w/w polyvinyl alcohol and 11% w/w gelatin properly in distilled water to get transparent solutions. Next, 21.6 % w/w polyvinyl pyrrolidone dissolved in the solution of ethyl alcohol and water, which was mixed with PVA-gelatin solution. The solution was mixed and reacted properly at 45 °C, followed by dispersion of 43% w/w of TiO₂ Degussa P25 powder in the mixture. Thereafter, the polymeric/TiO₂ solutions were cross linked by physical cross linking method while storing the solution at - 2 °C.

8.2.2.2 Photodegradation and LC/MS analysis

The photodegradation of 2 ppm aspirin solution was carried out in a batch reactor (250 ml) at pH 3.5, under solar light of Intensity-77 mW/cm². Samples were taken at various time intervals were analyzed by LC/MS (LCMS-2010 EV Liquid Chromatography Mass spectrometer, Shimadzu) to identify the intermediate compounds. A capillary column C-18 (5 μm , 100 x 4.6 mm length) was used for separation of product intermediates. The mobile phase was a mixture of acetonitrile–water (70/30, v/v) with 0.04% glacial acetic acid to maintain an acidic pH. The flow rate of elute was 0.1 ml min⁻¹ and the injection volume was 20 μl. The UV detection was at 298 nm. The eluent from the chromatographic column successively entered the UV–vis diode array detector, the ESI interface and the quadruple ion trap mass analyzer. MS analysis in the negative ions

mode was performed on a mass spectrometer equipped with an ESI ion source. The ESI probe tip and capillary potentials were set at 2.5 kV and 25 V, respectively. The mass range was 50–750 m/z. The heated capillary was set to 200 °C.

8.2.2.3 Fourier Transform Infra Red (FTIR)

Fourier transform infra red analysis of the aspirin solution and its degraded products were carried out in Bruker FTIR (model no- Vector 22) to analyse the intermediates formed at different time intervals. The analysis of one broad banded pass of radiation through the sample gives rise to a complete IR spectrum. The radiation containing all IR wavelengths ranges from 400 to 5000 cm^{-1} . Results of 32 scans were combined to average out random absorption artifacts, and excellent spectra from very little amount of samples were obtained.

8.2.2.4 High performance liquid chromatography

HPLC (Agilent) used to analyse the intermediates. C18 column used with eluent acetonitrile and water (70:30) with flow rate of 0.1 ml/min. UV detection was at 298 nm. Peaks were observed within 15 minutes of retention time. A number of analytical techniques such as high performance liquid chromatography (HPLC), FTIR were employed for determination of several organic intermediates for several dyes degradation [7, 8]. The literature review reveals that no studies have been carried out to detect the intermediates during aspirin photo degradation. Aspirin molecules are non-volatile and highly soluble in hot water therefore cannot be analyzed by GC/MS. Therefore, liquid chromatographic techniques were employed for the analysis of mixtures of aspirin photodegradation and identification of their intermediates and degraded end products. The present study is focused on degradation of acetylsalicylic acid in the presence of solar light and TiO_2 /polymeric photocatalyst, and to identify degradation products of aspirin by LC/MS and FTIR for establishing the mechanism of photocatalytic degradation.

8.3 Results and Discussions

Among h_{vb}^+ , e_{cb}^- , and $\cdot OH$, based on the observed reactions pathway, it seems that hydroxyl radical is the most dominant factor in the degradation of aspirin in aqueous TiO_2 suspension. On the basis of chemical structures and concentration profiles of identified intermediates, possible reaction pathways during the photocatalytic degradation have been explained. Concentration of the intermediates formed and their degradation time have also been studied, which reflects the rate of formation of each intermediate. Products formed during the photodegradation process were analysed by HPLC which reported formation of six new intermediates at different intervals. Most of the peaks were observed within 15 minutes of retention time. The concentrations of the intermediates were calculated from the area of the peaks. However it was not possible to detect the compounds directly, therefore, intermediates were further analysed by LC/MS.

The components eluted having different retention time were subjected to mass spectrometry and identified by interpretation of their fragment ions in the mass spectra. The chromatographic and TOC data suggested that the entire components and their disappearance after 5 hours of photocatalytic treatment. The mass spectra of degraded products showed species at 59 m/z which was acetic acid and 137 m/z attributes to salicylic acid. Further, hydroxylation produced products at 110 m/z, which again formed species upon hydroxylation, showing fragments at 116 m/z (maleic acid) and at 90 m/z (oxalic acid). Further hydroxylation gave species at 104 m/z (malonic acid), which on hydroxylation formed products to show fragments at 59 m/z.

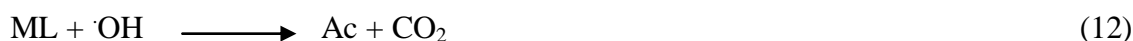
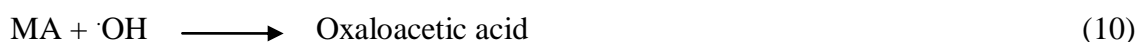
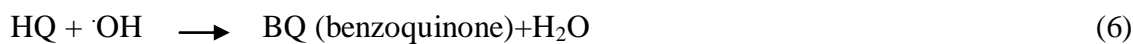
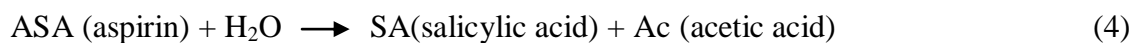
Table 8.1. Identification of intermediates

Compounds	Area of peaks	Rxn.time (min)	RT (min)	Rates ppm/min
Aspirin	1520362 100	0 20	14.3	
Salicylic acid	1398683 136.8 83.6	20 60 130	13.2	0.008
Hydroquinone	1091680	60	13	0.006
Muconic acid	289863 1052590	60 130	12.5	0.009
Maleic acid	15455 1000	130 220	10.5	0.005
Malic acid	505 14000	130 220	6.2	0.004
Oxalic acid	19005	130	1.5	0.008
Malonic acid	588103	220	6.7	0.0065
Acetic acid	121579 17000 77 117666 196264	20 60 130 220 260	5.8	0.008

Mass spectroscopy and the chromatograms showed the presence of only 8 intermediates. Few more compounds which have been assumed to have formed during the degradation, were not detected by the instrumental analysis. The absence of these compounds may be due to their unstable nature, which made them to degrade too fast to be detected. Benzoquinone, oxalo-acetic acid, formic acid were not detected in LC/MS.

8.3.1 The reaction mechanism

Based on the analysis, following reactions were most likely to have occurred during the degradation of aspirin.



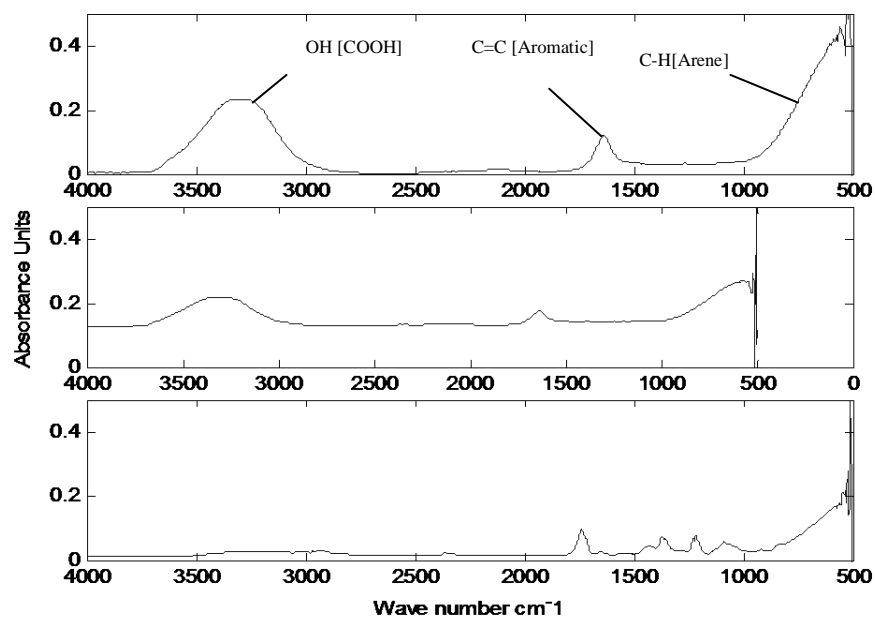
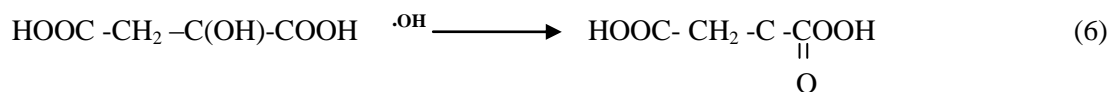
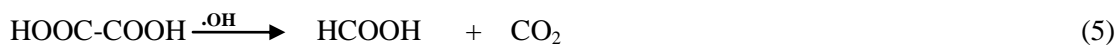
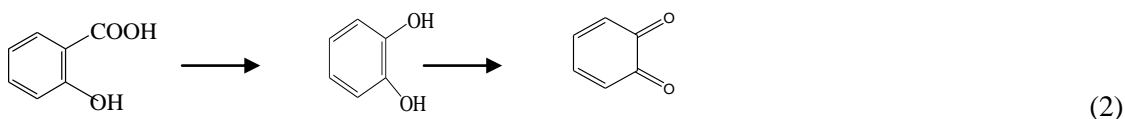
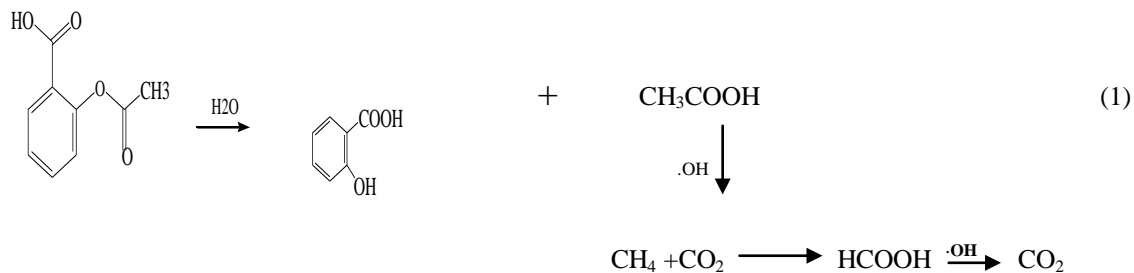


Figure 8.1: FTIR spectra of degraded aspirin solution

Aspirin solutions were subjected to Fourier transform infra red analysis before and after degradation. The band around $3000\text{-}3300\text{ cm}^{-1}$ attributed to the OH of COOH groups of aspirin. While the bands at $1000\text{-}1500$ and $500\text{-}1000(\text{cm}^{-1})$ attributed to the presence of C=C of benzene ring and secondary cyclic alcohols respectively. Also, Aromatic hydrocarbons are represented by the absorptions in the regions $1600\text{-}1585\text{ cm}^{-1}$. $1500\text{-}1400\text{ cm}^{-1}$ band attributed to C–C stretch (in-ring). Besides, C–H stretch has been represented by $3100\text{-}3000\text{ cm}^{-1}$ band.

From the study of all spectra, the presence of salicylic acid, butanedioic acid, malic acid, malonic acid and acetic acid were concluded. Gradually with time these compounds degraded and finally the end product did not show any of those peaks except for few aliphatic groups around 500cm^{-1} which can be related to negligible amount of CH_4 and C_2H_6 groups.

8.3.2 Pathways of aspirin degradation



Generally the sites near double bonds are attacked first in the degradation process. Aromatic intermediates were identified at the initial stages of degradation. Intermediates were formed were most probably aromatic acids and aliphatic acids. In this degradation

reaction, aspirin got hydrolysed in water by a mechanism involving an intramolecular generalised basis catalysis forming salicylic acid and acetic acid. Main products identified were salicylic acid, acetic acids, fumaric acid or maleic acid, malic acid and malonic. Salicylic acid got oxidised to 1, 2 dihydroxybenzene, which on further reaction $\cdot\text{OH}$ formed hydroquinone. While a part of salicylic acid also got oxidized to 2, 3 dihydroxybenzoic acid was less prominent than 1, 2 dihydroxy benzene formation reaction [8]. Hydroquinone hydroxylated to benzoquinone, which being unstable in aqueous solution underwent ring rupture followed by further oxidation forming muconic acid [8,9]. Addition of a hydroxyl radical to the double bond of muconic acid, yielded maleic acid and oxalic acid. Maleic/Fumaric acid then got oxidized to malic acid, which was a precursor of malonic acid. Malonic acid further produces acetic acid and carbon dioxide [10]. Oxalic acid got oxidized to CO_2 , through formation of formic acid. Acetic acid was observed to form both by hydrolysis of aspirin at the initial stage and also by oxidation of malonic acid. It was then oxidized to form CO_2 through formation of CH_4 , C_2H_6 and H_2O . The pathway of conversion of acetic acid to carbon dioxide [10-12] fitted well in degradation reaction pathway. The adsorbed CH_3COOH dissociated to CH_3COO^- species, which reacted with photogenerated holes to form $\cdot\text{CH}_3$ radicals and CO_2 (known as photo-Kolbe reaction) [13]. The active $\cdot\text{CH}_3$ radicals then reacted with H_2O to release CH_4 , or with another $\cdot\text{CH}_3$ radical to produce C_2H_6 . In consequence, $\cdot\text{CH}_3$ radicals reacted with $\cdot\text{OH}$ radicals to generate CH_3OH . Next, the photogenerated holes attacked the produced CH_3OH to form HCHO , which further oxidized by both $\cdot\text{OH}$ radicals and photogenerated holes to produce HCOOH [14]. At last step the HCOOH was decarboxylated by the photo-Kolbe reaction to release CO_2 . Decarboxylation of COOH group forms CO_2 by “photo-Kolbe” reaction [15]. Among most of the intermediates acetic acid was detected almost in larger amounts, compared to other aromatic acids. Formation of CO_2 is generally related to the degree of mineralization occurred during the photodegradation. In general at low reactant levels, reactants disappear exponentially, but at higher reactant levels, mineralization is slower than the degradation of the parent compound [15]. TOC values decreased with the increase of the irradiation time. This can be explained as; with time the acetylsalicylic acid gets hydrolysed and oxidized to lower molecular weight compounds so the TOC content was observed to decrease with time.

The TOC values though does not reach zero at the end but becomes negligible as compared to the initial value of the solution before degradation. Towards the end of the reaction, the parent compound forms acetic acid, which gradually forms carbon dioxide through the formation of CH_4 and C_2H_6 . It can be assumed that some of these CH_3 radicals were unable to form CO_2 at the end. These functional groups have also been identified in the FTIR spectrum at the end product.

Table 8.2. TOC content of aspirin solutions

Time (min)	Carbon content (mg/L)
0	1.19
20	1.13
180	0.35
300	0.01

8.4 Conclusion

Degradation of acetylsalicylic acid by solar stimulator in presence of TiO_2 -polymeric film catalyst was studied, revealing valuable information about the complex reactions during the process. This study was carried out to detect if the intermediates formed were more toxic than aspirin. The qualitative/quantitative analyses of the intermediates resulted in determination of the most probable reactions' mechanism governing the degradation process. Although some of the intermediates were not identified due to their instability and fast degradation, they were determined through the reaction's path. The results obtained corresponded well with the reported data on the degradation of acetic acid and phenolic compounds by other researchers. The resulting mechanism showed that salicylic acid, acetic acid, and muconic acid were the main components in the reactions. Major aliphatic acid like muconic, malic and malonic acids formation by the photocatalytic oxidation process explains the opening of the aromatic ring. The TOC results combined

with LC-MS and FTIR concluded that the products formed during the reactions decomposed into carbon dioxide and environmentally friendly non-toxic products.

8.5 Nomenclature

NSAIDs- Nonsteroidal anti-inflammatory drugs

ASA- Acetylsalicylic acid

SA- Salicylic acid

HQ- Hydroquinone

BQ- Benzoquinone

Mc- Muconic acid

ML- Malonic

Ac- Acetic acid

LC/MS - Liquid chromatography/Mass spectroscopy

FTIR - Fourier transform infra red

HPLC - High performance liquid chromatography

TOC - Total organic content

OH - Hydroxyl ion

h_{vb}^+ - Holes in valence band

8.6 References

1. Terry, L.A., *Water Pollution, Environ. Law practice*,4, (1996),19-29.
2. Poppe, Wayne, Hurst, Renee, *Water qual. Int.*, (1997),37-39.
3. Richman, M., *Ind. Wastewater*, 5, (1997), 24-29.
4. Nathan Wei, <http://www.arthritis-treatment-and-relief.com/aspirin-side-effects.html>, Retrieved May 2010.
5. A. Achilleos, E. Hapeshi, N.P. Xekoukoulotakis, D. Mantzavinos and Fatta-Kassinou, *Separation Science and Technology*, 45, (2000),1564-1570.
6. Fabiola Méndez-Arriaga, Santiago Esplugas, Jaime Giménez, *Water Research*,42, (2008),585- 595.
7. P. Calza, V.A. Sakkas, C. Medana, C. Baiocchi, A. Dimou, E. Pelizzetti, T. Albanis, *Applied Catalysis B: Environmental*, 67, (2006), 197-205.
8. D. R. A. Uges, H. Bloemhof and E. K. Juul Christensen, *Pharmacy World & Science* 3, (1986),1309-1315.
9. Arthur Winter, *organic chemistry 1, Science*, (2005), 388.
10. Christoph K. Scheck, Fritz Frimmel, *Wat. Res.* 29, (1995), 2346-2352.
11. A. Chemseddine, H.P. Boehm, *J. of Molecular Catalysis*, 60, (1990), 295-311.
12. S.D. Muggli, Falconer, *J. Catalysis*,187, (1999), 230-237.
13. Zheng X.Z., Wei L.F., Zhang Z.H., Jiang Q.J., Wei Y.J., Xie B., Wei M.B., *Int. J. of hydrogen energy*, 34, (2009), 9033-9041.
14. Méndez-Arriaga F., Esplugas S., Giménez J., *Water Res.* 42, (2008), 585-594.
15. Z.P.G. Masende , B.F.M. Kuster, K.J. Ptasinski, F.J.J.G. Janssen , J.H.Y. Katima, J.C. Schouten, *Applied Catalysis B: environmental.* 56, (2004), 189-199.

Chapter 9

Photodegradation of methyl orange in a large scale continuous reactor under LED lights in presence of TiO₂/polymeric film photocatalyst

9.1 Introduction

Approximately, 14,000 people die every day because of water pollution, all over the world [1]. According to official classification, 41.3% of the United States' water is polluted. China is the latest victim of impure water tragedies [2]. The environment is extremely fragile. Recent pollution offenses include mountaintop mining in the Appalachians, oil drilling at both the Arctic and Antarctic poles which results in massive wildlife death, and oil spills that sicken people, as was recently the case in United States. Canada flushes some 200 billion liters of raw sewage directly into natural waterways every year, from the St. Lawrence River to the Strait of Juan de Fuca and the Pacific Ocean [3, 4]. Scientists detected the traces of several organic dyes and prescription drugs in the water that comes from many people's faucets. These organic dyes come from textile and printing industries sewage. To be sure, the concentrations of these chemicals are really low, measured in quantities of parts per billion or trillion. It has been proved by scientists that the traces of these chemicals can cause several health problems to both human and wild life [5]. These dyes besides being carcinogenic to human health, also causes kidney and liver damage [6].

In our study, methyl orange has been taken up as the model organic pollutant. Methyl orange in Fig. 9.1 has been proved to be hazardous in case of skin contact (irritant), of eye contact (irritant), ingestion, inhalation. Severe over-exposure can result in death.

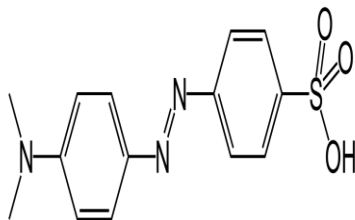


Figure 9.1: Structure of methyl orange [7].

These, organic pollutants though can be partially absorbed by charcoal or activated carbon but cannot be completely removed [8]. Also, the use of charcoal again pollutes our environment in several ways. Thus the traditional water treatment technologies can decolourize and absorb these chemicals but cannot degrade them completely. Distillation and reverse osmosis though remove a wide range of water supply contaminants but unable to degrade these aromatic functional groups containing dyes. The premier activated carbon water filter on the market, won't strip away these organic pollutants completely, either. Therefore, advanced oxidation processes have been introduced, to degrade these pollutants in water. Among all kind of advanced oxidation processes, photocatalytic oxidation is the most promising one. In recent years, photocatalytic degradation mediated by illuminated TiO₂ has received considerable attention as an alternative for treating polluted water. It has been proved that this process can degrade many toxic compounds in waste water into carbon dioxide. The most suitable semiconductor for the photocatalytic reaction is TiO₂ Degussa P25 [9, 10]. According to the proved theory of photocatalytic degradation of organic pollutants, the relevant reactions at the semiconductor surface causing the degradation of dyes can be expressed as follows:



The resulting $\cdot\text{OH}$ radical, being a very strong oxidizing agent (standard redox potential +2.8 V) can oxidize most of methyl orange dye the mineral end-products. Substrates not reactive toward hydroxyl radicals are degraded employing TiO₂ photocatalysis with rates of decay highly influenced by the semiconductor valence band edge position [11]. In our

study, a large scale continuous flow reactor has been employed to degrade methyl orange under LED lights in presence of TiO₂/polymeric photocatalyst films. The effects of initial concentration and flow rates have been studied and analysed. Several researches have been carried out on degradation of methyl orange by slurry TiO₂ under UV, solar and fluorescent lamps [12, 13]. In our studies almost similar trend has been observed for methyl orange degradation under visible lights. Effects of flow rate and initial concentrations, on the degradation rate, have been discussed.

9.2 Materials and Methods

9.2.1 Materials

Methyl orange (Sigma Aldrich), Gelatin (Sigma Aldrich), PVA (Sigma Aldrich), PVP (Sigma Aldrich), TiO₂ Degussa 25 (Evonik), Beaker (Chemistry store, UWO), Conical flask (Chemistry store, UWO), LED lights, Continuous reactor, peristaltic pump

9.2.2 Methods

9.2.2.1 Photodegradation of MeO under LED lights

A large scale continuous reactor of volume 5000 cc shown in Fig. 9.2, consisted of two concentric cylinders with the LED lights supported on a plastic support hold outside the reactor. The radius of the space between two cylinders was 5 cm and the thickness of the cylindrical wall was 0.45 cm. The light intensity measured was 7 mW/cm². The methyl orange solution containing 0.00025 cm² pieces of photocatalyst films was pumped by a peristaltic pump into the reactor. After photodegradation the solution was pumped out of the reactor into the same container which was continuously being stirred by a magnetic stirrer. The concentration change of the solutions were continuously monitored by a UV-Vis spectrophotometer at ($\lambda = 465$ nm).

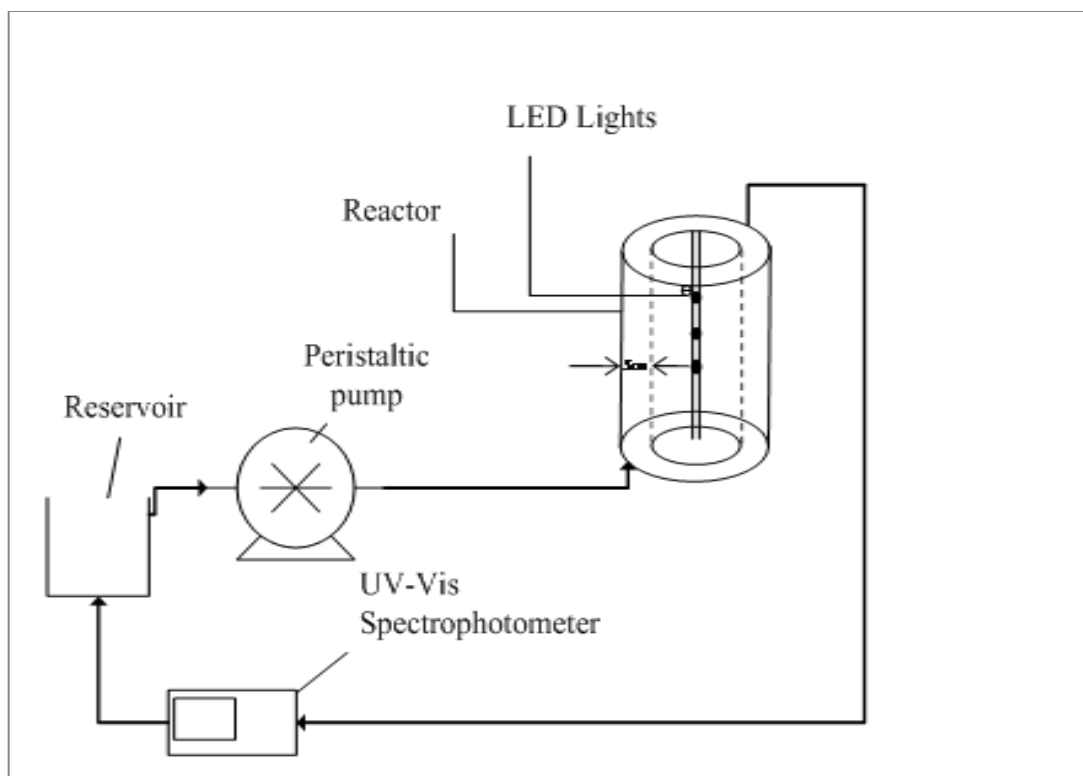


Figure 9.2: Experimental setup of methyl orange photodegradation under LED illumination. Experimental conditions [Large scale 5 L reactor, $I = 4.1 \text{ mW/cm}^2$, $\text{pH} = 5.8-6$, $H = 0.45 \text{ mm}$, Flow rate = 800 ml/min]

9.2.2.2 Preparation of TiO_2 -polymeric composite

The polymers used to prepare the catalyst have been considered non-toxic by WHO and also have been proved to be by toxicology researches [18, 19, 20]. 24.3 % w/w of PVA and 11% w/w of Gelatin were dissolved and mixed properly in distilled water and to get a transparent solution. Next, 21.6 % w/w of PVP dissolved in the solution of ethyl alcohol and water at 45°C . The solution was stirred for 15 minutes followed by dispersion of 43 % w/w TiO_2 Degussa P25 powder in the mixture. The photocatalyst film was cut into small pieces of area 0.00025 cm^2 .

9.2.2.3 Blank experiments

This experiment was carried out with photo catalyst but no illumination. Dark reactions were carried out at different concentrations (100 ppm, 30 ppm, 15 ppm and 2 ppm). It was observed in UV-Vis spectrophotometer that the concentration has changed after some time. These changes in the concentration, proved the adsorption of methyl orange on the catalyst surfaces. This dark reaction was carried out to saturate the catalyst surface by dye adsorption so that during reaction under LED lights no more adsorption of dye occurs.

9.3 Results and discussions

9.3.1 Photocatalytic oxidation

The detailed mechanism of MeO dye catalyzed degradation states that conduction band electrons (e^-) and valence band holes (h^+) are generated when aqueous TiO_2 suspension is irradiated with light energy greater than its band gap energy (3.2 eV). The photo-generated electrons could reduce the dye or react with electron acceptors such as O_2 adsorbed on the photocatalyst surface or dissolved in water reducing it to superoxide radical anion $O_2^{\bullet-}$. The photogenerated holes can oxidize the organic molecule to form R^+ , or react with H_2O forming $\cdot OH$ radicals. Together with other highly oxidant species (peroxide radicals) they are reported to be responsible for the heterogeneous TiO_2 photodecomposition of organic substrates as dyes [11, 13].

9.3.2 Effects of flow rates on the photodegradation of methyl orange

Experiments were carried out at several flow rates. In the graph below effect of the following flow rates [45, 85, 200, 450, 650, 800 (ml/min)] are depicted. The degradation rates increased with the increase of flow rates. Due to limitations on experimental set up, experiment at higher flow rate was not possible. The increase of degradation rate with the increase of flow rate, was due to the effect of external mass transfer. External mass

transfer played a significant role for the low flow rates. Therefore with increasing flow rates the degradation also increased but beyond this limit, the increment in flow rate does not affect the degradation anymore. Therefore 800 ml/min has been selected as ideal flow rate for the rest of the experiment. Also beyond this flow rate bubbles would be introduced in the reactor which would lead to experimental errors.

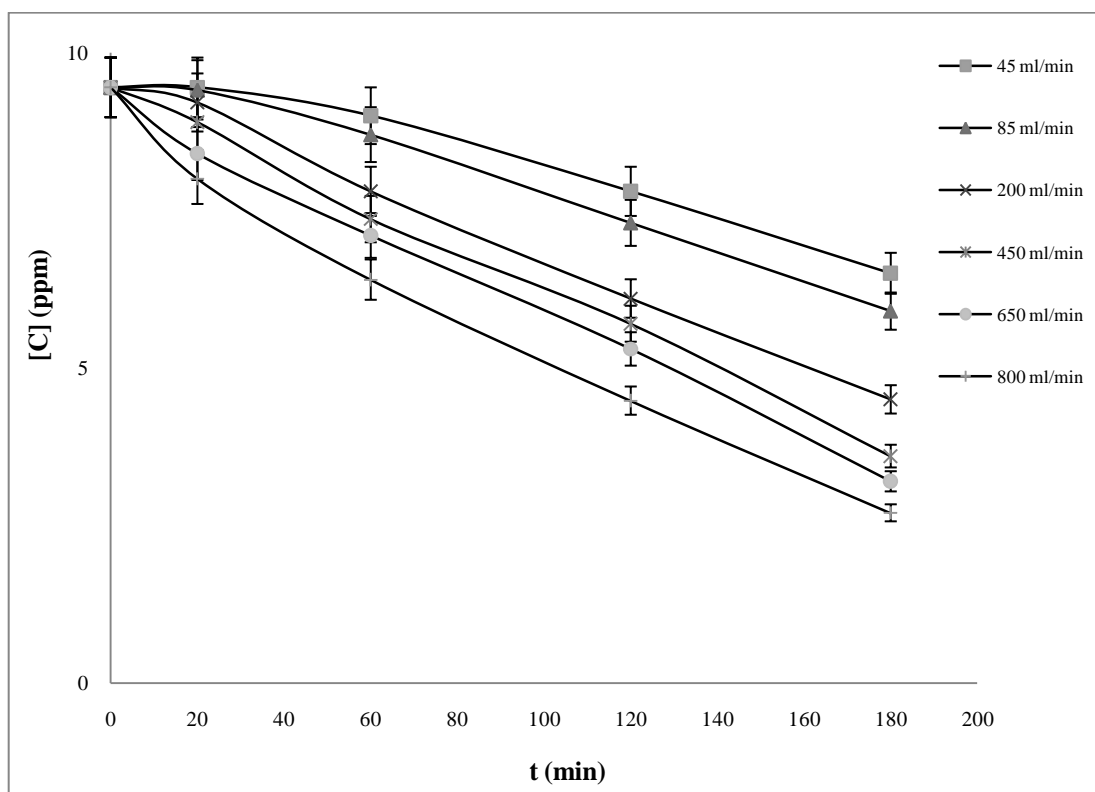


Figure 9.3: Effects of flow rates on photodegradation of MeO under LED lights. Experimental conditions [$C_0 = 10$ ppm, pH - 5.8, $I = 4.1$ mW/cm², H= 0.45 mm]

9.3.3 Photodegradation of MeO

After the dark reaction was carried out, methyl orange solution ($C_0 = 200$ ppm, after dark reaction 198 ppm) was photo degraded till 300 minutes. The photo degraded samples were collected for spectrophotometric observations at very small intervals of time both at the beginning and also towards the end of the reaction. From Fig. 9.4 the rate constant of

the photocatalysis was calculated. The rate constant was calculated to be 0.071 mg/L/min. It was also observed that degradation rate was independent of the concentration at very high concentrations. It was found that TiO₂-polymeric composite catalyst degraded 72% of the methyl orange under LED light.

$$\epsilon\% = (C_0 - C)/C_0 \times 100 = 72\%$$

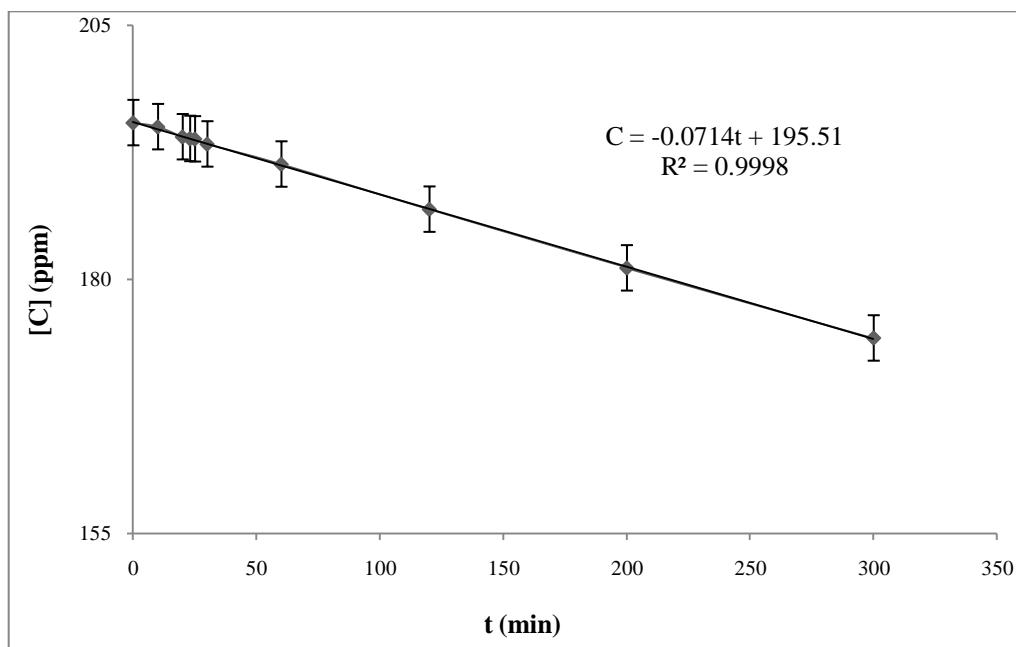


Figure 9.4: Photodegradation of MeO. Experimental conditions [$C_0 = 200$ ppm, pH – 5.8, $I = 4.1$ mW/cm², $H=0.45$ mm]

Here C_0 is the initial concentration of methyl orange and C is the final concentration after time T .

9.3.4 Effect of initial concentrations

The effect of initial concentrations of MeO was studied. To study the initial degradation rate the photodegradation was carried out for 30 minutes. The organic dyes

concentrations in waste water usually range from 0.01-0.05 g/dm³ [19]. Therefore, methyl orange solutions of different concentration were used ranging from 2 ppm to 200 ppm [200, 100, 30, 10, 2 (ppm)]. The solutions were subjected to photo degradation at pH 5.8 under LED lights, for 30 minutes to observe the initial degradation rate. Fig. 9.5 explained that the degradation of MeO followed the model of Langmuir-Hinshelwood. It was observed that the degradation rate decreased with the decrease of concentration. This phenomenon, can be explained as: i) Low concentrated solution degradation was affected by the mass transfer resistances. While at very high concentration the degradation rate remained independent of mass transfer effects. ii) With the increase of the initial concentration of the dye the probability of reaction between dye molecules and the photocatalyst also increased which lead to an enhancement in the degradation rate.

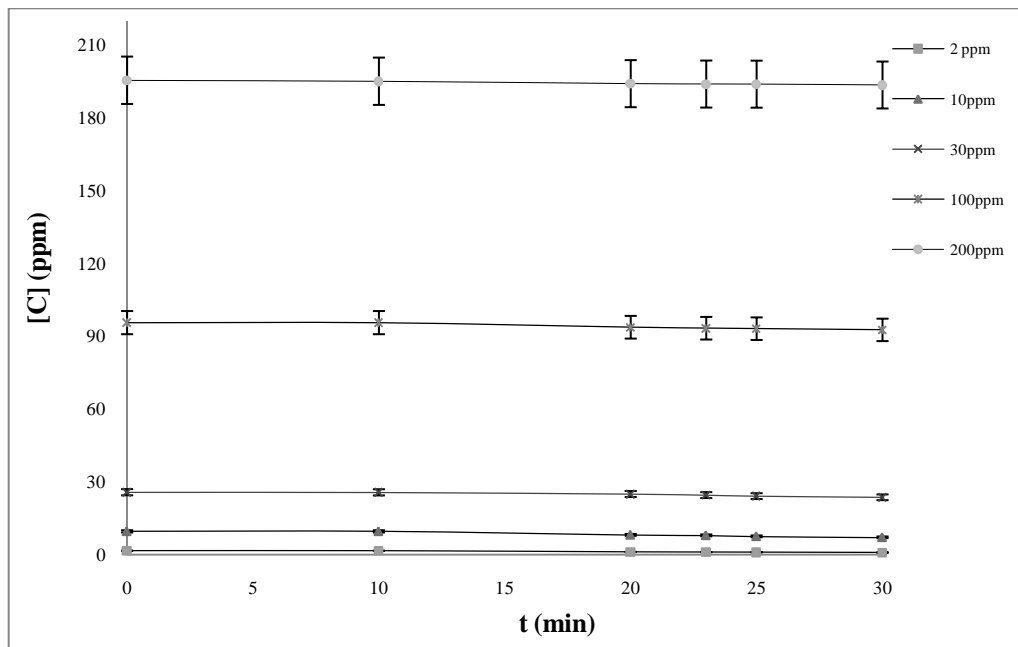


Figure 9.5: Effect of initial concentrations on photodegradation of MeO. Experimental conditions [pH = 5.8, I = 4.4 mW/cm², Flow rate= 800 ml/min, H= 0.45 mm]. $k_{200} = 0.1$ ppm/min, $k_{100} = 0.14$ ppm/min, $k_{50} = 0.07$, $k_{10} = 0.048$, $k_2 = 0.03$

While researchers reported that degradation rate increased with the increase of dye concentration to a certain limit and further increase lead to a decrease in degradation rate, which was due to the reduction in generation of $\cdot\text{OH}$ radicals on the catalyst surface [12,

13]. In this study the degradation increased with the increase of dye concentration up to 100 ppm, beyond which degradation rate decreased. The decrease of dye degradation as the dye concentration increase beyond 100 ppm was due to the reduction of $\cdot\text{OH}$ radicals formation on the catalyst surface (since the active sites were covered by the dye ions) [13]. Our results showed, that at irradiation of methyl orange by LED source, the degradation of the dye decreased as the dye concentration increased beyond a certain limit (100 ppm) [11-13]. This decrease in rate can be explained as, the result of decreased number of photon absorption by the catalyst at higher concentration [13].

9.3.5 Kinetic study

Photodegradation of 200 ppm MeO was carried out for 30 minutes, for calculating the initial degradation rate constant. At very high concentration, the rate remained independent of mass transfer resistances. Therefore, the rate constant determined from this Fig. 9.6 was compared with the k value obtained from Fig. 9.7.

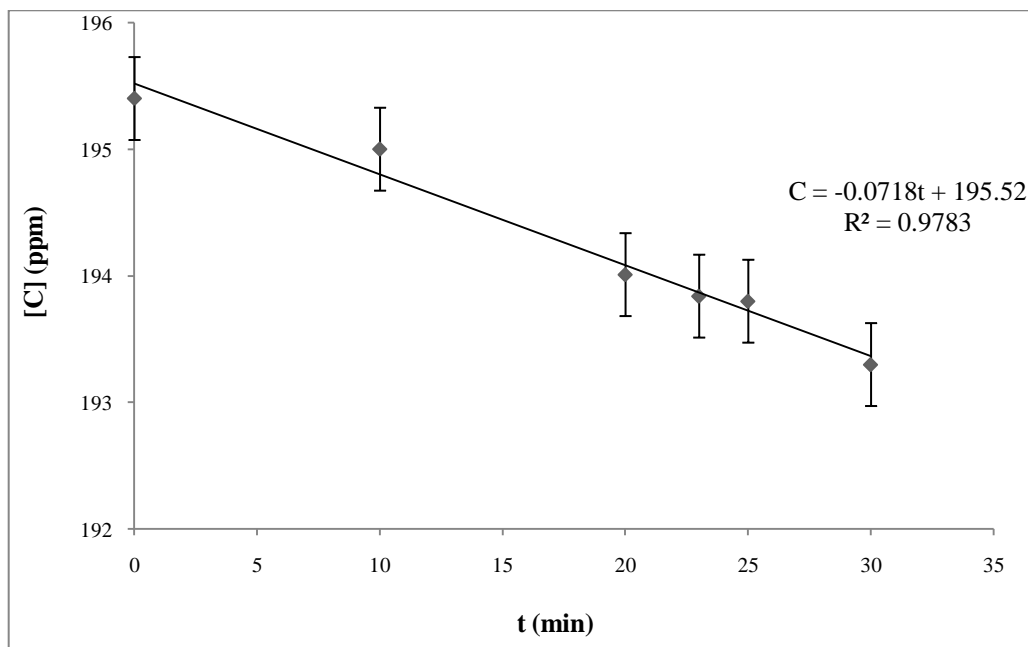


Figure 9.6: Photodegradation of MeO under LED lights. Experimental conditions $[C_0 = 200 \text{ ppm}, \text{pH} = 5.2, I = 4.1 \text{ mW/cm}^2, \text{TiO}_2 \text{ loading} = 1.5 \text{ g/L}]$

The rate constant obtained was $k = 0.071 \text{ mg/L/min}$

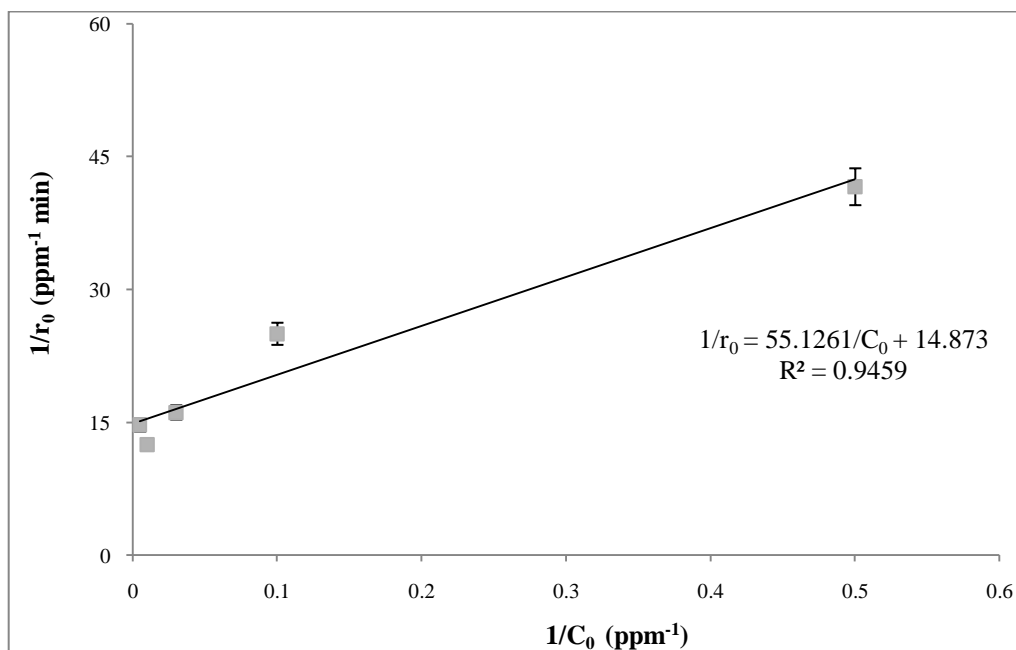


Figure 9.7: Photodegradation of MeO. Experimental conditions [$C_0 = 200, 100, 30, 10, 2$ (ppm), pH -5.2, $I = 4.1 \text{ mW/cm}^2$, TiO_2 loading = 1.5 g/L]

The rate constant and adsorption constant obtained from this plot were $k = 0.067 \text{ mg/L/min}$ and $K = 0.27 \text{ Lmg}^{-1}$

9.3.6 Total organic carbon measurement

The total organic carbon content was measured after the degradation of methyl orange under LED lights and in presence of the TiO_2 -polymeric photocatalyst. After photodegradation the total organic carbon content of methyl orange was observed to decrease with time. The decrease of carbon content signifies the degradation of the methyl orange into nontoxic decomposition compounds.

Table 9.1: Total organic carbon content measurement

Time	Carbon content (mg/L)
0	1007.1
10	1000
20	950
60	900
120	710
240	325
300	14

9.4 Conclusions

The porous TiO₂/polymeric composite catalyst developed in this experiment was observed to degrade MeO under LED lights. At very high concentration, the degradation kinetics was observed to fit into Langmuir-Hinshelwood model, while at low concentration, the kinetics followed was first order. It can be concluded that at higher flow rate the degradation was observed to be faster than at lower flow rates, which can be attributed to minimization of external mass transfer resistances. The pH of the solution remained unaltered on LED lights exposure, unlike UV lights. The photo-catalytic processes were influenced by the initial concentrations of methyl orange. Color change from orange to colorless was irreversible. With the increase of concentration, the degradation rate increased. At very high concentration, the rate of reaction was independent of the mass transfer effects. While at lower concentration, the mass transfer resistances being dominant, decreased the degradation rate. Beyond 100 ppm, MeO degradation was observed to decrease which was due to the less production of OH radicals due to the coverage of active sites by the high concentrated MeO molecules. The degradation rate was lower than under UV lamp, due to very low light intensity. LED lights had very little or no cross-linking effects on the photocatalyst film, thereby not affecting the rate with time. More studies required in this case. Increase of light intensity can be assumed to increase the degradation rate.

9.5 Recommendations

- 1) Studies can be carried out by increasing the intensity of the LED lights.
- 2) Different visible or fluorescent lamps can be installed and supported to the setup.
- 3) Slurry TiO_2 can be coated on the inner wall of the reactor, to study the effects of different catalyst nature on the degradation rate.
- 4) TiO_2 -polymeric photocatalyst can be immobilized on the inner wall of the reactor.

9.5 Nomenclature

MeO – Methyl orange

ppm – Parts per million

eV – Electron volt

UV – Ultra violet

TOC – Total organic carbon

9.6 References

1. Peter Vikeshland, Krista L Rule, <http://www.innovationmagazine.com/innovation/>, Retrieved April 2009.
2. Larry West, <http://scipeeps.com/articles-on-water-pollution/>, Retrieved April 2009.
3. U.S. Dept. of the Interior, Federal Water Pollution Control Administration, Great Lakes Region, http://openlibrary.org/books/OL5737954M/Water_pollution, (2011).
4. Alaton I.A., Balcioglu I.A., Bahnemann D.W., *Water Res.* 36, (2000), 1143–115.
5. Chatterjee D (2004). *Bull. Catal. Soc. India* 3, (1998), 56-58.
6. Chatterjee D, Mahata A, *Appl. Catal. B Environ.* 33,(2001), 119-125.
7. <http://www.tutorvista.com/content/chemistry/chemistry-iv/chemistry-in-life/methyl-Orange>, Retrieved June 2009.
8. Chun H, Yizhong W., *Chemosphere*, 39, (1999), 2107-2115.
9. Fujishima, K. Honda, *Nature*, 238, (1972), 37-3.
10. Tang J, Durrant JR, Klug DR., *J. Am Chem Soc.*, 130, (2008), 13885-91.
11. Hoffman M.R., Martin S., Choi W., Bahnemann DW, *Chem. Rev.* 95, (1995), 69-79
12. M.N. Rashed, A.A.El-Amin, *Int. J. of Physical Sciences*, 2, (2007), 131-145.
13. S.B. Sakthivela, M.V. Neppolianb, B. Shankarb, M. Arabindoob, V.Palanichamyb, and V. Murugesanb, *Sol. Energy Mater. Sol. Cells*, 77, (2003), 65-82.

10 Final Conclusions

10.1 Conclusions

A wide range of experiments were carried out at different conditions to study the degradation of pollutants using TiO_2 photo-catalyst. Methyl Orange and Aspirin were selected as two model compounds. In order to avoid the costly process of filtration/ultrafiltration of photo-catalyst, the TiO_2 particles were immobilized by a novel technique over a safe and environmentally friendly polymeric substance. The film photocatalyst were prepared by non-toxic polymers (approved by FDA and WHO), posing no threat to human health. It was concluded that the TiO_2 -polymeric film can be an efficient photocatalyst under both UV and solar lights but due to the cross-linking effects of the UV on the polymeric film, the rate changed with the progress of time under the UV lamp. This film showed best efficiency under solar light, since solar contains only 4% of UV light. It was observed that variation of the film thickness plays an important role in degrading pollutants due to internal mass transfer effects, (increasing diffusional length across the grain of the micro porous film). The external mass transfer effects were minimized by controlling the flow rates and mixing. In both cases (Methyl orange and Aspirin degradation), with the increase of concentrations, the degradation rates increased up to a certain limit, beyond which it decreased. The combined effect of mass transfer, photon absorption and $\cdot\text{OH}$ radical reproducibility were most probably the main reasons for such behaviour. Due to variation of the surface charge of TiO_2 particles, the pH of the solution was a crucial factor. The acidic pH would be the best for organic dyes having similar properties as methyl orange and all NSAIDs. In, degradation studies under the UV light, the pH of MeO was observed to change drastically with time which also affected the degradation rate, but under LED lights such drastic changes in pH were not observed. Similar experiments on canola oil showed the applicability of this photocatalyst for oil spill remediation. Addition of the photo catalyst, which remains suspended at the water surface due to its high porosity, creates an ideal situation where solar radiation activates the catalyst on one side while spilled oil degradation occurs on the other side. In case of off shore oil spill, the waves create enough mixing to overcome mass transfer resistances.

Degradation mechanism of aspirin showed that a number of intermediates were formed and finally converted to carbon dioxide and water. Incomplete degradation may result in release of these intermediates which could be a source of contamination in surrounding environment.

Experiments in larger scale reactor also showed the applicability of photocatalytic degradation in commercial sizes. The process undergoes different hydrodynamics in larger scales, which may affect the effectiveness of the degradation. More studies are required to investigate the effects of scale up on photocatalytic degradation of pollutant in large scales.

In brief, this novel polymeric-TiO₂ film photocatalyst holds the potential of an efficient, economical, photocatalyst of the future world for environmental detoxification.

Appendix I (Chapter 5)

I Photodegradation of methyl orange in presence of TiO₂/polymeric photocatalyst under UV lamp

I.1 Calculation of residence time

The photodegradation was carried out for 140 minutes but the resident time of methyl orange solution inside the reactor was taken into consideration.

$$t_r = t_{\text{expt}} \times V_r / V_l, \text{ here } [t_{\text{expt}} = 140 \text{ minutes, } V_r = 121 \text{ ml, } V_l = 150 \text{ ml}]$$

Therefore the residence time of methyl orange in the reactor was 112 minutes.

I.2 Calculation of total organic carbon content

Molecular wt. of methyl orange (C₁₄H₁₄N₃NaO₃S) is 327.33 g. mol⁻¹

Amount of carbon in 1 mg/L of MeO = $14 \times 12 / 327.33 = 0.51 \text{ mg}$

Therefore, after 140 minutes of degradation under UV lights 7.5 mg of carbon corresponds to 15 ppm of MeO.

Appendix II (Chapter 6)

II Photodegradation of Aspirin by slurry TiO₂ both under UV and solar lights

II.1 Dark reactions

Before the carrying out the photocatalytic reactions, experiments were conducted to investigate whether there is any direct photolysis (in the presence of light but in the absence of any catalyst). It was observed that no direct photolysis took place for aspirin. When experiments were conducted in the presence of catalyst but in the absence of light (dark reaction), a small decrease in the concentration of aspirin was observed because of adsorption onto the catalyst surface, which reached an equilibrium value within 30 minutes. Hence, before the light was turned on, it was always ensured that adsorption equilibrium was reached.

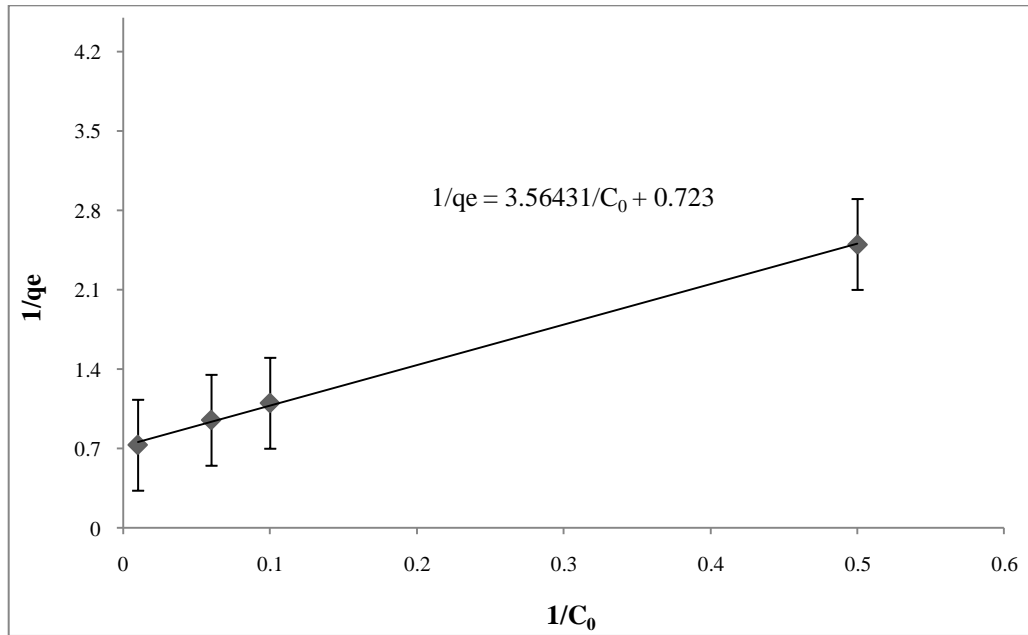


Figure II.1: Dark reaction of aspirin in presence of TiO₂ slurry

The small change in concentration of aspirin in absence of light (dark reaction) in presence of a slurry TiO_2 can be attributed to the adsorption of aspirin onto the surface of the TiO_2 . The concentration of aspirin adsorbed on the catalyst was calculated from the difference between the initial and equilibrium concentrations. Having prepared the plot of $1/q_e$ Vs $1/C_0$, where q_e is the amount of dye adsorbed on the catalyst surface and C_0 is the initial concentration, q_m and K were obtained. This reaction appeared to follow Langmuir adsorption isotherm:

$$q_e = q_m K C_0 / (1 + K C_0)$$

q_m and K are the saturation and adsorption equilibrium values respectively

$$K = 0.2 \text{ Lmg}^{-1}, q_m = 1.38 \text{ mg/L}$$

Here q_m is the maximum amount of dye adsorbed and K is the adsorption constant.

Appendix III (Chapter 7)

III Photodegradation of Aspirin under both UV and solar light in presence of polymeric-TiO₂ film

III.1 Dark reactions

When experiments were conducted in the presence of catalyst but in the absence of light (dark reaction), a small decrease in the concentration of aspirin was observed because of adsorption onto the catalyst surface, which reached an equilibrium value within 30 minutes. Hence, before the light was turned on, it was always ensured that adsorption equilibrium was reached. The small change in concentration of aspirin in absence of light (dark reaction) in presence of a TiO₂/polymeric film catalyst can be attributed to the adsorption of aspirin onto the surface of the film photocatalyst. The concentration of aspirin adsorbed on the catalyst was calculated from the difference between the initial and equilibrium concentrations. Having prepared the plot of $1/q_e$ Vs $1/C_0$, where q_e is the amount of dye adsorbed on the catalyst surface and C_0 is the initial concentration, q_m and K were obtained. This reaction appeared to follow Langmuir adsorption isotherm:

$$q_e = q_m K C_0 / (1 + K C_0)$$

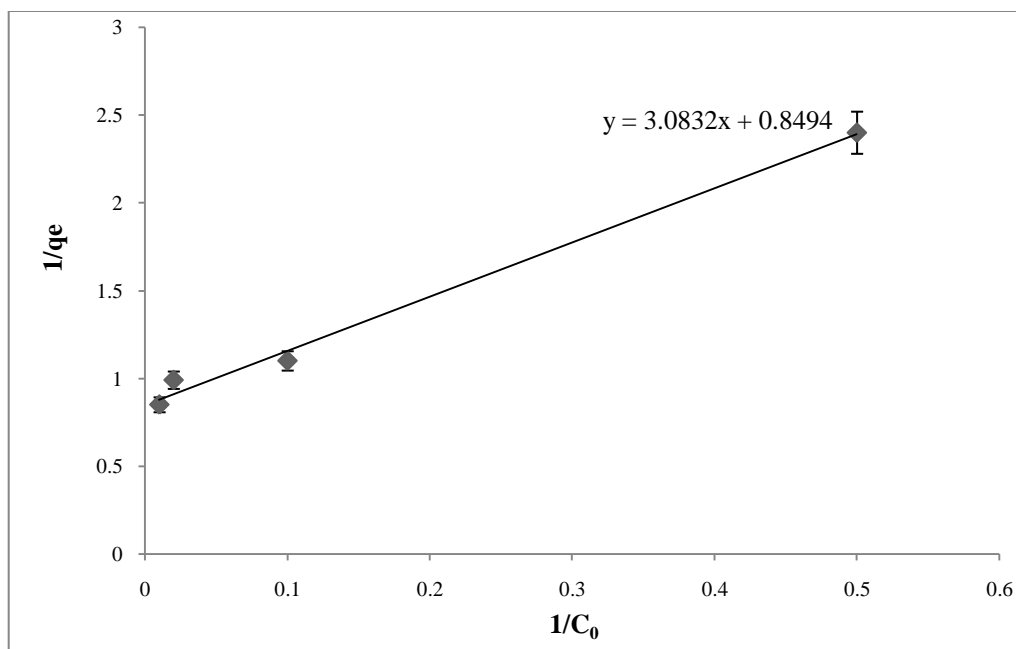


Figure III.1 Dark reactions of methyl orange in presence of TiO₂/polymeric photocatalyst

$$K = 0.27 \text{ Lmg}^{-1}, q_m = 1.17 \text{ mg/L}$$

Here q_m is the maximum amount of dye adsorbed and K is the adsorption constant.

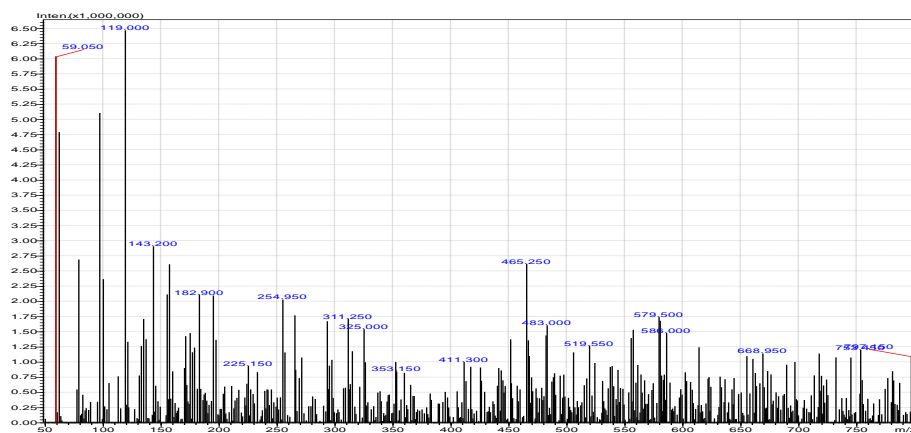
Appendix IV (Chapter 8)

IV Mechanism of aspirin degradation under solar light in presence of a TiO₂/polymeric film

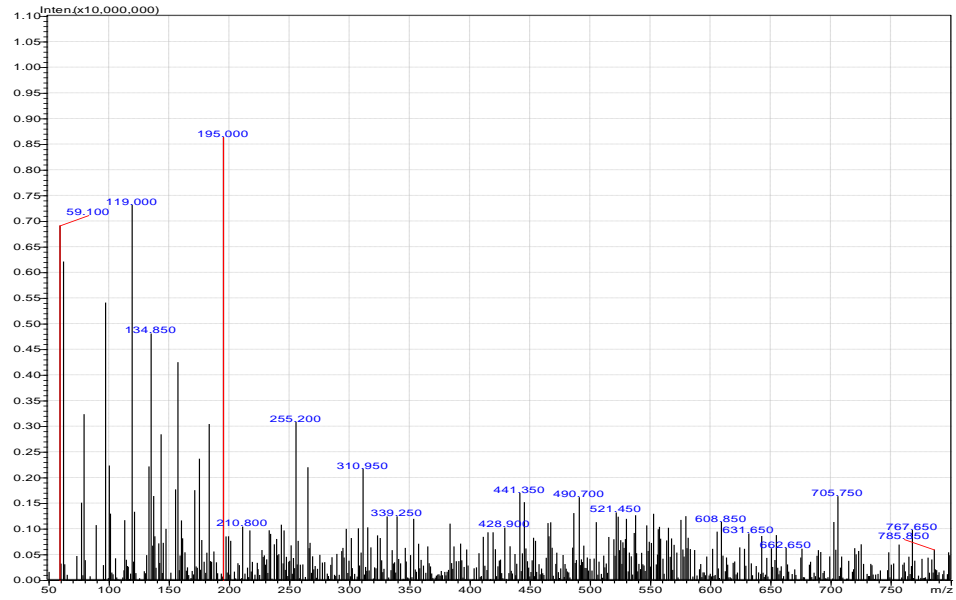
IV.1 LC/MS Analysis

The photodegradation of 2 ppm aspirin solution was carried out in a batch reactor (250 ml) at pH 3.5, under solar light of Intensity-77 mW/cm². Samples were taken at various time intervals were analyzed by LC/MS (LCMS-2010 EV Liquid Chromatography Mass spectrometer, Shimadzu) to identify the intermediate compounds. A capillary column C-18 (5 μm , 100 x 4.6 mm length) was used for separation of product intermediates. The mobile phase was a mixture of acetonitrile–water (70/30, v/v) with 0.04% glacial acetic acid to maintain an acidic pH. The flow rate of elute was 0.1 ml min⁻¹ and the injection volume was 20 μl. The UV detection was at 298 nm. The eluent from the chromatographic column successively entered the UV–Vis diode array detector, the ESI interface and the quadrupole ion trap mass analyzer. MS analysis in the negative ions mode was performed on a mass spectrometer equipped with an ESI ion source. The ESI probe tip and capillary potentials were set at 2.5 kV and 25 V, respectively. The mass range was 50–750 m/z. The heated capillary was set to 200 °C.

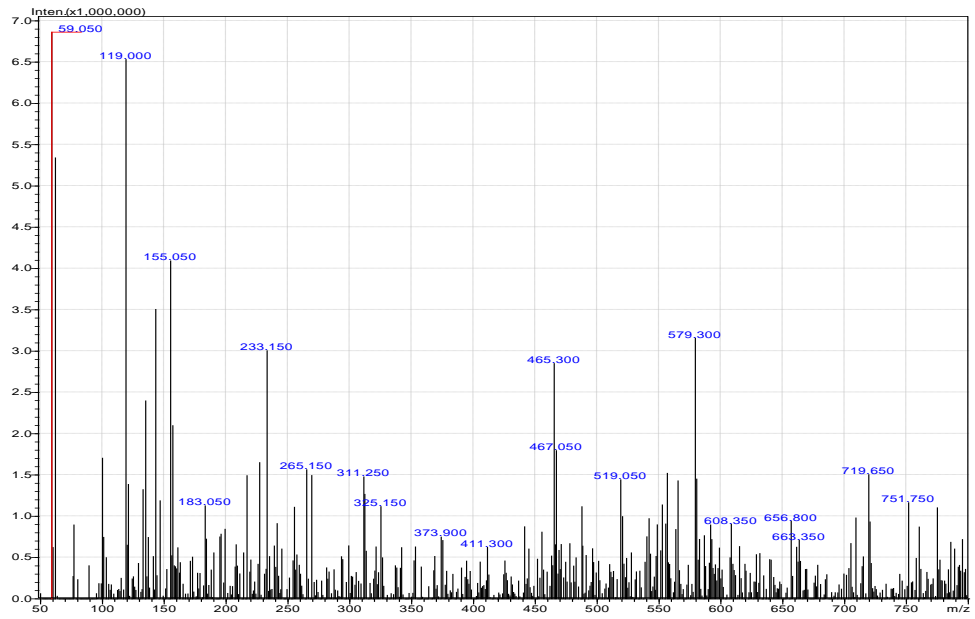
The mass spectroscopy spectrums are as follows:



[a]

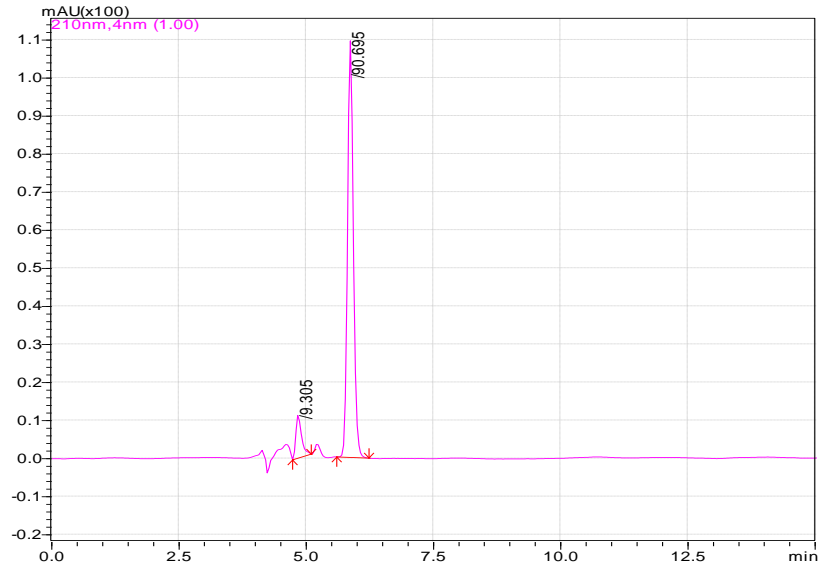


[b]

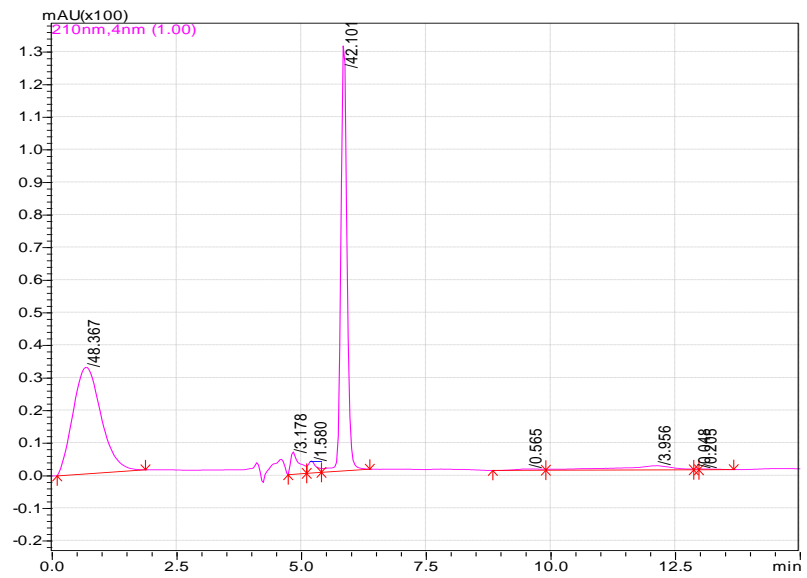


[c]

Figure IV.1: [a],[b], [c], MS spectra of the degraded aspirin



[d]



[e]

Figure IV.2: [d,e], LC spectra of degraded aspirin

IV.2 Calculation of total organic carbon content

Molecular wt of aspirin ($C_9 H_8 O_4$) is $180.15 \text{ g.mol}^{-1}$

No. Of carbons present in 1 mg of aspirin is $9 \times 12 = 108/180.15 = 0.59 \text{ mg}$

2 ppm aspirin contains 1.19 mg of Carbon

Therefore after 300 minutes of degradation 0.01 mg of carbon represents 0.016 ppm of aspirin

Appendix V (Chapter 9)

V Photodegradation of methyl orange in a large scale continuous reactor under LED lights in presence of TiO₂/polymeric film photocatalyst

V.1 Residence time of methyl orange inside the reactor

Photodegradation of MeO was carried out for 330 minutes in a 5000 cc continuous flow reactor under LED lights in presence of TiO₂/polymeric film photocatalyst.

$t_r = t_{\text{expt}} \times V_r/V_1$, where $V_r = 5$ Litres and $V_1 = 5500$ cc [V_1 and V_r are volume of liquid and volume of reactor respectively.]

Therefore, the residence time of the MeO in the reactor was $t_r = 300$ minutes

V.2 Total organic carbon content

Molecular wt. of methyl orange (C₁₄H₁₄N₃NaO₃S) is 327.33 g. mol⁻¹

Amount of carbon in 1 mg/L of MeO = $14 \times 12 / 327.33 = 0.51$ mg

Therefore, after 300 minutes of degradation under LED lights 14 mg of carbon corresponds to 28 ppm of MeO.

Curriculum Vitae

Name: Debjani Mukherjee

Post-secondary Education and Degrees: Rourkela, Sambalpur University, India
1997-2001 B.Tech. (Pharmaceutical Science and Technology)
Indian Institute of Technology (Kharagpur), India
2003-2005 M.S. (Materials Science and Engineering)
The University of Western Ontario
London, Ontario, Canada
2007-2011 Ph.D.

Related Work Experience

Research Assistant
K.I.S.T.
Seoul, S.Korea
2005-2006

Chemist
C.I. Laboratories
Kolkata, India
2006-2007

Teaching Assistant
The University of Western Ontario
2007-2011

Honours and Awards

WGRS
2007-2011

Sarnia research bridge symposium
(poster presentation)
2010

Publications:

Mukherjee, D. (2011). Development of novel photocatalyst for water purification under solar and UV light. Water Innovation Forum, Lawrence centre of Management and Policy, London, Canada, 3.

Mukherjee, D., Barghi, S., Ray, A. (2009). Development of TiO₂ polymeric composite for water purification. Abstract book of 8th World congress of chemical engineering, Montreal, 319-324.

Mukherjee, D. (2006). Preparation of adrenochrome hydrogel patch, gel, ointment and comparison of their blood coagulating and wound healing capability. Journal of Materials and Manufacturing Processes, 21, 297-301.

Mukherjee, D. (2004). Hydrogel transdermal patch as controlled drug delivery system of tetracycline. Proceedings of 2nd International Conference, SPPM, Bangladesh in association with United States, 1, 639-645.

Mukherjee, D. (2004). Comparative study of antibiotic drug release behavior by hydrogel transdermal patches as controlled drug delivery system. Proceedings of International Symposium, ISAKMAP-2K4, Materials Sc.Center, I.I.T Kharagpur, India, 1, 671-677.

Mukherjee, D. (2004). Preparation of blood coagulating dosage forms and their wound healing capabilities. Proceedings of International Symposium, ISAMAP-2K4, vol 1, Materials Sc.Center, I.I.T. Kharagpur, India, 1, 701-716.

Submitted/ on-desk papers

Mukherjee, D., Barghi, S., Ray, A. Development of TiO₂/polymeric photocatalyst for degradation of methyl orange and kinetic study of the photodegradation under UV light.

Mukherjee, D., Barghi, S., Ray, A. Analysis of the intermediates of aspirin degradation under solar light in presence of TiO₂/polymeric composite.

Mukherjee, D., Barghi, S., Ray, A. Preparation and characterization of novel TiO₂/polymeric photocatalyst films for water purification both under UV and solar light.

Mukherjee, D., Barghi, S., Ray, A. Degradation of Methyl orange in a continuous flow reactor under LED in presence of polymeric film photocatalysts.